Progress and perspectives on the electron-doped cuprates[*]

N.P. Armitage

The Institute of Quantum Matter, Department of Physics and Astronomy, The Johns Hopkins University, Baltimore, MD 21218, USA.

P. Fournier

Regroupement québécois sur les matériaux de pointe and
Département de Physique, Université de Sherbrooke, Sherbrooke, Québec, CANADA, J1K 2R1.

R.L. Greene

Center for Nanophysics and Advanced Materials, Department of Physics, University of Maryland, College Park, MD 20742, USA.

(Dated: March 12, 2010)

Although the vast majority of high-T_c cuprate superconductors are hole-doped, a small family of electron-doped compounds exists. Under investigated until recently, there has been tremendous recent progress in their characterization. A consistent view is being reached on a number of formerly contentious issues, such as their order parameter symmetry, phase diagram, and normal state electronic structure. Many other aspects have been revealed exhibiting both their similarities and differences with the hole-doped compounds. This review summarizes the current experimental status of these materials. We attempt to synthesize this information into a consistent view on a number of topics important to both this material class as well as the overall cuprate phenomenology including the phase diagram, the superconducting order parameter symmetry, electron-phonon coupling, phase separation, the nature of the normal state, the role of competing orders, the spin-density wave mean-field description of the normal state, and pseudogap effects.

Contents

I. INTRODUCTION

It has now been over 20 years since the discovery of high temperature superconductivity in the layered copper-oxide perovskites by Bednorz and Müller (1986). Despite an almost unprecedented material science effort, the origin of the superconductivity or indeed even much consensus on their dominate physics remains elusive(Alloul *et al.*, 2009; Campuzano *et al.*, 2004; Damas-

---

celli *et al.*, 2003; Fischer *et al.*, 2007; Kastner *et al.*, 1998; Lee *et al.*, 2006b; Orenstein and Millis, 2000; Scalapino, 1995; Timusk and Statt, 1999).
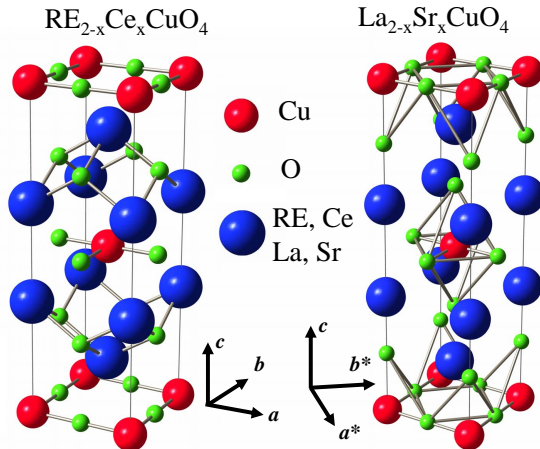

FIG. 1 A comparison of the crystal structures of the electron-doped cuprate $RE_{2-x}Ce_xCuO_4$ and of its closest hole-doped counterpart $La_{2-x}Sr_xCuO_4$. Here RE is one of a number of rare earth ions, including Nd, Pr, Sm, or Eu. One should note the different directions for the in-plane lattice parameters with respect to the Cu-O bonds.
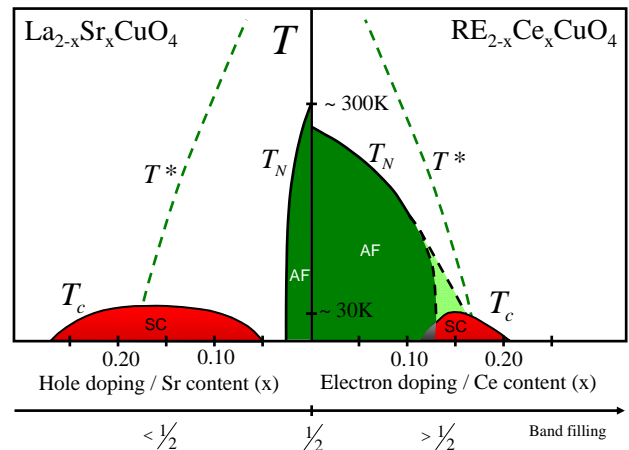

FIG. 2 Joint phase diagram of the LSCO/NCCO material systems. The uncertainty regarding the extent of AF on the electron-doped side and its coexistence with superconductivity is shown by the white/green dotted area. Maximum Néel temperatures have been reported as 270 K on the electron-doped side in NCO (Mang *et al.*, 2004b), 284 K in PCO (Sumarlin *et al.*, 1995) and 320 K on the hole-doped side in LCO(Keimer *et al.*, 1992). T^* indicates the approximate extent of the pseudogap (PG) phase. It is not clear if PG phenomena have the same origin on both sides of the phase diagram. At low dopings on the hole-doped side, a spin-glass phase exists (not-shown). There is as of yet no evidence for a spin-glass phase in the electron-doped compounds.

The undoped parent compounds of high-temperature cuprate superconductors are known to be antiferromagnetic (AFM) Mott insulators. As the CuO_2 planes are doped with charge carriers, the antiferromagnetic phase subsides and superconductivity emerges. The symmetry, or the lack thereof, between doping with electrons (*n*-type) or holes (*p*-type) has important theoretical implications as most models implicitly assume symmetry. One possible route towards understanding the cuprate superconductors may come through a detailed comparison of these two sides of the phase diagram. However, most of what we know about these superconductors comes from experiments performed on *p*-type materials. The much fewer measurements from *n*-type compounds suggest that there may be both commonalities and differences between these compounds. This issue of electron/hole symmetry has not been seriously discussed, perhaps, because until recently, the experimental database of *n*-type results was very limited. The case of electron doping provides an important additional example of the result of introducing charge into the CuO_2 planes. The hope is that a detailed study will give insight into what aspects of these compounds are universal, what aspects are important for the existence of superconductivity and the anomalous and perhaps non-Fermi liquid normal state, what aspects are not universal, and how various phenomena depend on the microscopics of the states involved.

The high-temperature cuprate superconductors are all based on a certain class of ceramic perovskites. They share the common feature of square planar copper-oxygen layers separated by charge reservoir layers. Fig. 1 presents the crystal structures for the canonical single layer parent materials La_2CuO_4 (LCO). The undoped materials are antiferromagnetic insulators. With the substitution of Sr for La in La_2CuO_4, holes are introduced into the CuO_2 planes. The Néel temperature precipitously drops and the material at some higher hole doping level becomes a superconductor (Fig. 2).

Although the majority of high-T_c superconductors are hole-doped compounds there are a small number that can be doped with electrons (Takagi *et al.*, 1989; Tokura *et al.*, 1989b). Along with the mostly commonly investigated compound $Nd_{2-x}Ce_xCuO_4$ (NCCO), most members of this material class have the chemical formula $RE_{2-x}M_xCuO_4$ where the lanthanide rare earth (RE) substitution is Pr, Nd, Sm or Eu and M is Ce or Th (Dalichaouch *et al.*, 1993; Maple, 1990). These are single-layer compounds which, unlike their other brethren 214 hole-doped systems (for instance the T crystal structured $La_{2-x}Sr_xCuO_{4\pm\delta}$ discussed above), have a T' crystal structure that is characterized by a lack of oxygen in the apical position (see Fig. 1 left).

The most dramatic and immediate difference between electron- and hole-doped materials is in their phase diagrams. Only an approximate symmetry exists about zero doping between *p*- and *n*-type, as the antiferromagnetic phase is much more robust in the electron-doped material

and persists to much higher doping levels (Fig. 2). Superconductivity occurs in a doping range that is almost five times narrower. In addition, these two ground states occur in much closer proximity to each other and may even coincide unlike in the hole-doped materials. Additionally, in contrast to many $p-$type cuprates, it is found that in doped compounds spin fluctuations remain commensurate(Thurston *et al.*, 1990; Yamada *et al.*, 1999). Various other differences are found including a resistivity that goes like $\approx T^2$ near optimal doping, lower superconducting T_c's and much smaller critical magnetic fields. One of the other remarkable aspects of the n-type cuprates, is that a mean-field spin-density wave treatment of the normal metallic state near optimal doping describes many material properties quite well. Such a description is not possible in the hole-doped compounds. Whether this is a consequence of the close proximity of antiferromagnetism and superconductivity in the phase diagram, smaller correlation effects than the p-type, or the absence of other competing effects (stripes etc.) is unknown. This issue will be addressed more completely in Sec. IV.G.

In the last few years incredible progress has been made both in regards to material quality as well as in the experimental understanding of these compounds. Unfortunately even in the comparatively under-investigated and well-defined scope of the n-type cuprates, the experimental literature is vast and we cannot hope to cover all the excellent work. Important omissions are regrettable, but inevitable.

II. OVERVIEW

A. General aspects of the phase diagram

Like many great discoveries in material science the discovery of superconductivity in the $Nd_{2-x}RE_xCuO_4$ material class came from a blend of careful systematic investigation and serendipity (Khurana, 1989). Along with the intense activity on the hole-doped compounds in the late 1980's, a number of groups had investigated n-type substitutions. The work on the $Nd_{2-x}RE_xCuO_4$ system was motivated after the discovery of 28K superconductivity in $Nd_{2-x-y}Sr_xCe_yCuO_4$, by Akimitsu *et al.* (1988), where it was found that higher cerium concentrations eventually killed the superconducting T_c (Tokura *et al.*, 1989a).

The original work on NCCO at the University of Tokyo was done with the likely result in mind that the material when doped with electrons may become an n-type metal, but it would not become a *superconductor*. This would indicate the special role played by superconducting holes. Initial work seemed to back up this prejudice. The group found that indeed the conductivity seemed to rise when increasing cerium concentration and that for well-doped samples the behavior was metallic ($d\rho/dT > 0$) for much of the temperature range. Hall effect measure-

ments confirmed the presence of mobile electrons, which underscored the suspicion that cerium was substituting tetravalently ($+4$) for trivalent neodymium ($+3$) and was donating electrons for conduction.

At the lowest temperatures the materials were not good metals and showed residual semiconducting tendencies with $d\rho/dT < 0$. In an attempt to create a true metallic state at low temperature, various growth conditions and sample compositions were tried. A breakthrough occurred when a student, H. Matsubara, accidently quenched a sample in air from 900°C to room temperature. This sample, presumed to be destroyed by such a violent process, actually showed superconductivity at 10K. Later it was found that by optimizing the conditions T_c could be pushed as high as 24K (Takagi *et al.*, 1989; Tokura *et al.*, 1989b).

The first reports of superconductivity in $Nd_{2-x}Ce_xCuO_4$ and $Pr_{2-x}Ce_xCuO_4$ by Takagi *et al.* (1989) also presented the first phase diagram of this family (see Fig. 3). In comparison to $La_{2-x}Sr_xCuO_4$, the doping dependence of the critical temperature (T_c) of these materials was sharply peaked around $x_{opt} = 0.15$ (optimal doping) corresponding to the maximum value of $T_{c,opt} \sim 24K$. In fact, at first glance, the $T_c(x)$ relation showed no underdoped regime ($x < x_{opt}$) with T_c rising from zero to its maximum value within a Δx of ~ 0.01 (from $x = 0.13$ to 0.14). Even the overdoped regime ($x > x_{opt}$) presents a sharp variation of T_c ($\frac{dT_c}{dx} \sim 600K/$ Ce atom). As discussed below, such steep dependence of $T_c(x)$ makes the exploration of the phase diagram very difficult.
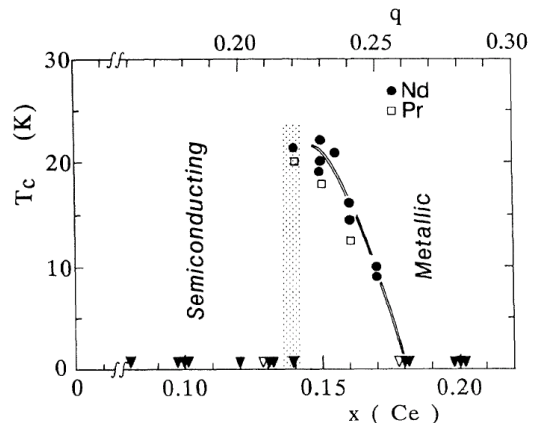
FIG. 3 Transition temperature T_c as a function of the Ce concentration in reduced NCCO (circles) and PCCO (squares). The closed and open triangles indicate that bulk superconductivity was not observed above 5 K for the Nd or Pr systems respectively. From the original paper of Takagi *et al.* (1989).

An important difference in the phase diagram of electron-doped cuprates with respect to their hole-doped cousins is the close proximity of the antiferromagnetic

phase to the superconducting phase. Using muon spin resonance and rotation on polycrystalline samples, Luke *et al.* (1990) first found that the Mott insulating parent compound Nd_2CuO_4 has a Néel temperature (T_N) of approximately 250K[1]. Upon substitution of Nd by Ce, T_N of $Nd_{2-x}Ce_xCuO_4$ decreases gradually to reach zero close to optimal doping (x $\sim$ 0.15)[2]. As noted previously, this should be contrasted with the case of $La_{2-x}Sr_xCuO_4$ in which antiferromagnetism collapses completely with dopings as small as $x = 0.02$ (Kastner *et al.*, 1998; Luke *et al.*, 1990). In the case of NCCO, the antiferromagnetic phase extends over a much wider range of cerium doping. This difference gives us a first hint that electron doping and hole doping are not affecting the electronic properties in the exact same manner in the cuprates. The proximity of the AF phase to the superconducting one is reminiscent of the situation in other strongly correlated electronic systems like some organic superconductors(Lefebvre *et al.*, 2000; McKenzie, 1997) and heavy fermion compounds (Coleman, 2007; Joynt and Taillefer, 2002; Pfleiderer, 2009). However, it still remains unclear up to now whether or not AF actually coexists with superconductivity. This will also be discussed in detail below.

B. Specific considerations of the cuprate electronic structure upon electron doping

As emphasized early on (Anderson, 1987), the central defining feature of all the cuprates is their ubiquitous CuO_2 layers and the resulting strong hybridization between Cu and O orbitals, which is the primary contributor to their magnetic and electronic properties. It is believed that the states relevant for superconductivity are formed out of primarily in-plane Cu $d_{x^2-y^2}$ and O $p_{x,y}$ orbitals. Small admixtures of other orbitals like Cu $d_{z^2-r^2}$ are also typically present, but these make usually less than a 10 % contribution (Nücker *et al.*, 1989; Pellegrin *et al.*, 1993). The formal valences in the CuO_2 planes of the undoped parent compounds are Cu^{+2} and O^{-2}. With one hole per unit cell, band theory predicts the undoped parent compounds (for instance La_2CuO_4 and Nd_2CuO_4) of these materials to be metallic. In fact they are insulators, which is believed to be driven by a strong local Coulomb interaction that suppresses charge fluctuations. Mott insulators, where insulation is caused by a strong on-site correlation energy that discourages double occupation, are frequently described by the single-band Hubbard Hamiltonian $H = \sum_{ij} t_{ij} c_j^\dagger c_i + \sum_i U n_{i\uparrow} n_{i\downarrow}$. If

$U \gg t_{ij}$ the single band is split into two, the so-called upper and lower Hubbard bands (see Fig. 4 (top)) that are respectively empty and completely full at half-filling. The Hubbard Hamiltonian is the minimal model that includes the strong local interactions, which are believed to be so central to these compounds. Although frequently referred to as Mott insulators, the cuprates are more properly referred to as charge-transfer band insulators within the Zaanen-Sawatsky-Allen scheme (Zaanen *et al.*, 1985). Here the energy to overcome for charge motion is not the strong on-site Coulomb interaction on the Cu site, but instead the energy associated with the potential difference beween Cu $d_{x^2-y^2}$ and O $p_{x,y}$ orbitals Δ_{pd} (Fig. 4 (middle)). The optical gap in the undoped La_2CuO_4 is found to be $1.5 - 2$ eV (Basov and Timusk, 2005), which is close to the expected value of Δ_{pd}. This means that doped holes preferentially reside in the so-called 'charge transfer band' composed primarily of oxygen orbitals (with a local configuration primarily $3d^9\underline{L}$ where $\underline{L}$ is the oxygen 'ligand' hole), whereas doped electron preferentially reside on the Cu sites (Fig. 4 (bottom)) (with a local configuration mostly $3d^{10}$). In the half-filled cuprates, with a single electron on the Cu $d_{x^2-y^2}$ orbital and filled O $p_{x,y}$ orbitals these compounds can be then described by a three band Hubbard model, which generally takes into account hopping, the onsite Coulomb interactions U_d, the energy difference between oxygen and copper orbitals Δ_{pd}, and intersite interactions V_{pd} (Varma *et al.*, 1987).

A number of simplifications of the three band model may be possible. Zhang and Rice (1988) argued that the maximum gain in hybridization energy is gained by placing doped holes in a linear combination of the O $p_{x,y}$ orbitals with the same symmetry as the existing hole in the Cu $d_{x^2-y^2}$ orbital that they surround. This requires an antisymmetry of the wave function in their spin coordinates, so that the two holes must form a singlet. They argued that this split-off state retained its integrity even when intercell hopping is taken into account. With this simplification, the separate degrees of freedom of the Cu and O orbitals are removed and the CuO_2 plaquette is real space renormalized to an effective site centered on Cu. In this case, it may be possible to reduce the three band model to an effective single band one, where the role of the lower Hubbard band is played by the primarily oxygen based charge transfer band (of possibly singlet character) and an effective Hubbard gap given primarily by the charge transfer energy Δ_{pd}. Even though the local structure of the states is different upon hole or electron doping (Fig. 4 (bottom)), both would be of singlet character ($3d^9\underline{L}$ and $3d^{10}$ respectively).

In general, it may be possible to reduce the one band Hubbard model even further by taking the limit of large effective U (the charge transfer energy Δ_{pd} in the cuprates). One can find an effective Hamiltonian in the subspace of only singly occupied sites. Localized electrons with oppositely aligned spins on adjacent sites can still reduce their kinetic energy by undergoing virtual

---

[1] T_N is a very sensitive function of oxygen concentration. Subsequent work has shown that the Néel temperature of ideally reduced NCO is probably closer to 270 K (Mang *et al.*, 2004b)

[2] The precise extent of the AF state and its coexistence or not with SC is a matter of much debate. See Sec. IV.H for further details.
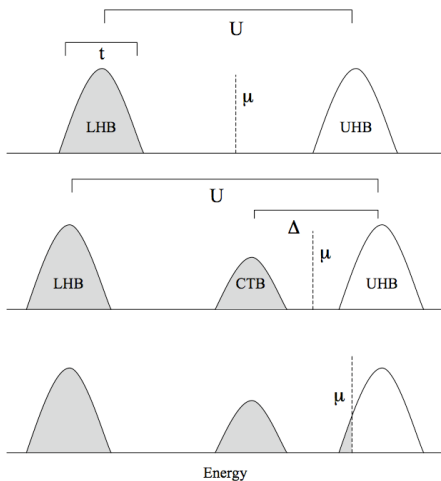
FIG. 4 (top) Schematic of the one band Hubbard model with $U \gg t$. At half-filling the chemical potential μ lies in the middle of the Mott gap. (middle) Schematic for a charge-transfer band insulator. Δ_{pd} may play the role of an effective Hubbard U with the charge transfer band (CTB) standing in for the lower Hubbard band. (bottom) Upon doping the CTB insulator with electrons, the chemical potential μ presumably moves into the upper Hubbard band.

hops to neighboring sites. As such, hops are only allowed with neighboring electrons being anti-aligned, this gives an effective spin exchange interaction which favors anti-ferromagnetism. The effect of the upper Hubbard band comes in only through these virtual hops. Second order perturbation theory gives an energy lowering for oppositely directed spins of $4t^2/U$. By neglecting correlated hopping terms, the one band Hubbard model can then be replaced by the so-called '$t - J$' model which is a possible minimal model for the cuprates. The $t - J$ model can be refined by the inclusion of next-nearest t' and next-next-nearest t'' neighbor hopping terms.

We should note that the reduction of the three band model to models of the $t - U$ or $t - J$ variety is still very controversial. Emery and Reiter (1988) argued that in fact the quasiparticles of the three band model have both charge and a spin of 1/2, in contrast to the singlets of Zhang and Rice and that the $t - J$ model is incomplete. Similarly, Varma has proposed that one must consider the full three band Hubbard model (Varma, 1997, 1999) and that non-trivial phase factors between the bands become possible at low energies, which leads to a state with orbital currents on the O-Cu-O triangular plaquettes. The order associated with these currents has been proposed to be a candidate for the pseudogap phase. Moreover, questions regarding even the validity of the parameter J remain. It is derived for the insulating case of localized electrons. Is it still a valid parameter when many holes or electrons have been introduced? Although throughout this review we will frequently appeal to the insight given by these simpler models (single band

Hubbard or $t - J$), we caution that it is far from clear whether or not these models are missing some very important physics.

As mentioned, doped electrons are believed to reside primarily on Cu sites. This nominal $3d^{10}$ atomic configuration of an added electron has been confirmed *via* a number of resonant photoemission studies which show a dominant Cu $3d$ character at the Fermi level (Allen *et al.*, 1990; Sakisaka *et al.*, 1990) in electron-doped compounds. Within the context of the single band Hubbard or $t - J$ models, the effective orbital of a hole-doped into the CuO_2 plane $3d^9\underline{L}$ may be approximated as a singlet formed between the local Cu^{+2} spin and the hole on the oxygen atoms. This is viewed as symmetry equivalent to the state of a spinless hole $3d^8$ on the copper atom (albeit with different effective parameters). Although their actual local character is different, such an approximation makes the effective model describing holes and electrons doped into $3d^9$ virtually identical between the $p-$ and $n-$type cuprates leading to the prediction of an electron-hole symmetry. The noted *asymmetry* between the two sides of the phase diagram means that there are specific extra considerations that must go into the two different cases.

There are a number of such considerations regarding the cuprate electronic structure that apply specifically to the case of electron doping. One approach to understanding the relative robustness of antiferromagnetism in the electron-doped compounds has been to consider *spin-dilution models*. It was shown *via* neutron scattering that Zn doping into La_2CuO_4 reduces the Néel temperature at a similar rate as Ce doping in $Pr_{2-x}Ce_xCuO_{4\pm\delta}$ (Keimer *et al.*, 1992). Since Zn substitutes in a configuration that is nominally a localized d^{10} filled shell, it can be regarded as a spinless impurity. In this regard Zn substitution can be seen as simple dilution of the spin system. The similarity with the case of Ce doping into $Pr_{2-x}Ce_xCuO_{4\pm\delta}$ implies that one of the effects of electron doping is to dilute the spin system by neutralizing the spin on a d^9 Cu site. It subsequently was shown that the reduction of the Néel temperature in $Nd_{2-x}Ce_xCuO_{4\pm\delta}$ comes through a continuous reduction of the spin stiffness ρ_s which is consistent with this model (Matsuda *et al.*, 1992). In contrast, in the hole-doped case Aharony *et al.* (1988) have proposed that only a small number of holes is required to suppress antiferromagnetism because they primarily exist on the in-plane oxygen atoms and result in not spin-*dilution* but instead spin-*frustration*. The oxygen-hole/copper-hole interaction, whether ferromagnetic or antiferromagnetic, induces an effective ferromagnetic Cu-Cu interaction. This interaction competes with the antiferromagnetic superexchange and frustrates the Néel order so a small density of doped holes has a catastrophic effect on the long-range order. This additional frustration does not occur with electron doping as electrons are primarily introduced onto Cu sites. This comparison of Ce with Zn doping is compelling, but cannot be exact as Zn does not add itinerant charge carriers like Ce does, as its

d^{10} electrons are tightly bound and can more efficiently frustrate the spin order. Models or analysis which takes into account electron itinerancy must be used to describe the phase diagrams. But this simple model gives some indication how the principle interactions can be very different between electron and hole-doping if one considers physics beyond the $t-J$ or single band Hubbard models.

Alternatively, it has been argued that the observed asymmetry between hole and electron doping (say for instance in their phase diagrams) can be understood within single band models by considering the fact that the hopping terms, which have values $t > 0$, $t' < 0$, and $t'' > 0$ for hole doping assume values $t < 0$, $t' > 0$, and $t'' < 0$ for electron doping. These sign reversals arise in the particle-hole transformation $c_{i\sigma}^{\dagger} \rightarrow (-1)^i c_{i\sigma}$ where c and $c^{\dagger}$ are particle creation and annihilation operators and i is a site index[3].

Since the next nearest t' and next-next nearest neighbor t'' terms facilitate hopping on the same sub-lattice of the Néel state, the energy and stability of antiferromagnetic order is very sensitive to their values. For instance, it has been argued that the greater stability of antiferromagnetism in the electron-doped compounds is primarily a consequence of $t' > 0$. This scenario is supported by a number of numerical calculations and analytical treatments (Gooding *et al.*, 1994; Pathak *et al.*, 2009; Singh and Ghosh, 2002; Tohyama and Maekawa, 1994, 2001).

Models that account for the effective sign change of the hopping parameter, successfully account for the fact that the lowest energy hole addition (electron removal) states are near $(\pi/2, \pi/2)$ (Wells *et al.*, 1995), while the lowest energy electron addition states (hole removal) are near $(\pi, 0)$ (Armitage *et al.*, 2002). This manifests as a small hole-like Fermi arc (or perhaps pocket (Doiron-Leyraud *et al.*, 2007; LeBoeuf *et al.*, 2007)) for low hole dopings near the $(\pi/2, \pi/2)$ point and a small electron-pocket near the $(\pi, 0)$ point for low electron dopings (Armitage *et al.*, 2002). Such considerations also mean that the insulating gap of the parent compounds is indirect. Aspects of $t-J$ type models applied to both sign of charge carriers have been reviewed by Tohyama (2004).

Although it may be that such a mapping can be applied so that the same model (for instance $t-J$) captures aspects of the physics for both hole and electron doping, the object that is undergoing hopping in each case has very different spatial structure and local character ($3d^9\underline{L}$ ZR singlet vs. $3d^{10}$ respectively). It is reasonable to expect that the values for their effective hopping parameters could be very different[4]. In this regard, Hozoi

et al. (2008) found *via ab initio* quantum chemical calculations very different values for the *bare* hopping parameters of the $3d^{10}$ and $3d^9\underline{L}$ states. They found $|t| = 0.29$, $|t'| = 0.13$, and $|t''| = 0.045$ for $3d^{10}$ and $|t| = 0.54$, $|t'| = 0.305$, and $|t''| = 0.115$ for $3d^9\underline{L}$. Interestingly, they find that after including interactions the *renormalized* values are much closer to each other, but still with some significant differences. ($|t| = 0.115$, $|t'| = 0.13$, and $|t''| = 0.015$ for $3d^{10}$ and $|t| = 0.135$, $|t'| = 0.1$, and $|t''| = 0.075$ for $3d^9\underline{L}$. All values in eV.). Similar magnitudes of t and t' for electron and hole doping have also been found in Cu-O cluster calculations. Hybertsen *et al.* (1990) used *ab initio* local-density-functional theory to generate input parameters for the three-band Hubbard model and computed spectral functions exactly on finite clusters using the three band Hubbard model and compared the results with the spectra of the one band Hubbard and the $t-t'-J$ models. The extracted effective nearest neighbor and next-nearest neighbor hopping parameters were found to be almost identical at $t = 0.41$ and $|t'| = 0.07$ eV for electron doping and $t = 0.44$ and $|t'| = 0.06$ eV for hole doping. J was found in this study to be 128 ± 5 meV which is in reasonable agreement with neutron (Mang *et al.*, 2004b) and two-magnon Raman scattering (Blumberg *et al.*, 1996; Lyons *et al.*, 1988; Singh *et al.*, 1989; Sulewski *et al.*, 1990). Somewhat similar results for the hole-doped case were obtained by Bacci *et al.* (1991). However these results conflicted with those of Eskes *et al.* (1989) who found slightly different values between hole ($t = -0.44$, $t' = 0.18$ eV) and electron doping ($t = 0.40$, $t' = -0.10$ eV) in their numerical diagonalization study of Cu_2O_7 and Cu_2O_8 clusters. In a similar calculation but with slightly different parameters and also taking into account the apical oxygen for the hole-doped case Tohyama and Maekawa (1990) found the even more different $t = -0.224$ and $t' = 0.124$ eV for the p-type and $t = 0.3$ and $t' = -0.06$ eV for the n-type cases. This shows the strong sensitivity that these effective parameters likely have on the local energies and the presence of apical oxygen. Despite differences in the estimates for these parameters it is still remarkable that in all these studies the values of the hopping parameters for holes and electrons are so close to each other considering the large differences in these states' local character. This shows the principal importance that correlations have in both cases in renormalizing their dispersions.

It is interesting to note that although very different behavior of the electronic structure is expected and indeed found at low dopings (FS pockets around $(\pi,0)$ vs. $(\pi/2,\pi/2)$), it appears that at higher dopings in both systems the set of small Fermi pockets go away and a large Fermi surface centered around the (π, π) point emerges (Anderson *et al.*, 1993; Armitage *et al.*, 2002; King *et al.*,

---

[3] Note that for the case of long-range AF order, the final results in either doping case are invariant with respect to the sign of t, as a change in the sign of t is equivalent to a shift of the momentum by the AF reciprocal lattice vector (π,π).

[4] It is also reasonable to expect that their interaction with degrees of freedom not explicitly considered in these electronic models, such as the strength of their lattice coupling, could also be very

---

different. Aspects related to lattice coupling are discussed in Sec. IV.D below.

1993). In the electron-doped materials, aside from the 'hot-spot' effect discussed in detail below, the Fermi surface resembles the one calculated *via* LDA band structure calculations.

A number of workers (Kusko *et al.*, 2002; Kyung *et al.*, 2004, 2003; Tremblay *et al.*, 2006) have pointed out that due to the different size of the effective onsite repulsion U and the electronic bandwidth W in the n-type systems, the expansion parameter U/W is less than unity, which puts the electron-doped cuprates in a weaker correlated regime than the p-type compounds. Among other things, this makes Hubbard model-like calculations more amenable[5]. Smaller values of U/W physically derive from better screening and the Madelung potential differences noted above, as well as a larger occupied bandwidth. This weaker coupling may allow for more realistic comparisons between theoretical models and experiment and even serve as a check on what models are most appropriate for the more correlated hole-doped materials. The fact that we may be able to regard the n-type systems as somewhat weaker correlated is manifest in a number of ways, including the remarkable fact that a mean-field spin-density wave (SDW) like treatment of the normal state near optimal doping can capture many of the gross features of transport, optics, and photoemission quite well (Sec IV.G). It also makes the issue of AF fluctuations easier to incorporate. For instance, the Two-Particle Self-Consistent (Kyung *et al.*, 2004) approach to the Hubbard model allows one to predict the momentum dependence of the PG in the ARPES spectra of the n-type cuprates, the onset temperature of the pseudogap T^*, and the temperature and doping dependence of the AF correlation length. A similar treatment fails in hole-doped compounds with their corresponding larger values of U/W. The n-type compounds appear to be the first cuprate superconductors whose normal state lends itself to such a detailed theoretical treatment. Recent work by Weber *et al.* (2009), even claims that U/W in the electron-doped cuprates is low enough to be below the critical value for the Mott transition and hence that the $x \rightarrow 0$ insulating behavior must derive from antiferromagnetism. To distinguish from the p-type Mott systems, they call such a system a Slater insulator. These issues are dealt with in more detail below.

C. Crystal structure and solid-state chemistry

RE$_2$CuO$_4$ with RE = Nd, Pr, Sm, Eu, Gd crystallizes in the so-called T' crystal structure and are typi-

cally doped with Ce[6][7]. These compounds are tetragonal with typical lattice parameters of a = b $\sim$ 3.95 Å and c $\sim$ 12.15 Å . Their structure is a close cousin of T structure La$_2$CuO$_4$ (LCO) compound. T' is represented by the D_{4h}^{17} point group (I4/mmm). It has a body-centered unit cell where the copper ions of adjacent copper-oxygen CuO$_2$ layers are displaced by (a/2,a/2) with respect to each other (Kastner *et al.*, 1998). In Fig. 1, we compare the crystal structure of these parent compounds.

Although aspects of the LCO and NCO crystal structures are similar, closer inspection (Kwei *et al.*, 1989; Marin *et al.*, 1993) reveals notable differences. First, the coordination number of the in-plane copper is different. The T' structure has no apical oxygen above the in-plane Cu and hence only four oxygen ions O(1) surround each copper. The T structure has 6 surrounding O atoms, two of which are in the apical position.

The different relative positions of the reservoir oxygens O(2) with respect to the T-structure results in an expanded in-plane unit cell with respect to La$_2$CuO$_4$ that allows a further decrease of the unit cell volume with decreasing rare earth ionic radius (see Table I). While La$_2$CuO$_4$ with the T-structure has typical in-plane lattice parameters on the order of a = b $\sim$ 3.81 Å and c $\sim$ 13.2 Å (Kastner *et al.*, 1998)[8] and a unit cell volume of 191.6 Å^3, the largest undoped T' phase cuprate, Pr$_2$CuO$_4$, has a = b $\sim$ 3.96 Å and c $\sim$ 12.20 Å and similar unit cell volume of 191.3 Å^3. The smallest, Eu$_2$CuO$_4$, has a = b $\sim$ 3.90 Å and c $\sim$ 11.9 Å (Fontcuberta and Fabrega, 1996; Nedil'ko, 1982; Uzumaki *et al.*, 1991; Vigoureux, 1995)[9]. The second notable difference arising from the expanded in-plane lattice parameters is that the rare-earth and oxygen ions in the reservoirs are not positioned in the same plane.

Until recently it was believed that only T' crystal structures without apical oxygen can be electron doped. This was understood within a Madelung potential analysis, where the local ionic potential on the Cu site is influenced strongly by the presence of an O^{-2} ion in the apical site immediately above it (Ohta *et al.*, 1991; Torrance and Metzger, 1989). As doped elec-

---

[5] In a reanalysis of optical and ARPES data Xiang *et al.* (2008) in fact have argued that the charge transfer gap Δ, which is the effective onsite Hubbard repulsion is even smaller than usually assumed in the electron-doped compounds. They claim $\Delta \approx 0.5$ eV.

[6] There is at least one more class of superconducting electron-doped cuprates, the so-called infinite layer compounds. Sr$_{0.9}$La$_{0.1}$CuO$_2$ (SLCO) has been known for almost as long as the (RE)CCO material class (Siegrist *et al.*, 1988). It has the highest T$_c$ ($\approx$ 42K) of any $n-$doped cuprate. However, there has been comparatively little research performed on it due to difficulties in sample preparation. This system will be touched only briefly here.

[7] Another intriguing path to doping in the (RE)CCO electron-doped family is Nd$_2$CuO$_{4-y}$F$_y$, which uses an under investigated fluorine substitution for oxygen (James *et al.*, 1989) and no Ce doping

[8] Note that the real crystallographic in-plane lattice parameters of LCO are actually a* $\sim$ b* = $\sqrt{2}$a as shown in Fig. 1. In this case, a* and b* are 45° with respect to the Cu-O bonds.

[9] The other (RE)CCO compound in this series Gd$_2$CuO$_4$ is not a superconductor upon Ce doping

8

trons are expected to primarily occupy the Cu site, while doped holes primarily occupy in-plane O sites the local ionic potentials play a strong role in determining which sites mobile charges can occupy. Recent developments may not be entirely consistent with this scenario as there has been a report of superconductivity in T phase $La_{2-x}Ce_xCuO_4$ (Oka $et\ al.$, 2003). However this report contrasts with various thin film studies, which claim that although T phase $La_{2-x}Ce_xCuO_4$ can be electron-doped (i.e with Ce in valence state +4) it does not become a superconductor (Tsukada $et\ al.$, 2005, 2007). There has also been the recent remarkable work by Segawa and Ando (2006) who reported ambipolar doping of the $(Y_{1-z}La_z)(Ba_{1-y}La_y)_2Cu_3O_y$ (YLBLCO) system. They found that La^{+3} substitutes for Ba^{+2} at the 13 % level. By varying oxygen content y between 6.21 and 6.95 by controlled annealing, they could tune the in-plane resistivity through a maximum at 6.32. This was interpreted as an ability to tune the material through the Mott insulating state from hole- to electron-doping. Electron-doping was confirmed by negative Hall and Seebeck coefficients for $y < 6.32$. Subsequent photoemission work has shown that the chemical potential crosses a CT gap of ~ 0.8 eV upon cross the n/p threshold (Ikeda $et\ al.$, 2009a) . This work represents the first demonstration of ambipolarity in a single material system, which deserves further investigation.

As observed originally by Takagi $et\ al.$ (1989) and expanded upon by Fontcuberta and Fabrega (1996), the actual phase diagram of the (RE)CCO electron-doped family is sensitive to the rare-earth ion size. The smaller the ionic radius of the rare earth the smaller the optimal $T_{c,max}$ (see Table I, Fig. 5, and Fontcuberta and Fabrega (1996); Vigoureux (1995) and references therein). The most obvious effect of the decreasing ionic size (Table I) is a decrease of roughly 2.6% of the c-axis and 1.5% of the in-plane lattice constant across the series. One should note that the lattice also contracts with Ce substitution in $Pr_{2-x}Ce_xCuO_4$ (PCCO) and NCCO (Fontcuberta and Fabrega, 1996; Tarascon $et\ al.$, 1989; Vigoureux, 1995) as shown in Fig. 6.

As the RE-O distance gradually decreases with decreasing ionic radius, the crystal structure is subjected to increasing internal stress indicated by a decreasing tolerance factor $t \equiv \frac{r_{RE}+r_O}{\sqrt{2}(r_{Cu}+r_O)}$ where r_{RE}, r_O and r_{Cu} are respectively the ionic sizes of the rare earth, the oxygen and the copper ions (see Table I). Several neutron and high-resolution x-ray scattering studies report structural distortions when the Cu-O bond length becomes too large with respect to the shrinking RE-O ionic distance which promotes Cu-O-Cu bond angles that deviate from 180°. The most striking result is the distorted structure of (non-superconducting) Gd_2CuO_4 with its commensurate distortion corresponding to the rigid rotation of the four planar oxygen atoms around each copper sites(Braden $et\ al.$, 1994; Vigoureux $et\ al.$, 1997). This distortion leads to antisymmetric exchange term of Dzyaloshinski-Moriya type that may account for the weak ferromagnetism of

	La^{3+}	Pr^{3+}	Nd^{3+}	Sm^{3+}	Eu^{3+}	Gd^{3+}	Ce^{4+}
Ionic radius (Å)	1.30	1.266	1.249	1.219	1.206	1.193	**1.11**
a (Å)	−	3.9615	3.942	3.915	3.901	3.894	-
c (Å)	−	12.214	12.16	11.97	11.90	11.88	-
t	−	0.856	0.851	0.841	0.837	0.832	-
$T_{c,max}(K)$	−*	22	24	20	13	0	-

TABLE I Dependence on ionic radius of unit cell parameters of the parent compound, the tolerance factor t (Cox $et\ al.$, 1989; Muller-Buschbaum and Wollschlager, 1975; Nedil'ko, 1982; Uzumaki $et\ al.$, 1991), and the maximum transition temperature $T_{c,max}$ obtained by cerium doping for $x \sim 0.15$ (Fontcuberta and Fabrega, 1996; Maple, 1990). The T' $(La,Ce)_2CuO_4$ can only be easily stabilized in thin films, giving $T_{c,max} \sim 25K$ (Naito $et\ al.$, 2002). Ionic radii are given for a coordination of 8 according to Shannon (1976) and references therein. See Sec. II.D.
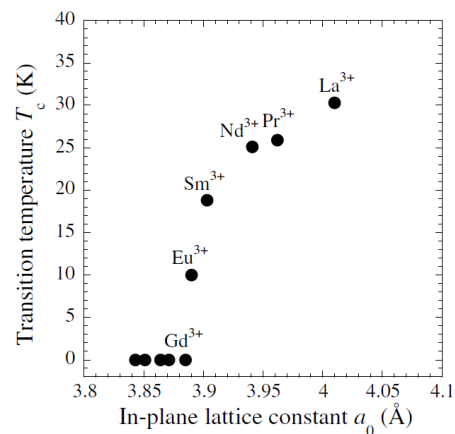

FIG. 5 The highest superconducting onset temperature versus in plane lattice constant in $RE_{2-x}Ce_xCuO_{4+\delta}$. Note that T' phase $La_{2-x}Ce_xCuO_{4+\delta}$ can only be stabilized in thin film form as discussed in the text. From Naito $et\ al.$ (2002).

Gd_2CuO_4 (Oseroff $et\ al.$, 1990; Stepanov $et\ al.$, 1993).

At the other extreme, for large ionic radius, the crystal structure approaches the T' to T structural transition, which is expected for an ionic radius between those of Pr and La (Fontcuberta and Fabrega, 1996). PCO is at the limit of the bulk T' phase: the next compound in the RE series with a larger atomic radius is LCO which crystallizes not in the T' phase, but instead in the more compressed T-phase form where the out-of plane oxygens are in apical positions as mentioned previously. It does seem to be possible to stabilize a doped T' phase of $La_{2-x}Ce_xCuO_{4+\delta}$ by substitution of La by the smaller Ce ion, although bulk crystals are not of that high quality due to the low growth temperatures required (Yamada $et\ al.$, 1994). However it has been shown by Naito
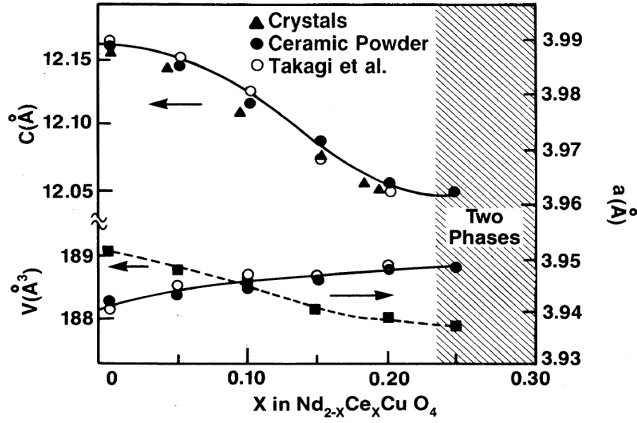
FIG. 6 The lattice parameters of NCCO single crystals and ceramic powders as a function of cerium content x showing the decreasing unit cell volume with increasing x. Solid circles and triangles refer to powder samples and single crystals respectively. Open circles are the results from (Takagi *et al.*, 1989). From Tarascon *et al.* (1989).

and Hepp (2000); Naito *et al.* (2002); Wu *et al.* (2009) that the T' phase of $La_{2-x}Ce_xCuO_{4+\delta}$ (LCCO) can be strain stabilized in thin film form leading to high quality superconducting materials with T_c as high as 27K. One can also drive the T' structure even closer to the structural instability by only partial substitution of Pr by La (Fontcuberta and Fabrega, 1996; Koike *et al.*, 1992) as $Pr_{1-y-x}La_yCe_xCuO_{4\pm\delta}$. This substitution provokes a significant modification to the phase diagram, with an optimal $T_{c,opt} \sim 25K$ for $Pr_{1-x}LaCe_xCuO_{4\pm\delta}$ at $x \sim 0.11$ and superconductivity extending as low as $x = 0.09$ and as high as $x = 0.20$ (Fujita *et al.*, 2003) (See Fig. 7). The mechanism leading to a different phase diagram in PLCCO remains a mystery, but it has been suggested that it corresponds to the ability to remove a larger amount of oxygen during the necessary reduction process compared to PCCO and NCCO, which leads to larger electron concentrations (Kuroshima *et al.*, 2003).

There have been many fewer studies of the infinite layer class of electron-doped cuprate superconductors $Sr_{1-x}Nd_xCuO_2$ (SNCO)(Smith *et al.*, 1991) and $Sr_{1-x}La_xCuO_2$ (SLCO)(Kikkawa *et al.*, 1992). To date no single crystals have been produced and the data up to now relies on ceramic samples(Ikeda *et al.*, 1993; Jorgensen *et al.*, 1993; Khasanov *et al.*, 2008; Kim *et al.*, 2002) and thin films(ichi Karimoto and Naito, 2004; Leca *et al.*, 2006; Li *et al.*, 2009; Naito *et al.*, 2002; Nie *et al.*, 2003). Its simple structure is based on alternating of CuO_2 planes with Sr (La) layers with lattice parameters a = b $\sim$ 3.94 Å and c $\sim$ 3.40 Å. Electron doping is suggested because the La (Nd) nominal valence is +3 as compared to Sr's +2 valence. Electron-type doping is supported by a negative thermopower(Kikkawa *et al.*,
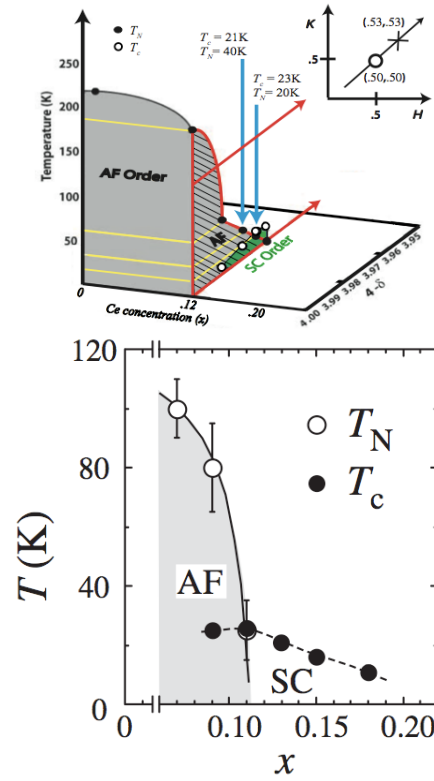

FIG. 7 (top) $\delta - x$ phase diagram of PLCCO (Wilson *et al.*, 2006b). (bottom) Phase diagram for PLCCO as a function of Ce content x (Fujita *et al.*, 2008a) as determined by neutron scattering and SQUID measurements.

1992) and XANES results (Liu *et al.*, 2001) confirming the presence of Cu^{1+} ions. However, a systematic study of the Hall effect with doping is still lacking, which makes difficult any comparison with the well-established behavior of transport for T' electron-doped (RE)CCO (see Section III.A).

The most complete phase diagram for the $Sr_{1-x}La_xCuO_2$ system has been established from the MBE film studies (ichi Karimoto and Naito, 2004). In this exploration the ab-plane resistivity shows that superconductivity exists in the doping range $0.08 < x < 0.15$ with the maximum $T_c \sim 40K$ for x$\sim$0.1 as shown in Fig. 8. Because of the limited sample size, very little is known about the possibility of an antiferromagnetic phase in the lightly doped materials and a complete phase diagram showing antiferromagnetic and superconducting phase boundaries has not been produced. However, muon spin rotation (uSR) measurements (Shengelaya *et al.*, 2005) on ceramic samples have claimed that magnetism and SC do not coexist at the La=0.1 doping and that the superfluid density is four times larger than in p-type cuprates with comparable T_c (i.e. off the 'Uemura line' (Uemura *et al.*, 1991, 1989)). A similar doping dependence of T_c with substitution of Pr(Smith *et al.*, 1991), Sm

and Gd(Ikeda *et al.*, 1993) rules out the possibility that superconductivity in SLCO arises due to the intercalation of the $(La,Sr)_2CuO_4$ phase. Early neutron scattering studies on bulk materials have shown that superconducting SLCO is perfectly stoichiometric and presents no excess (interstitial) oxygen in the Sr(La) layers (Jorgensen *et al.*, 1993). Thus, neither oxygen vacancies nor interstitial oxygen seem to play a role in the doping of this compound, although a recent report on thin films may be indicating a required reduction process (Li *et al.*, 2009).
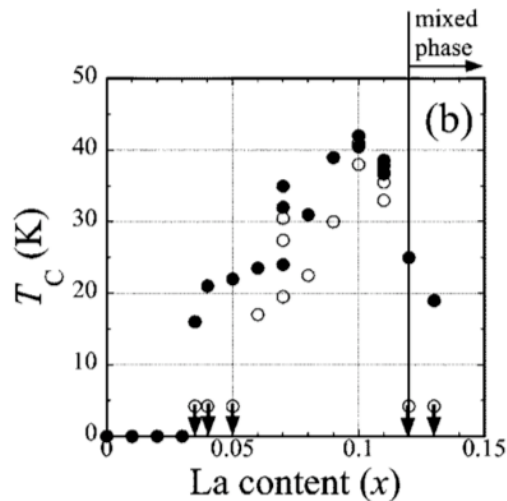

FIG. 8 Extracted values of T_c for SLCO as a function of doping. Solid and open circles are for the onset and zero resistivity respectively. From ichi Karimoto and Naito (2004).

D. Materials growth

The growth of electron-doped cuprate materials has been a challenge since their discovery. Because there are in principle two doping degrees of freedom (cerium and oxygen), the optimisation of their growth and annealing parameters is tedious and has been the source of great variability in their physical properties. For instance, it took almost 10 years after the discovery of the n-type compounds until superconducting crystals of sufficient size and quality could be prepared to perform inelastic neutron scattering (Yamada *et al.*, 1999). It is obvious that many properties, for example the temperature dependence of the resistivity, are strongly affected by grain boundaries. Due to these difficulties we focus our attention here on the growth of single crystals and epitaxial thin films.

1. Single crystals

Two main techniques have been used to grow single crystals of the n-type family: in-flux solidification and traveling-solvent floating zone (TSFZ). The first single crystals of $Nd_{2-x}Ce_xCuO_4$ were grown using the directional solidification flux technique taking advantage of the stability of the NCCO T' phase in a flux of CuO close to an eutectic point(Tarascon *et al.*, 1989). As shown in Fig. 9, the $T - x$ phase diagram of the NdCeO-CuO mixture presents a large region between 1030 and $1250°C$ for which the growth of NCCO crystals is possible within a liquid phase(Maljuk *et al.*, 1996; Oka and Unoki, 1990; Pinol *et al.*, 1990). Typical crucibles used for the flux growth of the electron-doped cuprates are high purity alumina(Brinkmann *et al.*, 1996a; Dalichaouch *et al.*, 1993; Peng *et al.*, 1991; Sadowski *et al.*, 1990), magnesia, zirconia(Kaneko *et al.*, 1999) and platinum(Kaneko *et al.*, 1999; Matsuda *et al.*, 1991; Tarascon *et al.*, 1989). After reaching temperatures high enough for melting the whole content of a crucible (above $1250°C$ following the phase diagram in Fig. 9), the temperature is slowly ramped down with typical rates of 1 to $6°C/h$ while imposing a temperature gradient at the crucible position promoting the growth of the CuO_2 planes along its direction. As the crucible is further cooled down, the flux solidifies leaving the NCCO single crystals usually embedded in a solid matrix. Platelet crystals can reach sizes on the order of several millimeters in the $a - b$ direction, with the c axis limited to a few tens to several hundred microns.

When their growth and annealing processes are under control, flux grown single crystals present very high crystalline quality with few defects. They also have well-defined faces which necessitate little cutting and polishing to prepare for most experiments. Flux grown crystals can have however a cerium content that can vary substantially even within the same batch(Dalichaouch *et al.*, 1993) and moreover, the thickest crystals have been shown to have an inhomogeneous cerium distribution along their thickness(Skelton *et al.*, 1994). Finally, since the flux properties change considerably with composition, it remains quite difficult to vary the cerium content substantially around optimal doping and preserve narrow transitions. A variant of this directional flux technique, top seeded solution, has also been developed(Cassanho *et al.*, 1989; Maljuk *et al.*, 2000) which leads to large single crystals with apparently more uniform cerium content.

These millimeter-size crystals are large enough for many experiments, however, their limited volume is a drawback for others like neutron scattering. As is also the case for the p-type cuprates, larger single crystals can be grown by the TSFZ technique using image furnaces(Gamayunov *et al.*, 1994; Kurahashi *et al.*, 2002; Tanaka *et al.*, 1991). Large boules of electron-doped cuprates several centimeters in length and half a centimeter in diameter(Tanaka *et al.*, 1991) can be produced with close to stoichiometric flux in various atmospheres and
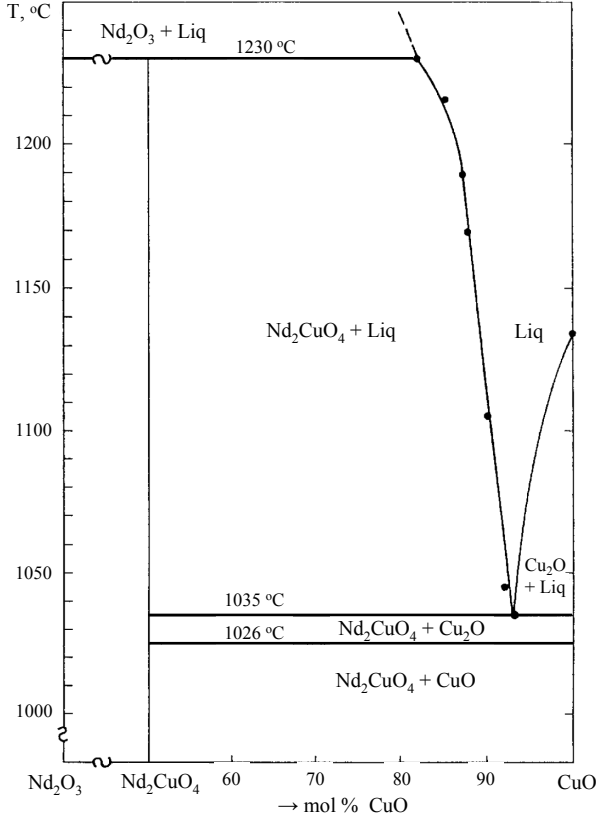
FIG. 9 Phase diagram of the Nd_2O_3-CuO binary system. Without Ce, the eutectic point corresponds to approximatively 90% CuO content in the flux. From Maljuk *et al.* (1996).

pressures. Using such conditions, NCCO crystals with x as large as 0.18, the solubility limit, could be grown and studied by neutron scattering(Mang *et al.*, 2004b; Motoyama *et al.*, 2007). Large TSFZ single crystals of $Pr_{1-y-x}La_yCe_xCuO_{4\pm\delta}$ have also been grown successfully in recent years (see Ref. (Kuroshima *et al.*, 2003; Wilson *et al.*, 2006c) and references therein). Interestingly, it appears that the presence of La stabilizes their growth(Fujita *et al.*, 2003; Lavrov *et al.*, 2004).

2. Role of the reduction process and effects of oxygen stochiometry

Superconductivity in the electron-doped cuprates can *only* be achieved after reducing the as-grown materials (Takagi *et al.*, 1989; Tokura *et al.*, 1989b). Unannealed crystals are never superconducting. This reduction process removes only a small fraction of the oxygen atoms as measured by many techniques(Klamut *et al.*, 1997; Moran *et al.*, 1989; Navarro *et al.*, 2001; Radaelli *et al.*, 1994; Schultz *et al.*, 1996; Tarascon *et al.*, 1989), but has dramatic consequences for its conducting and magnetic properties. The oxygen removed in general ranges

between 0.1 and 2% and generally decreases with increasing cerium content (Kim and Gaskell, 1993; Schultz *et al.*, 1996; Suzuki *et al.*, 1990; Takayama-Muromachi *et al.*, 1989). The exact effect of oxygen reduction is still unknown. Although reduction in principle should contribute electrons, it clearly has additional effects as it is not possible to compensate for a lack of reduction by the addition of extra Ce.

There are many different procedures mentioned in the literature for the reduction process. In general, the single crystals are annealed at high temperature (850 to 1080°C in flowing inert gas or vacuum) for tens of hours to several days. In some of these annealing procedures, the single crystals are also covered by polycrystalline materials, powder and pellets, in order to protect them against decomposition(Brinkmann *et al.*, 1996a). As revealed by a thermogravimetric study(Navarro *et al.*, 2001) of polycrystalline $Nd_{1.85}Ce_{0.15}CuO_{4+\delta}$, the annealing process in small oxygen partial pressures at a fixed temperature (900°) consists of two distinct regimes as shown in Fig. 10: a first one at high pressure leading to non-superconducting materials and a second one at low pressure inducing superconductivity. Interestingly, the separation of these two regimes coincides with the phase stability line between CuO and Cu_2O with their respective Cu^{2+} and Cu^{1+} oxidation states(Navarro *et al.*, 2001). A similar conclusion was reported by Kim and Gaskell (1993) in the phase stability diagram shown in Fig. 11. The coincidence of the Cu^{2+}/Cu^{1+} (CuO/Cu_2O) transition and the onset of superconductivity may be interpreted as a sign that oxygen reduction removes oxygen atoms in the CuO_2 planes leaving behind localized electrons on the Cu sites in proximity to the oxygen vacancies (these Cu ions then have oxidation state +1). Fig. 11 also shows that annealing electron-doped cuprates in lower pressures and/or higher temperatures leads eventually to the decomposition of the materials into a mixture of Nd_2O_3, $NdCeO_{3.5}$ and Cu_2O. As emphasized by Kim and Gaskell (1993) and more recently by Mang *et al.* (2004a) it is interesting that the highest T_c samples are found when the reduction conditions push the crystal almost to the limit of decomposition (Fig. 11). This underlines the difficulty of achieving high quality reduction when it requires exploring annealing conditions on the verge of decomposition.

This annealing and small changes in oxygen content have a dramatic impact on the physical properties. As-grown materials are typically antiferromagnetic with a Néel temperature T_N above 100K for x = 0.15(Mang *et al.*, 2004b; Uefuji *et al.*, 2001). It shows fairly large resistivity with a low temperature upturn (see section III.A). After reduction, antiferromagnetism is suppressed and superconductivity emerges. As mentioned, there is still no consensus on the exact mechanism for this striking sensitivity to oxygen stoichiometry and the annealing process. There are three main (not necessarily exclusive) proposals to explain how as small a change as 0.1% change in oxygen content can have such an impor-
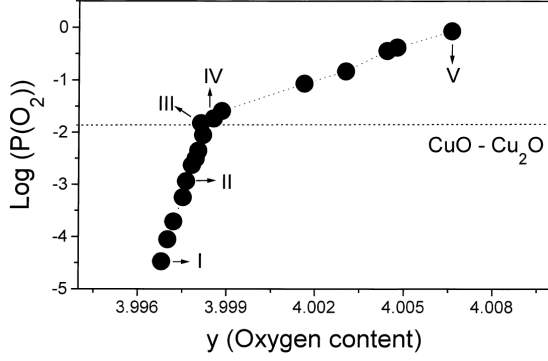
FIG. 10 Equilibrium oxygen partial pressure $p(O_2)$ as a function of oxygen content y for $Nd_{1.85}Ce_{0.15}CuO_y$ at 900°C. The dashed line indicates the Cu^{2+}/Cu^{1+} transition. Samples below this line are superconducting, while those above are not. From Navarro *et al.* (2001).
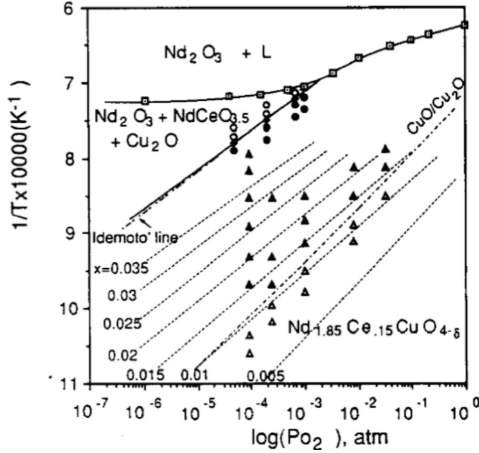

FIG. 11 The phase stability diagram for x=0.15 NCCO. The filled diamond symbols are obtained by thermogravimetric analysis and the filled and open circles are compounds which lie within and outside the field of stability respectively. The filled triangles represent superconducting samples and the open triangles at the bottom represent nonsuperconducting oxides. The dash-dot-dash line is for the Cu_2O - CuO transition and the dotted lines are isocompositions. From Kim and Gaskell (1993).

tant effect, which is similar to the impact of changing the cerium doping by $\Delta x \sim 0.05$ - 0.10.

The first proposal and historically the mostly widely assumed, proposes that apical oxygen atoms, an interstitial defect observed in the T' structure by neutron scattering in Nd_2CuO_4(Radaelli *et al.*, 1994), acts as a strong scattering center (increasing resistivity) and as a source of pair breaking(Xu *et al.*, 1996). By Madelung potential consideration, one expects that apical oxygen may strongly perturb the local ionic potential on the Cu

site immediately below it (Ohta *et al.*, 1991; Torrance and Metzger, 1989). Radaelli *et al.* (1994) showed that reduction leads to a decrease in apical occupancy to approximately 0.04 from 0.1 for the *undoped compounds* (Radaelli *et al.*, 1994). In doped compounds, the oxygen loss is less and almost at the detection limit of the diffraction experiments, however Schultz *et al.* (1996) claimed that their results in $Nd_{1.85}Ce_{0.15}CuO_{4+\delta}$ were consistent with a loss of a small amount of oxygen at the apical position.

However, there are several recent reports that favor a second scenario in which only oxygen ions on the intrinsic sites [O(1) in-plane and O(2) out-of-plane in Fig. 1] are removed. It was found that a local Raman mode which is associated with the presence of apical oxygen is not affected at all by reduction in cerium-doped crystals (Richard *et al.*, 2004; Riou *et al.*, 2001, 2004). This appears to indicate that reduction does not change the apical site's oxygen occupation as originally believed. In the same reports, crystal-field spectroscopy of the Nd or Pr ions on their low symmetry site show also that the excitations associated with the interstitial oxygen ions are not changed by reduction while new sets of excitations appear(Richard *et al.*, 2004; Riou *et al.*, 2001, 2004). These new excitations were naturally related to the creation of O(1) and O(2) vacancies; in-plane O(1) vacancies appear to be favored at large cerium doping. Such a surprising conclusion was first formulated by Brinkmann *et al.* (1996b) from the results of a wide exploration of the cerium and oxygen doping dependence of transport properties in single crystals. In order to explain the appearance of a minimum in resistivity as a function of oxygen content (for a fixed cerium content), these authors proposed that the increasing scattering rate (increasing ρ_{xx}) with decreasing oxygen content for extreme annealing conditions could only be due to an increasing density of defects (vacancies) into or in close proximity to the CuO_2 planes. They targeted the reservoir O(2) as the likely site for vacancies.

Finally, a third scenario has been suggested by recent detailed studies of the microstructure of $Nd_{1.85}Ce_{0.15}CuO_{4+\delta}$. Kurahashi *et al.* (2002) reported the appearance and disappearance of an unknown impurity phase associated with an annealing/re-oxygenation process. Mang *et al.* (2004a) showed that this phase was $(Nd,Ce)_2O_3$, which grew in epitaxial register with material under reduction. This observation has an important repercussions on the interpretation of neutron scattering experiments (Sec. III.F), but it also suggests a scenario for the role of reduction in this family. In Fig. 12, high resolution transmission electron microscopy (HRTEM) images reveal the presence of narrow bands of this parasitic phase about 60Å thick on average extending well over $1\mu m$ along the CuO_2 planes. This phase represents approximately 1% of the entire volume. Since this phase is claimed to appear with reduction and to disappear surprisingly with oxygenation, it was proposed that these zones act as copper reservoirs to cure intrinsic

Cu vacancies in the as-grown CuO_2 planes (Kang *et al.*, 2007; Kurahashi *et al.*, 2002). Within this scenario, during the reduction process Cu atoms migrate from these layers to the NCCO structure to "repair" defects present in the as-grown materials resulting in Cu deficient regions with the epitaxial $(Nd,Ce)_2O_3$ intercalation. Thus, the decreasing density of Cu vacancies in the CuO_2 planes removes pair-breaking sites favoring superconductivity.
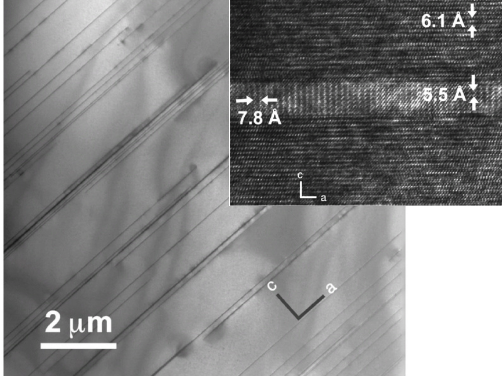

FIG. 12 HRTEM images of a reduced $Nd_{1.84}Ce_{0.16}CuO_{4+\delta}$ single crystal showing the intercalated layers. The $(Nd,Ce)_2O_3$ layers are found to be parallel to the CuO_2 planes. From Mang *et al.* (2004a).

In addition to whatever role it plays in enabling superconductivity, the oxygen reduction process probably also adds charge carriers. Using neutron scattering on TSFZ single crystals with various values of x and annealing conditions to tune the presence of superconductivity, Mang *et al.* (2004b) confirmed Luke *et al.* (1990)'s results for reduced samples, with the $T_N(x)$ line plunging to zero at $x \sim 0.17$ as shown in Fig. 13(a). They found that for unreduced samples $T_N(x)$ extrapolated somewhere around $x = 0.21$. For a fixed x value below 0.17, reduction lowers T_N and the corresponding staggered in-plane magnetization, while promoting superconductivity. The change in $T_N(x)$ with oxygen content was interpreted as a direct consequence of carrier doping i.e. that removal of oxygen acts exactly like cerium substitution (Mang *et al.*, 2004b), because one could simply rigidly shift the as-grown $T_N(x)$ line by $\Delta x \approx 0.03$ to overlay the reduced one. However, the conclusions of Mang *et al.* (2004b) may be called into question by later work of Motoyama *et al.* (2007), who claim that the AF state terminates at x approximately 0.134 for reduced samples. It may be then that this picture of shifting the $T_N(x)$ line by an amount corresponding to the added electron contribution from reduction is only valid at low dopings. Different physics may come into play near superconducting compositions. Arima *et al.* (1993) had found that reduced and unreduced infrared spectra which differed by $\Delta x \approx 0.05$ could be overlayed on top of each other. If one considers the reduction of oxygen content corresponds to an addition of electron carriers to the CuO_2 plane this implies an

oxygen reduction of 0.02-0.03, which is consistent with thermogravimetric studies (Arima *et al.*, 1993).
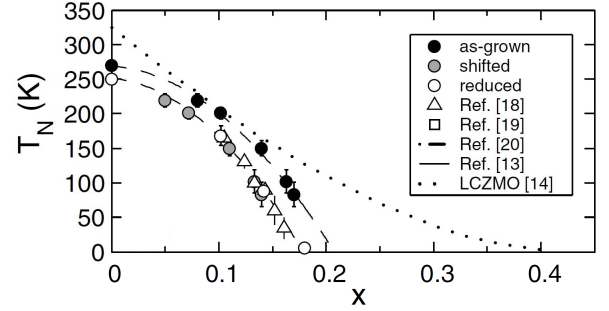

FIG. 13 (a) Phase diagram for $Nd_{2-x}Ce_xCuO_{4+\delta}$ single crystals as determined by neutron scattering. It shows the Néel temperature as a function of cerium content (x). Full circles: as-grown (oxygenated) samples. Open symbols : reduced samples. Grey circles are the data for the as-grown crystals shifted to simulate the carrier density change with reduction. From Mang *et al.* (2004b).

3. Thin films

Thin film growth offers additional control on the stoichiometry of the electron-doped system, for both cerium and oxygen content. Thin films have been grown using most of the usual techniques for the deposition of other cuprates and oxides, including pulsed-laser deposition (PLD) (Gauthier *et al.*, 2007; Gupta *et al.*, 1989; Maiser *et al.*, 1998; Mao *et al.*, 1992) and molecular beam epitaxy (MBE) (Naito *et al.*, 2002, 1997). Both techniques lead to a single crystalline phase with the cerium content accuracies better than 3%. Since film thicknesses are in the range of 10 to 500 nm and the flux and proportion of each constituent can be accurately controlled during deposition, their cerium content is more homogeneous in contrast to single crystals. Moreover, since oxygen diffusion along the c-axis is easier they can be reduced much more uniformly and efficiently with post-annealing periods on the order of one to several tens of minutes(Maiser *et al.*, 1998; Mao *et al.*, 1992). As a consequence of the greater stoichiometry control, superconducting transition widths as small as $\Delta T_c \sim 0.3K$ (from AC susceptibility) have been regularly reported(Maiser *et al.*, 1998). For PLD films, growth in a nitrous oxide (N_2O) atmosphere (Maiser *et al.*, 1998; Mao *et al.*, 1992) instead of molecular oxygen(Gupta *et al.*, 1989) has also been used in an effort to decrease the time needed for reduction. Unlike single crystals, it is possible to finely control the oxygen content using in-situ post-annealing in low pressure of O_2. Within a narrow range of increasing pressure, the resulting films show a gradual decrease of

T$_c$ and related changes in transport properties(Gauthier *et al.*, 2007) (see section III.A.4 and Fig. 25).

Since they are grown on single crystalline substrates with closely matching lattice parameters (LaAlO$_3$, SrTiO$_3$, etc.), films are generally epitaxial with a highly ordered (001) structure with their *c* axis oriented normal to the substrate and providing the needed template for the exploration of in-plane transport and optical properties. Unlike other high-T$_c$ cuprates like YBa$_2$Cu$_3$O$_7$ (Covington *et al.*, 1996), there have been very few reports on films with other orientations. There is evidence that films with (110) and (103) orientations can be grown on selected substrates as confirmed by x-ray diffraction and anisotropic resistivity(Ponomarev *et al.*, 2004; Wu *et al.*, 2006), but the width of their superconducting transition ($\Delta T_c \sim$1K) shows that there is room for further optimisation as compared to c-axis films. These particular film orientations could be of interest for directional tunneling experiments (Covington *et al.*, 1996).

A number of drawbacks to thin films do exist. There has been reports of parasitic phases detected by x-ray diffraction in PLD films(Gupta *et al.*, 1989; Lanfredi *et al.*, 2006; Maiser *et al.*, 1998; Mao *et al.*, 1992) and HRTEM(Beesabathina *et al.*, 1993; Roberge *et al.*, 2009). These phases have been indexed to other crystalline orientations(Maiser *et al.*, 1998; Prijamboedi and Kashiwaya, 2006) or Cu-poor intercalated phases(Beesabathina *et al.*, 1993; Lanfredi *et al.*, 2006; Mao *et al.*, 1992; Roberge *et al.*, 2009), which have also been observed in single crystals(Mang *et al.*, 2004a). These parasitic phases are mostly absent in MBE films(Naito *et al.*, 2002) except for extreme cases when the substrate/film lattice mismatch becomes important. This microstructural difference between MBE and PLD films may be at the origin of the difference in the magnitude of their in-plane resistivity(Naito *et al.*, 2002) as was confirmed recently by Roberge *et al.* (2009) in a new set of films grown with off-stochiometric targets to remove the parasitic phase. Moreover, a significant effect of a strain-induced shift of T$_c$ shown in Fig. 14 has been observed as it decreases with decreasing thickness(Mao *et al.*, 1994).

Strain from the substrate however can also play a crucial role to help stabilizing the T' structure. As mentioned previously, usual bulk LCO grows in the T phase. It was shown by Naito *et al.* that La$_{2-x}$Ce$_x$CuO$_{4+\delta}$ (LCCO) can actually be grown successfully in T' by MBE leading to superconducting materials with T$_c$ as high as 27K(Krockenberger *et al.*, 2008; Naito and Hepp, 2000; Naito *et al.*, 2002). These electron-doped films also exhibit a modified phase diagram with superconductivity extending to x values below 0.10 as shown in Fig. 15, which is fairly similar to that of the (Pr,La)$_{2-x}$Ce$_x$CuO$_{4+\delta}$ compounds(Fontcuberta and Fabrega, 1996; Fujita *et al.*, 2003, 2008a). The LCCO T' phase has also been successfully grown by DC magnetron sputtering(Zhao *et al.*, 2004) and PLD (Sawa *et al.*, 2002).
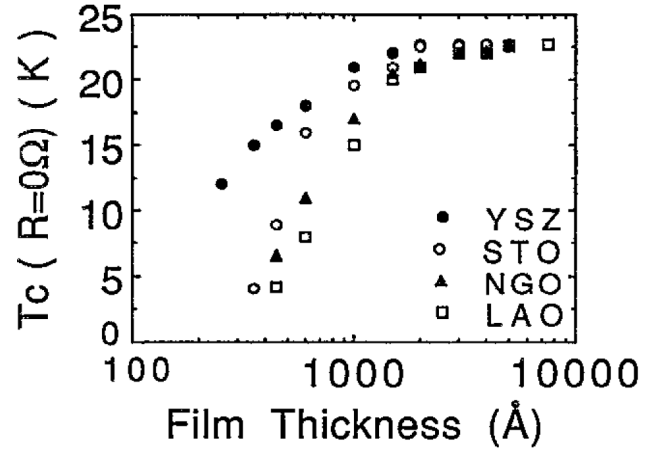
FIG. 14 Variation of the transition temperature with the thickness of the PLD films on various substrates. From Mao *et al.* (1994).
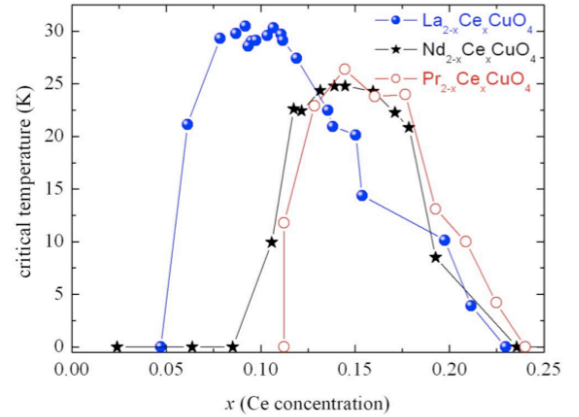
FIG. 15 The transition temperature as a function of cerium doping for T' La$_{2-x}$Ce$_x$CuO$_{4+\delta}$, NCCO, and PCCO thin films grown by MBE. From Krockenberger *et al.* (2008).

Recently, Matsumoto *et al.* (2009) have shown that it is possible to grow *superconducting* thin films of the undoped T' structure RE$_2$CuO$_4$ with RE = Pr, Nd, Sm, Eu, Gd with T$_c$'s as high as 30K using metal-organic deposition (MOD). This is obviously quite a different behavior compared to the abovementioned trends, in particular the observation of superconductivity in Gd$_2$CuO$_4$. The authors claim that a complete removal of all the apical oxygen acting as a scatterer and a source of pair breaking during the reduction process explains the observation of superconductivity in these undoped compound. It could also be that such films are the T' electron-doped analog of superconducting La$_2$CuO$_{4+\delta}$ where δ is excess interstitial 'staged' oxygen. Obviously, such behavior is intriguing and may raise important questions on the actual mechanism of superconductivity and definitely deserves further

investigation.

E. Unique aspects of the copper and rare earth magnetism

Irrespective of the actual superconductivity mechanism, it is clear that the magnetism of the high-T_c superconductors dominates their phenomenology. The magnetic properties of the electron-doped cuprates are unusually complex and intriguing and demand special consideration. On top of the usual AF order of the in-plane Cu spins observed for example in Nd_2CuO_4 at $T_{N,Cu} \sim$ 270K (Mang et $al.$, 2004b), additional magnetism arises from the response of the rare-earth ions to the local crystal field. In the T' structure, rare-earth ions sit on a low-symmetry site (point group C_{4v}) where they experience a local electric field leading to a splitting of their $4f$ atomic levels(Nekvasil and Divis, 2001; Sachidanandam et $al.$, 1997). In Table II, we present the estimated magnetic moment of the most common RE ions used in the n-type family. Some of these magnetic moments are large and interactions between the RE ions and localized Cu spins give rise to a rich set of properties and signatures of magnetic order. As an emblematic example, Nd magnetic moments are known to grow as the temperature is decreased since it is a Kramers doublet (Kramers, 1930), implying a complex temperature-dependent interaction with the Cu sub-lattice and other Nd ions. Among other things, these growing Nd moments at low temperature have an impact on several low temperature properties that are used to characterize the pairing symmetry (see Section IV.A.1). Here we summarize the different magnetic states observed in the electron-doped cuprates. We first focus on the Néel order of the Cu spins, and then follow with a quick overview of its interaction with the RE moments.

	PCO	NCO	SCO	ECO	GCO	PLCO
J	4	9/2	5/2	0	7/2	
effective moment Curie-Weiss	$3.65\mu_B$	$3.56\mu_B$	$0.5\mu_B$	$0\mu_B$	$7.8\mu_B$	
ordered moment measured	$0.08\mu_B$	$1.23\mu_B$	$0.37\mu_B$	$0\mu_B$	$6.5\mu_B$	$0.08\mu_B$
RE Néel Temp. (K)	–	1.7	5.95	–	6.7	–

TABLE II Table summarizing the magnetic properties arising from RE moments. The RE effective moment is from a fit of the high-temperature susceptibility to the Curie-Weiss law while the ordered moment is estimated at low temperature from 0.4 to 10K mostly from neutron scattering experiments. The Néel temperature corresponding to the magnetic ordering of the RE moments was determined using specific heat. From Ghamaty et $al.$ (1989); Lynn and Skanthakumar (2001); Matsuda et $al.$ (1990); Vigoureux (1995) and references therein.

1. Cu spin order

The commensurate antiferromagnetic order of the Cu spins observed for the parent compounds of the electron-doped family is quite different from that of La_2CuO_4, despite close values of $T_{N,Cu} \sim 300K$, similar crystal structures and Cu-O bond lengths[10]. In Fig. 16, we compare the magnetic orders deduced from elastic neutron scattering for both families. Although the magnetic moments lie in the CuO_2 planes for both systems with fairly strong intraplane AF exchange interaction, the in-plane alignment differs as the spins lie along the Cu-O bonds in the case of electron-doped cuprates(Skanthakumar et $al.$, 1993, 1995) while they point at roughly 45° to the Cu-O bond directions for LCO(Kastner et $al.$, 1998). Since the resulting isotropic exchange between planes cancels out due to this in-plane alignment and crystal symmetry, the 3D magnetic order in the case of the electron-doped cuprates is governed by a delicate balance of RE-Cu coupling, superexchange, spin-orbit, and Coulomb exchange interactions (Lynn and Skanthakumar, 2001; Petitgrand et $al.$, 1999; Sachidanandam et $al.$, 1997; Yildirim et $al.$, 1994, 1996). They lead to a spin configuration where the in-plane magnetization alternates in directions between adjacent layers (Lynn and Skanthakumar, 2001; Sachidanandam et $al.$, 1997; Sumarlin et $al.$, 1995) in a non-collinear structure, which is compatible with the tetragonal crystal structure as shown in Fig. 16. For orthorhombic LCO, the spin structure is collinear along the c-axis(Kastner et $al.$, 1998). A noncollinear structure of the Cu spins has been confirmed for NCO, Sm_2CuO_4 (SCO), Eu_2CuO_4 (ECO), PCO and PLCCO using elastic neutron scattering(Chattopadhyay et $al.$, 1994; Lavrov et $al.$, 2004; Skanthakumar et $al.$, 1991, 1993, 1995; Sumarlin et $al.$, 1995). Various different non-collinear Cu spin patterns are stabilized depending on the nature of the RE-Cu interaction. The Cu spin wave spectrum is gapped due to anisotropy by about 5 meV in PCO (Sumarlin et $al.$, 1995) and (Bourges et $al.$, 1992), which can be compared with the anisotropy gap of 2.5 meV in LCO (Peters et $al.$, 1988). Magnetic exchange constants are of the same order as the hole-doped compound. See for instance the two magnon Raman data of Sulewski et $al.$ (1990), who find exchange constants of 128, 108 and 110 meV for LCO, NCO and SCO respectively. These values are similar to those found by fits to spin-wave theory (Sumarlin et $al.$, 1995). One may expect these numbers to be refined as new time-of-flight

---

[10] Note that the maximum Néel temperature of NCO is reported differently in various studies, which is presumably due to a strong sensitivity to oxygen content. For instance, Matsuda et $al.$ (1990) report 255 K, Bourges et $al.$ (1997) report 243 K, whereas Mang et $al.$ (2004b) report $\approx$ 270 K. The maximum reported T_N for PCO appears to be 284 K (Sumarlin et $al.$, 1995). In contrast, the maximum reported T_N for LCO is 320 K (Keimer et $al.$, 1992).
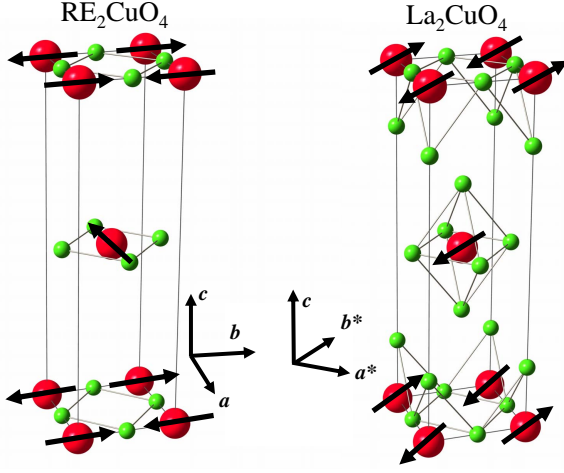
neutron spectrometers come online.

FIG. 16 Cu spin structures for the non-collinear phase of NCO in Phase II at 30 K < T < 75 K or SCO. Nd Phases I and III are equivalent to a structure with the central Cu spin of the figure flipped 180°. (left) The collinear structure of La_2CuO_4 (right). The moments (arrows) are aligned along the nearest neighbor Cu along the Cu-O bonds [(100) and (010)] for RE_2CuO_4 while they point toward the next-nearest neighbor Cu at 45° with respect to the Cu-O bonds [along (110)] for La_2CuO_4.

For at least small cerium doping (x $\sim$ 0.01 - 0.03), non-collinear commensurate magnetic structure persists and has a detectable impact on the electronic properties, in particular electrical transport in large magnetic fields, indicate the coupling of the free charge carriers to the underlying antiferromagnetism (Lavrov $et~al.$, 2004). The carriers couple strongly to the AF structure leading to large angular magnetoresistance (MR) oscillations for both in-plane and out-of-plane resistivity when a large magnetic field is rotated in the CuO_2 plane(Chen $et~al.$, 2005; Lavrov $et~al.$, 2004; Li $et~al.$, 2005a; Wu $et~al.$, 2008; Yu $et~al.$, 2007a). Although originally thought to be related to magnetic domains (Fournier $et~al.$, 2004), these oscillations are now believed to be related to the first-order spin-flop transition at a magnetic field of order 5T observed in magnetization and elastic neutron scattering measurements(Cherny $et~al.$, 1992; Plakhty $et~al.$, 2003). At that field applied along the Cu-O bonds, the in-plane and c-axis MRs change dramatically as the magnetic structure changes from the non-collinear order to a collinear one (Cherny $et~al.$, 1992; Lavrov $et~al.$, 2004) as shown in Fig. 17. Similar signatures but with smaller amplitudes were also observed at higher doping(Fournier $et~al.$, 2004; Yu $et~al.$, 2007b) for as-grown non-superconducting $x = 0.15$ PCCO crystals indicating that AF correlations are preserved over a wide range of

doping in these as-grown materials[11]. The effect of doping on the Cu spin structure is dealt with in more detail below.
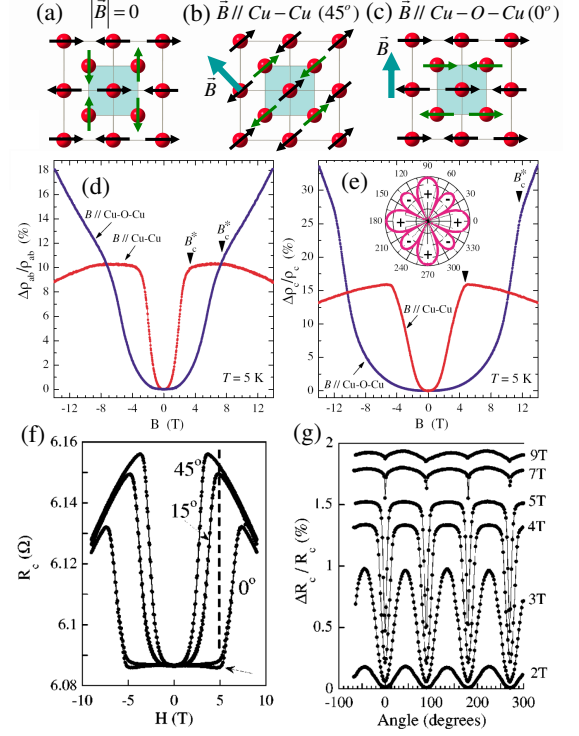
FIG. 17 In-plane Cu spin structures for (a) zero applied magnetic field and a large magnetic field beyond the spin-flop field applied at (b) 45° and (c) 0° with respect to the Cu-O-Cu bonds. (d) in-plane and (e) c-axis magnetoresistance of lightly doped $Pr_{1.3}La_{0.7}Ce_xCuO_4$ ($x = 0.01$) single crystals at 5K for a magnetic field applied along the (100) or (010) Cu-O bonds and along the (110) Cu-Cu direction (from Lavrov $et~al.$ (2004)). (f) c-axis magnetoresistance at 5K for non-superconducting as-grown $Pr_{1.85}Ce_{0.15}CuO_4$ as a function of field for three selected in-plane orientations (0, 15 and 45°) and (g) as a function of angle at selected magnetic fields below and above the spin-flop field of 5T (from Ref. Fournier $et~al.$ (2004)).

2. Effects of rare earth ions on magnetism

Additional magnetism arises from the large magnetic moments that can exist at the RE sites. Because of their different spin magnitudes different RE ions lead to very different magnetic structures, some of which with well-defined order. For more details on the magnetism of the

---

[11] Recently, Jin $et~al.$ (2009) found no four-fold effect in the in-plane angular magnetoresistance of thin films of T' LCCO. This is interesting in view of the fact that La has no RE moment and the role that RE-Cu coupling plays in determining the stability of the particular forms of non-collinear order as discussed below.

rare earths in these compounds, see the excellent review by Lynn and Skanthakumar (2001). We will discuss the various cases separately, but briefly.

In the case of RE = Nd, the fairly strong magnetic moment of the Nd ion was found early on to couple to the Cu spins sub-lattice(Cherny *et al.*, 1992; Lynn *et al.*, 1990). A number of successive Cu spin transitions can be observed in Nd_2CuO_4 with decreasing temperature using neutron scattering(Endoh *et al.*, 1989; Matsuda *et al.*, 1990; Matsuura *et al.*, 2003; Skanthakumar *et al.*, 1993, 1995). These transitions are seen as sharp changes of intensity for specific magnetic Bragg reflections (see Fig. 18) and reveal a growing interaction between the Cu and Nd spins as the temperature decreases. First, Cu spins order below $T_{N1} \approx 276$ K in a non-coliinear structure defined as phase I. At still lower temperatures there are two successive spin reorientations transitions at $T_{N2} = 75$ K (shown in Fig. 16) and again at $T_{N3} = 30$ K. At T_{N2} the Cu spins rotate by 90 degree about the c axis (phase II). The rotation direction is opposite for two successive Cu planes. At T_{N3} they realign back to their initial direction (phase III). Phases I and III are identical with the exception that the Nd magnetic moment is larger at low temperature since it is a Kramers doublet. Finally (inset of Fig. 18) additional Bragg intensity is detected below 1K arising from the AF ordering of the Nd moments in the same structure as the Cu. This feature is a clear indication that substantial Nd-Nd interaction is present on top of the Nd-Cu ones that lead to the transitions at T_{N2} and T_{N3}. These reorientations are the result of the competition between three energy scales : 1) the Cu-Cu ; 2) the Nd-Nd ; and 3) the Nd-Cu interactions. Since the Nd moment grows with decreasing temperature, the contributions from 2) and 3) grow accordingly.
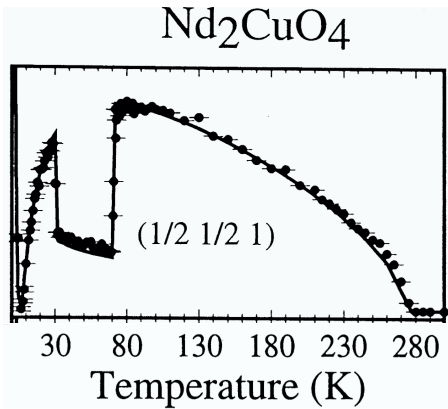

FIG. 18 Elastic neutron scattering intensity as a function of temperature at the (1/2 1/2 0) reciprocal space position for as-grown Nd_2CuO_4. The sudden changes in intensity occur at the transition from Type-I to Type-II, then Type-II to Type-III Nd-Cu moment configurations with decreasing temperature. From Lynn and Skanthakumar (2001) and references therein.

The reordering and the low temperature interaction of

Nd with Cu can be observed in various other ways. The reorientations were first observed by muon spin resonance and rotation experiments (Luke *et al.*, 1990) and were confirmed later on by crystal-field spectroscopy(Jandl *et al.*, 1999), and more recently by ultrasound propagation experiments(Richard *et al.*, 2005b). The growing competition between the three energy scales leads also to a wide variety of anomalies at low temperature(Cherny *et al.*, 1992; Li *et al.*, 2005a,b; Richard *et al.*, 2005a,b; Wu *et al.*, 2008).

The larger moments at the Sm sites in SCCO order quite differently than in NCCO. Sm_2CuO_4 shows a well-defined antiferromagnetic order below $T_{N,Sm} = 6$K with a transition easily observed by specific heat (Cho *et al.*, 2001; Dalichaouch *et al.*, 1993; Hundley *et al.*, 1989), magnetization(Dalichaouch *et al.*, 1993) and elastic neutron scattering(Sumarlin *et al.*, 1992). Here ferromagnetically aligned in-plane RE moments orient themselves antiferromagnetically along the c-axis (Sumarlin *et al.*, 1992). This special arrangement should lead to no significant coupling between the Sm and the Cu moments. A lack of coupling is supported by the absence of spin transitions in the Cu moments like in NCO. The non-collinear Cu spin order is the same as NCO in Phase II.

$Pr_{2-x}Ce_xCuO_4$ and $Pr_{1-y-x}La_yCe_xCuO_{4\pm\delta}$ exhibit the same non-collinear c-axis spin order as Phase I NCO. At low doping the magnetic moments at the Pr site have been shown to be small, but non-zero due to exchange mixing with a value of roughly $0.08\mu_B/Pr$ (Lavrov *et al.*, 2004; Sumarlin *et al.*, 1995). Due to the small moment the magnetic transitions associated with RE-Cu and RE-RE interaction in NCO do not appear to take place in PCO (Matsuda *et al.*, 1990). Nevertheless, there is evidence for Pr-Pr interactions in both the in-plane and out-of-plane directions(Sumarlin *et al.*, 1995) mediated by Cu spins. This is supported by the onset of a weak polarization of the Pr moments at the Néel temperature for Cu spin ordering ($T_N \sim 270$K for Pr_2CuO_4 and $T_N \sim 236$K for $Pr_{1.29}La_{0.7}Ce_{0.01}CuO_{4\pm\delta}$). Despite this induced magnetic moments at the Pr sites, PCO and PLCCO have a very small uniform magnetic susceptibility on the order of 1 % that of NCCO(Fujita *et al.*, 2003). This is a great advantage in the study of their magnetic and superconducting properties without the influence from the RE moments. For instance, the small DC susceptibility of PCCO as compared to NCCO allows precision measurements of the superconducting penetration depth and symmetry of the order parameter (see Section IV.A.5).

Finally, there has been less effort directed towards Eu_2CuO_4 (ECO) and Gd_2CuO_4 (GCO), but both systems present evidence of weak ferromagnetism, albeit with different sources. There are indications that the small size of the rare earth ions and subsequent lattice distortions are playing a crucial role in both cases(Alvarenga *et al.*, 1996; Mira *et al.*, 1995; Thompson *et al.*, 1989). For GCO, specific heat and magnetization anomalies at 9K demonstrate antiferromagnetic order on the Gd sublattice with signatures very similar to

SCO. It is believed that like SCO, the Gd RE spins orient ferromagnetically in-plane and anti-ferromagnetically out-of-plane. A notable difference however is that the Gd spin direction is in-plane. A large anisotropy of the DC susceptibility with its onset at the Cu spin order temperature ($\sim 260K$) indicates the contribution of a Dzyaloshinskii-Moriya (DM) interaction between the Cu spins leading to the weak ferromagnetism. For ECO, there have been reports of weak ferromagnetism Cu correlations(Alvarenga *et al.*, 1996), but clearly no RE ordering as the Eu ion is non-mangnetic. Eu exhibits the same non-collinear Cu spin order as SCO due also to an absence of a RE-Cu coupling.

III. EXPERIMENTAL SURVEY

A. Transport

1. Resistivity and Hall effect

The ab-plane electrical resistivity (ρ_{ab}) and Hall effect for the n-type cuprates have been studied by many groups. The earliest work found $\rho_{ab} = \rho_o + AT^2$ at optimal doping over the temperature range from T_c to approximately 250K (Tsuei *et al.*, 1989) and a temperature dependent Hall number in the same temperature range (Wang *et al.*, 1991). The T^2 behavior is in contrast to the linear in T behavior found for the optimal hole-doped cuprates. Although $\rho \sim T^2$ is a behavior consistent with electron-electron scattering in a normal (i.e., Fermi liquid) metal, it is quite unusual to find such behavior at temperatures above 20K. This suggested that there is some anomalous scattering in the n-type cuprates, but that phonons do not make a major contribution to the resistivity up to 250K.

The general doping and temperature evolution of the ab-plane resistivity is illustrated in ρ_{ab} data on NCCO crystals as shown in Fig. 19 (left) (Onose *et al.*, 2004). These data shows that even at rather low doping (i.e., in the AFM state) a "metallic"-like resistivity is observed at higher temperatures which becomes "insulator-like" at lower temperatures. The temperature of the minimum resistivity decreases as the doping increases and it extrapolates to less than T_c near optimal doping. The development of "metallic" resistivity at low doping is consistent with the ARPES data, which shows electron states near the Fermi level around $(\pi, 0)$ for $x > 0.04$ (Armitage *et al.*, 2002) and an increased Fermi energy density of states in other regions of the Brillouin zone (BZ) as doping increases (see ARPES discussion below). Recent work (Dagan *et al.*, 2007) showed a scaling of the T^2 resistivity above 100K for dopings x=0.11 to 0.19. Sun *et al.* (2004) emphasizes that despite the upturns in the ab-plane resistivity, the mobility over much of the temperature range is still quite high in even lightly doped AFM samples (5 cm^2/V · sec). They interpreted this as consistent with the formation of metallic stripe domains.
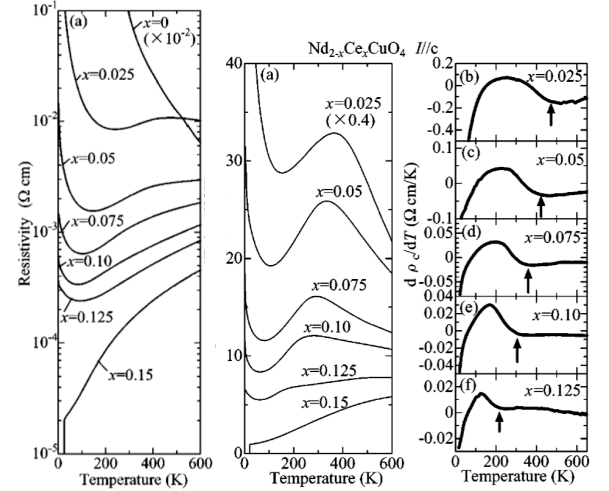

FIG. 19 (left) Temperature dependence of the in-plane resistivity of NCCO crystals at various doping levels x. (center) The temperature dependence of the out-of-plane resistivity of NCCO at various doping. (right) The temperature derivative of the out-of-plane resistivity ($d\rho_c/dT$). The nominal T^* is indicated by the arrow. From Onose *et al.* (2004).

The dependence of the high field "insulator to metal" crossover with Ce doping at low temperature ($T \ll T_c$, $H \gg H_{c2}$) has been studied in detail by Fournier *et al.* (1998a) and Dagan *et al.* (2004). Important aspects of their data to note are: 1) the linear in T resistivity from 35mK to 10K at one particular doping ($x = 0.17$ in (Fournier *et al.*, 1998a)), 2) the crossover from insulator to metal occurs at a $k_F l$ value of order 20, 3) the resistivity follows a T^2 dependence for all Ce doping at temperatures above the minimum or above 40K, and 4) the resistivity follows T^β with $\beta < 2$ in the temperature range less than 40K for samples in which there is no resistivity minimum.

The doping dependent "insulator to metal" crossover in the resistivity data appears very similar to behavior found in the hole-doped cuprates (Boebinger *et al.*, 1996). However, electron-doped cuprates are much more convenient to investigate such physics as much larger magnetic fields are needed to suppress the superconductivity in p-type compounds. In the few cases that sufficient fields have been used in the hole-doped compounds the low temperature upturn in resistivity occurs in samples near optimal doping with similar $k_F l$ values of order 20. The behavior of the resistivity at low T below is very similar in hole and electron-doped materials ($\rho \sim \log 1/T$) but the exact cause of the upturn is not known at present. Work by Dagan *et al.* (2005b) suggests that it is related to the onset of AFM in the $n-$doped cuprates. Disorder may also play a role in the appearance of the resistivity upturn (and metal-insulator crossover) as recently suggested for hole-doped cuprates (Rullier-Albenque *et al.*, 2008).

An insulator-metal crossover can also be obtained at a fixed Ce concentration by varying the oxygen reduction conditions (Fournier *et al.*, 1997; Gantmakher *et al.*, 2003; Gauthier *et al.*, 2007; Gollnik and Naito, 1998; Jiang *et al.*, 1994; Tanda *et al.*, 1992). Under these conditions the crossover occurs at a $k_F l$ value of order unity and near a 2D sheet resistance (treating a single copper-oxide plane as the 2D conductor) appropriate for a superconductor to insulator transition (SIT) (Goldman and Markovic, 1998). Some authors have interpreted their data as giving convincing evidence for a SIT (Tanda *et al.*, 1992) while others have argued against this view (Gantmakher *et al.*, 2003). More detailed study will be needed to resolve this issue.
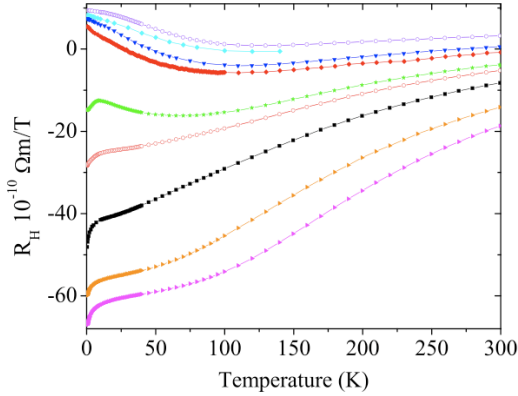

FIG. 20 The Hall coefficient R_H in $Pr_{2-x}Ce_xCuO_4$ films as function of temperature for the various doping levels (top to bottom): x = 0.19, x = 0.18, x = 0.17, x = 0.16, x = 0.15, x = 0.14, x = 0.13, x = 0.12, and x = 0.11 (Dagan and Greene, 2004).
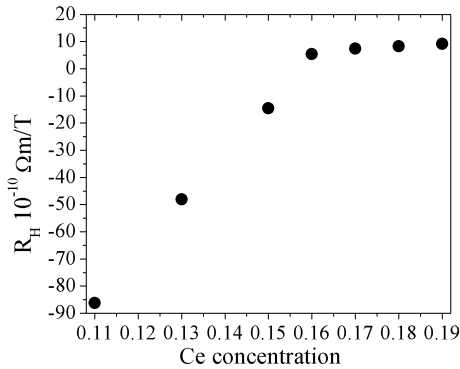

FIG. 21 The Hall coefficient at 0.35K (using the data from Fig. 20). A distinct kink in the Hall coefficient is seen between $x = 0.16$ and $x = 0.17$. The error on the concentration is approximately 0.003. The error in R_H comes primarily from the error in the film thickness; it is approximately the size of the data points(Dagan *et al.*, 2004).

The doping and temperature dependence of the normal state $(H > H_{c2})$ ab-plane Hall coefficient (R_H) are shown in Fig 20 (Dagan *et al.*, 2004) for PCCO films.

These recent results agree with previous work (Fournier *et al.*, 1997; Gollnik and Naito, 1998; Wang *et al.*, 1991) but cover a wider temperature and doping range. Notable features of these data are the significant temperature dependence for all but the most overdoped samples and the change in sign from negative to positive near optimal doping at low temperature. This latter behavior is most dramatically seen by plotting R_H versus Ce doping at 350mK (the lowest temperature measured) as shown in Fig 21 (Dagan *et al.*, 2004). At this low temperature one expects that only elastic scattering will contribute to ρ_{xy} and R_H and thus the behavior seen in Fig. 21 suggests some significant change in the Fermi surface near optimal doping. Qualitatively, the behavior of R_H is consistent with the Fermi surface evolution shown *via* ARPES in Fig. 28, which suggests that a SDW-like band structure rearrangement occurs, which breaks up the Fermi surface into electron and hole regions (Armitage, 2001; Armitage *et al.*, 2001b; Matsui *et al.*, 2007; Zimmers *et al.*, 2005). A mean field calculation of the $T \rightarrow 0$ limit of the Hall conductance showed that the data are qualitatively consistent with the reconstruction of the Fermi surface expected upon density wave ordering (Lin and Millis, 2005). A convincing demonstration of such a FS reconstruction is the recent observation of Shubinkov-de Haas oscillations in NCCO by Helm *et al.* (2009), who found quantum oscillations consistent with a small FS pocket for $x = 0.15$ and a large FS for $x = 0.17$. We will discuss these results and two-band transport in more detail below (Secs. IV.G and IV.H).

The Hall angle (θ_H) follows a behavior different than the well-known T^2 dependence found in the *p*-doped cuprates. Several groups (Dagan *et al.*, 2007; Fournier *et al.*, 1997; Wang *et al.*, 2005; Woods *et al.*, 2002) have found an approximately T^4 behavior for $\cot \theta_H$ in optimal *n*-type cuprates. Dagan *et al.* (2007) (but not Wang *et al.* (2005)) find the power law dependence on temperature of $\cot \theta_H$ becomes less than 4 for underdoped materials but cannot be fit to any power law for overdoped. This change may be related to the purported QCP which occurs near x=0.16, but more detailed studies will be needed to verify this. The unusual power law dependence for the Hall angle agrees with the theoretical model of Abrahams and Varma (2003) at optimal doping. These authors showed that the Hall angle is proportional to the square of the scattering rate if this rate is measured by the T dependence of the ab-plane resistivity. Since a resistivity proportional to T^2 is found at all dopings for T above 100K (Dagan *et al.*, 2007), but the Hall angle does not vary as T^4 for all dopings in this range this theoretical model can only be valid at optimal doping. The origin of the temperature dependence for other dopings is not understood.
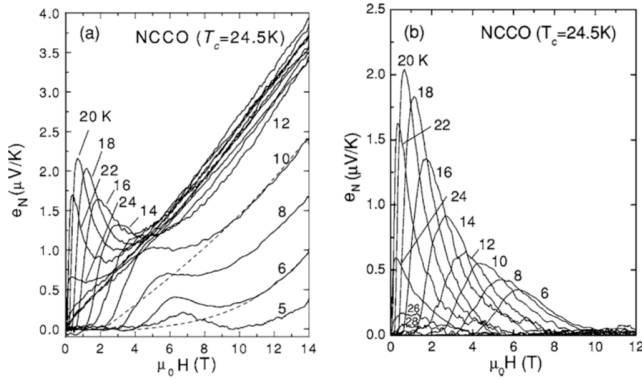
FIG. 22 (a) The experimentally measured Nernst signal e_N vs H in optimally doped $x = 0.15$ NCCO and $T_c = 24.5$ K from temperatures of 5 K to 30 K. The dashed lines are fits of the high-field segments to a quasiparticle term of the form $e_N^n(T, H) = c_1 H + c_3 H^3$ as detailed in Ref. (Wang $et\ al.$, 2006b). (b) The vortex contribution to the Nernst effect e_N^s as extracted from the data of panel (a) as also detailed in Ref. (Wang $et\ al.$, 2006b).

2. Nernst effect, thermopower and magnetoresistance

The Nernst effect has given important information about the normal and superconducting states in the cuprates. It is the thermal analog of the Hall Effect, whereby a thermal gradient in the $\hat{x}$ direction and a magnetic field in the $\hat{z}$ direction, induces an electric field in the $\hat{y}$ direction. The induced field comes from the thermal drift of carriers and their deflection by the magnetic field or by the Josephson mechanism if moving vortices exist (for details see Wang $et\ al.$ (2006b) and references therein). In conventional superconductors one finds a large Nernst signal in the superconducting state from vortex motion and a very small signal in the normal state from the carriers. Boltzmann theory predicts a zero Nernst signal from a single band of carriers with energy independent scattering (Sondheimer, 1948; Wang $et\ al.$, 2001). Surprisingly, a large Nernst signal is found in the normal state of both electron and hole-doped cuprates. However, the origin of this signal appears to be quite different in the two cases. For p-type cuprates the large normal state Nernst effect has been attributed to superconducting fluctuations in a large temperature region above T_c, especially in the range of doping where the pseudogap exists (Wang $et\ al.$, 2001). For n-type cuprates the large Nernst signal was attributed to two types of carriers in the normal state(Balci $et\ al.$, 2003; Fournier $et\ al.$, 1997; Gollnik and Naito, 1998; Jiang $et\ al.$, 1994; Li $et\ al.$, 2007a). The evidence for a difference in behavior between p- and n-type cuprates is persuasive.

The Nernst signal as a function of magnetic field at various temperatures for optimal-doped NCCO is shown in Fig. 22 (Wang $et\ al.$, 2006b). A vortex signal non-linear in field is seen for $H < H_{c2}$ for $T < T_c$ whereas for $T > T_c$ a linear in H normal state dependence is found. This is behavior typical of low-T_c superconductors, i.e.,

the non-linear superconducting vortex Nernst signal disappears for $T > T_c$ and $H > H_{c2}$. There is evidence for a modest temperature range of superconducting (SC) fluctuations just above T_c in the underdoped compositions (Balci $et\ al.$, 2003; Li and Greene, 2007). However, these data contrasts dramatically from the data found in most hole-doped cuprates. In those cuprates there is a very wide parameter range (in both T and H) of Nernst signal due to SC fluctuations, interpreted as primarily vortex-like phase fluctuations(Wang $et\ al.$, 2006b). This interpretation of the large Nernst signal above T_c in the hole-doped cuprates is supported by recent theory (see Podolsky $et\ al.$ (2007) and references therein)[12]. The inference that phase fluctuations are larger in hole-doped cuprates than the electron-doped is consistent with "phase fluctuation" models and estimates from various material parameters (Emery and Kivelson, 1995).

However, the magnitude of the Nernst signal is large for $T > T_c$ for both $n-$ and p-type cuprates for most doping levels above and below optimal doping. The temperature dependence of the Nernst signal at 9T ($H\|_c > H_{c2}$) for several PCCO dopings is shown in Fig. 23 (Li and Greene, 2007). It was found that at fixed temperature the signal is linear in field, so that it can be assigned to normal state carriers. In contrast, in the p-doped materials the field dependence is non-linear for a wide T range above T_c, which suggests a SC origin for the large Nernst signal. As mentioned earlier, the large signal in the normal state of the $n-$doped materials has been interpreted as arising from two carrier types. This is consistent with the ARPES and optics data, which shows that both electron and hole regions of the Fermi surface (FS) exist for dopings near optimal (Armitage, 2001; Armitage $et\ al.$, 2001b; Zimmers $et\ al.$, 2005). See Li and Greene (2007) for a thorough discussion on these points. Recent theoretical work of Hackl and Sachdev (2009), shows that the effects of FS reconstruction due to SDW order can give a magnitude and doping dependence of the low temperature Nernst signal that agrees with the measurements of Li and Greene. However, further work will be needed for a quantitative explanation of the complete temperature dependence of the Nernset signal shown in Fig. 23.

The ab-plane thermoelectric power (TEP) of the $n-$doped cuprates has been measured by many authors (Budhani $et\ al.$, 2002; Fournier $et\ al.$, 1997; Gollnik and Naito, 1998; Li $et\ al.$, 2007c; Li and Greene, 2007; Wang $et\ al.$, 2005; Xu $et\ al.$, 1996) (for work prior to 1995 see Fontcuberta and Fabrega (1996)). To date, there has been few quantitative interpretation of the temperature, doping and field dependence of the TEP in the cuprates (Gasumyants $et\ al.$, 1995; Sun $et\ al.$, 2008). However,

----

[12] This interpretation has been recently challenged by a detailed Nernst effect measurement in Eu-LSCO as a function of Sr doping for which the Nernst signature assigned to the onset of the PG disappears at a doping where superconductivity persists (Cyr-Choiniere $et\ al.$, 2009).
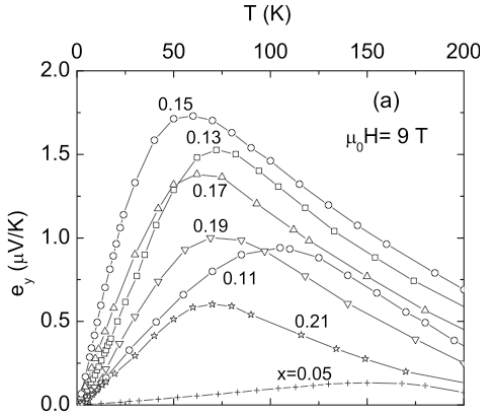
FIG. 23 Temperature dependence of normal-state Nernst signal at $\mu_0 H = 9$ T for all the doped PCCO films from Li and Greene (2007).

a number of qualitative conclusions have been reached for the n-type compounds. The doping dependence of the low temperature magnitude and sign of the TEP is consistent with the evolution of the FS from electron-like at low doping to two-carrier-like near optimal doping to hole-like at the highest doping. For example, at low doping ($x = 0.03$) the low-T TEP is "metallic-like" and negative (Hagen et $al.$, 1991; Wang et $al.$, 2005) even though the resistivity has an "insulator-like" temperature dependence. This reveals the presence of significant density of states at Fermi level and is consistent with the small pocket of electrons seen in ARPES and a possible 2D localization of these electrons at low temperature. A recent detailed study of the doping dependence of the low-temperature normal state TEP has given additional evidence for a quantum phase transition (QPT) that occurs near x=0.16 doping (Li et $al.$, 2007c). It is remarkable that the appearance of superconductivity in the compounds is almost coincident with the appearance of a hole-like contribution to their transport. Note that the existence of holes in this otherwise electron-doped metal is essential to the existence of superconductivity within some theories (Hirsch and Marsiglio, 1989).

The unusual and large magnetoresistance found in the $n-$doped cuprates has been studied by a number of authors. The most striking behavior is the large negative MR found for optimal and underdoped compositions at low temperature ($T < T_{min}$). This has been interpreted as arising from 2D weak localization(Fournier et $al.$, 2000; Hagen et $al.$, 1991), 3D Kondo scattering from Cu^{+2} spins in the CuO_2 plane (Sekitani et $al.$, 2003), or scattering from unknown magnetic entities associated with the AFM state(Dagan et $al.$, 2005b). At low doping ($x \leq 0.05$) the MR is dominated by an anisotropic effect, largest for $H\|c$, and can reasonably be interpreted as an orbital 2D weak localization effect (especially since the ab-plane resistivity lead to $k_F l < 1$ and follows a log T temperature dependence). At dopings between x=0.1 and 0.17 the negative MR is dominated by an isotropic

effect and the orbital contribution becomes weaker as the doping increases.

Dagan et $al.$ (2005b) have isolated the isotropic MR and shown that it disappears for $x \sim 0.16$. This suggests that this MR is associated with a QCP occurring at this doping and is caused by some heretofore unknown isotropic magnetic scattering related to the AFM state. Dagan et $al.$ (2005b) also showed that the isotropic negative MR disappears above a T_{min} and this suggests that the upturn in the ab-plane resistivity is associated with the AFM state. Recent high-field transverse magnetoresistance measurements (i.e., H applied along the c-axis)(Li et $al.$, 2007b) and angular magnetoresistance measurements (H rotated in the ab plane)(Yu et $al.$, 2007b) support the picture of a AFM to PM quantum phase transition near $x = 0.165$ doping [13].

3. c-axis transport

The temperature and field dependence of the DC c-axis resistivity has been studied in single crystals by many authors [for earlier work see the review of Fontcuberta and Fabrega (1996)]. The behavior of the $n-$doped c-axis resistivity is quite different than that found in p-type cuprates. Some representative data as a function of doping and temperature is shown in Fig 19 (center) and (right) (Onose et $al.$, 2004). This may reflect the different gapped parts of the FS in $n-$ and p-type, since c-axis transport is dominated by specific FS dependent matrix elements (Andersen et $al.$, 1995; Chakravarty et $al.$, 1993) which peak near (π,0) and the SDW-like state in the n-type as opposed to the unknown nature of the pseudogap in the p-type. As shown by Onose et $al.$ (2004) (Fig 19) the c-axis resistivity has a distinct change from "insulating-like" to "metallic-like" below a temperature T^*, near the temperature at which the SDW gap is observed in optical experiments (Onose et $al.$, 2004; Zimmers et $al.$, 2005), before going insulating at the lowest temperature for the most underdoped samples. Below T^*, the T dependence of the c-axis and ab-plane resistivity are similar although with an anisotropy ratio of 1000-10000. This behavior is strikingly different than that found in p-type cuprates. In p-type compounds the c-axis resistivity becomes "insulator-like" below the pseudogap temperature while the ab-plane resistivity remains "metallic" (down to T_{min} in underdoped compositions (Ando et $al.$, 2001). The interpretation of the c-axis resistivity upturn as a signature of the pseudogap formation in p-type cuprates has been reinforced by magnetic field studies, where the T^* is suppressed by

---

[13] The existence of a QPT associated with the termination of the AF state at this doping is at odds with the work of Motoyama et $al.$ (2007) who concluded via inelastic neutron scattering that the spin stiffness ρ_s fell to zero at a doping level of $x \approx 0.134$ (Fig. 35a). This issue is discussed in more detail in Sec. IV.H.

field in a Zeeman-splitting-like manner (Shibauchi *et al.*, 2001). A recent field-dependent study of *n*-type SCCO near optimal doping has been interpreted as for the *p*-type cuprates (Kawakami *et al.*, 2006, 2005). However, the T* found in this work is much lower than that found in the optical studies, casting some doubt on this interpretation. In contrast, Yu *et al.* (2006) have interpreted their field dependent c-axis resistivity results in terms of superconducting fluctuations. The origin of the c-axis resistivity upturn and its relation to the ab-plane upturn requires more investigation.

4. Effects of disorder on transport

Disorder has a significant impact on the *ab*-plane transport properties of the cuprates. This has been studied most extensively in the *p*-type materials [Alloul *et al.* (2009); Rullier-Albenque *et al.* (2008) and references therein]. The results obtained to date on the *n*-type cuprates seem to agree qualitatively with those found in *p*-type. Disorder in these compounds is caused by the cerium doping itself, the annealing process (where oxygen may be removed from some sites), doping of Zn or Ni for Cu, and by ion or electron irradiation. The general behavior of $\rho_{ab}(T)$ as defects are introduced by irradiation is shown in Fig. 24 (Woods *et al.*, 1998) for optimally doped NCCO. The general trends are: T_c is decreased, the residual resistivity increases while the metallic T dependence at higher T remains roughly the same, and an "insulator-like" upturn appears at low temperature. As the irradiation level increases the superconductivity is eventually completely suppressed and the upturn dominates the low temperature resistivity. The decrease of T_c is linearly proportional to the residual resistivity and extrapolates to zero at $R_\square$ per unit layer of 5-10 kΩ, which is near the quantum of resistance for Cooper pairs (Woods *et al.*, 1998), similar to behavior seen in YBCO (Rullier-Albenque *et al.*, 2003). Defects introduced by irradiation do not appear to change the carrier concentration since the Hall coefficient is basically unchanged. Oxygen defects (vacancies or impurity site occupancy) can cause both changes in carrier concentration and in impurity scattering. In two recent papers (Gauthier *et al.*, 2007; Higgins *et al.*, 2006) have studied the effects of oxygen on the Hall effect and ρ_{ab} of slightly overdoped PCCO. As oxygen is added to an optimally prepared x=0.17 film the $\rho(T)$ behavior (Fig. 25) becomes quite similar to the $\rho(T)$ data under increased irradiation as shown in Fig 24. Gauthier *et al.* (2007) attribute the role of oxygen not to changing the carrier concentration significantly but to having a dramatic impact on the quasiparticle scattering rate. Higgins *et al.* (2006) compare resistivity and Hall effect for films with oxygen variation and with irradiation. They conclude that oxygen changes both the carrier concentration and the scattering rate. The exact origin of all these disorder effects on T_c and the transport properties has not yet

been determined. However, various recent proposals (Alloul *et al.*, 2009; Rullier-Albenque *et al.*, 2008) for how defects influence the properties of hole-doped cuprates are probably valid for $n-$doped cuprates as well.
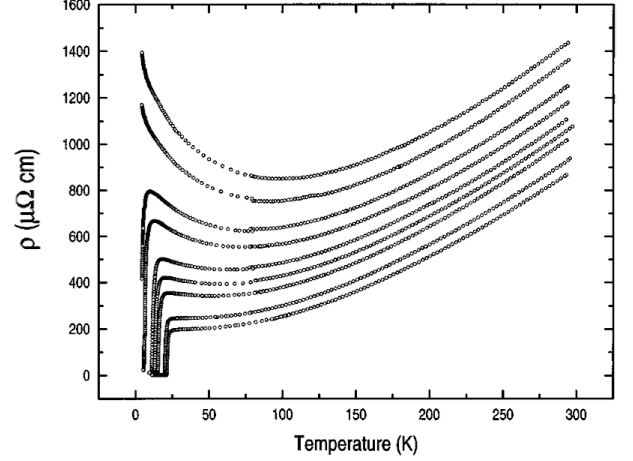
FIG. 24 Temperature dependent resistivity for NCCO $x = 0.14$ films damaged with He$^+$ ions. From bottom to top, ion fluences are 0, 0.5, 1, 1.5, 2, 2.5, 3, 4, and 4.5 $*10^{14}$ ions/cm^2. From Woods *et al.* (1998).
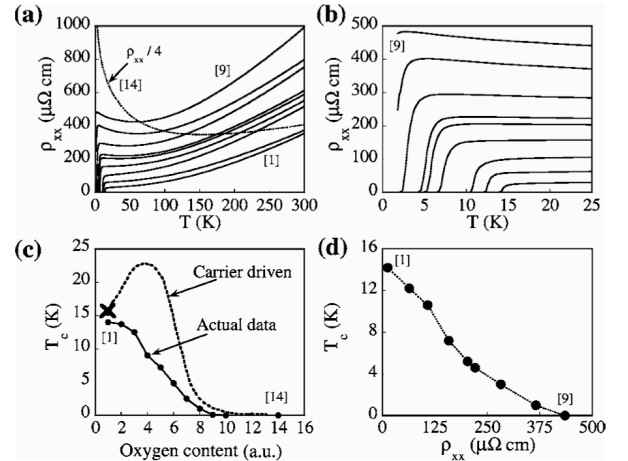
FIG. 25 (a) Resistivity as a function of temperature for $x = 0.17$ thin films with various oxygen contents. (b) Low-temperature region of the same data. (c) Critical temperature T_c as a function of oxygen content for x = 0.17 for films grown in oxygen full circles, solid line is a guide to the eye. Cross: highest T_c under N$_2$O. Dashed line: schematic of the expected behavior for a carrier driven T_c (see (Gauthier *et al.*, 2007)). (d) T_c as a function of the in-plane resistivity at 30 K. From Gauthier *et al.* (2007).

5. Normal state thermal conductivity

In general the ab plane thermal conductivity κ of the $n-$type materials resembles that of the hole-doped compounds. In the best crystals an increase in κ_{ab} is found at T_c and can be attributed to a change in electron-phonon scattering as in the hole-doped cuprates (Yu *et al.*, 1992). The most significant κ data has been taken below T_c at temperatures down to 50mK for $H > H_{c2}$. A striking result was the report of a violation of the Wiedemann-Franz law below 1K in slightly underdoped PCCO (Hill *et al.*, 2001) samples, which was interpreted as a possible signature of a non-Fermi liquid normal state. This will be discussed in more detail in section IV.F below.

Sun *et al.* (2004) measured the *ab*-plane and c-axis thermal conductivity for underdoped crystals of $Pr_{1.3-x}La_{0.7}Ce_xCuO_4$. They found that the low T phonon conductivity κ has a very anisotropic evolution upon electron doping; namely, the low-T peak of κ_c was much more rapidly suppressed with doping than the peak in κ_{ab}. Over the same doping range the ab-plane resistivity develops a "high mobility" metallic transport in the AFM state. They interpret these two peculiar transport features as evidence for stripe formation in the underdoped n-type cuprates. Essentially the same features are seen in underdoped p-type cuprates (Ando *et al.*, 2001) where the evidence for stripe formation is stronger.

In the underdoped n-type compounds, phonons, magnons and electronic carriers (quasiparticles) all contribute to the thermal conductivity. Only at very low temperature it is possible to separate out the various contributions. However since phonons and magnons both have a T^3 variation, it has been necessary in undoped and AFM Nd_2CuO_4 to use the magnetic field induced spin-flop transition to switch on and off the acoustic Nd magnons and hence separate the magnon and phonon contributions to the heat transport (Li *et al.*, 2005b).

B. Tunneling

Tunnelling experiments on $n-$doped cuprates have been difficult and controversial. This is likely due to the problems associated with preparing adequate tunnel barriers and the sensitivity of the electron-doped material to preparation conditions. Some of these difficulties have been discussed by Yamamoto *et al.* (1997). Improvements have been made in recent years and we will focus on the most recent results. It is important to keep in mind that the surface layer being probed by tunnelling is very thin (of order the coherence length) and the surface may have properties different than the bulk because the oxygen reduction conditions at the barrier may not be the same as the interior. Experiments that show a bulk T_c or H_{c2} in their tunnel spectra are most likely to represent properties of the bulk. We only discuss what appear to be measurements representative of the bulk. Tunnelling experiments have been performed on films and

single crystals using four methods; natural barriers with metals such as Pb, Sn, Al, In, and Au, point contact spectroscopy with Au or Pt alloy tips, bi-crystal grain boundary Josephson junctions (GBJ) on STO substrates, and Scanning Tunnelling Measurements (STM). Thus, these experiments are either in superconductor-insulator-superconductor (SIS), superconductor-insulator-normal metal (SIN), or SN configurations.
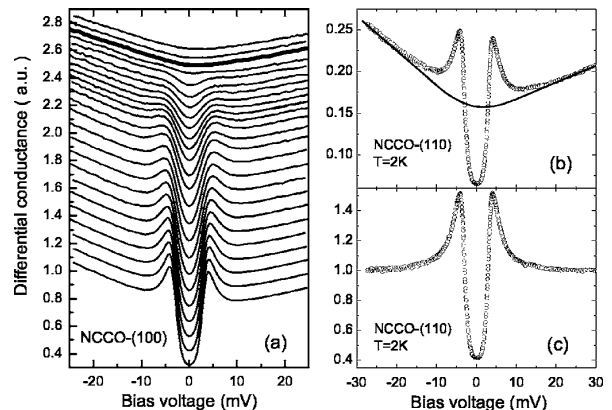

FIG. 26 Raw data of the directional tunneling measurements for optimally doped NCCO. (a) Temperature dependence of the tunnelling spectra measured along (100) direction. The curves have been shifted for clarity. The temperature increases from the bottom upwards in steps of 1 K (from 2 to 22 K) and then 2 K (from 22 to 30 K). The thick solid line denotes the data at 26 K which is approximately T_c. (b) An illustration of the constructed normal conductance background above T_c. (c) The normalized 2 K spectrum in the (110) direction. From Shan *et al.* (2005).

The aim of the tunnelling experiments has been to determine the SC energy gap, find evidence for bosonic coupling, the SC pairing symmetry, and evidence for a normal state gap (pseudogap). Typical quasi-particle conductance $G(V)=dI/dV$ spectra on optimal-doped NCCO using point contact spectroscopy are shown in Fig 26. Similar spectra are found for Pb/PCCO natural barrier junctions (Dagan *et al.*, 2005b) and GB junctions (Alff *et al.*, 1998a; Chesca *et al.*, 2005). The main features of the $n-$doped tunnel spectra are: prominent coherence peaks (which give an energy gap of order 4 meV at 1.8K), an asymmetric linear background $G(V)$ for voltage well above the energy gap, a characteristic 'V' shape, coherence peaks which disappear completely by $T \approx T_c$ at H=0 (and by $H \approx H_{c2}$ for T=1.8K), and typically the absence of a zero bias conductance peak (ZBCP) at V=0. Issues related to the determination of the order parameter are discussed in more detail in Sec. IV.A.2 below.

Tunneling experiments have also found evidence for a normal state energy gap with energy ~5 meV at 2K, which is of the same order as the superconducting gap energy (Biswas *et al.*, 2001; Kleefisch *et al.*, 2001). This normal state gap (NSG) is found in SIS experiments and point contact spectroscopy experiments which probe the
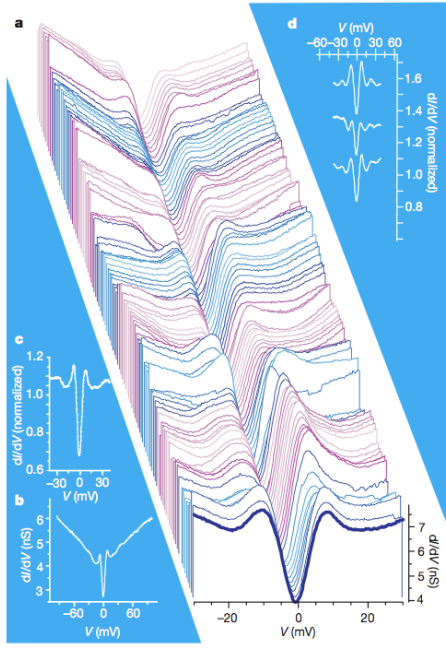
FIG. 27 (Color) (a) A 200 Å linecut that shows the variations in coherence peak heights and gap magnitude (Δ) The spectra have been offset for clarity. The gap magnitude, which is defined as half the energy separation between the coherence peaks varies from 5 meV to 8 meV in this linecut. (b) A representative ± 100-mV range (dI/dV) spectrum that illustrates the dominate 'V'-shaped background. (c) The spectrum in (b) after division by a linear V-shaped function. (d) Additional examples of dI/dV spectra that demonstrate the clearly resolved coherence peaks and modes resulting from a V-shaped division. From Niestemski *et al.* (2007).

ab-plane by applying a c-axis magnetic field greater than H_{c2}. The low energy NSG is distinctly different than the high energy (~ 100 meV) "pseudogap" seen in ARPES and optical experiments (Armitage *et al.*, 2001b; Zimmers *et al.*, 2005) and most recently in a local tunneling spectroscopy experiment (Zimmers *et al.*, 2007a). The high energy gap is suggested to be associated with SDW-like gapping of the FS. The origin of the low energy NSG is not conclusively determined at this time. Proposed explanations include: Coulomb gap from electron-electron interactions (Biswas *et al.*, 2001); hidden and competing order parameter under the SC dome which vanishes near optimal doping (Alff *et al.*, 2003); and preformed SC singlet pairs (Dagan *et al.*, 2005a). Dagan *et al.* (2005a) claim to rule out the Coulomb gap and competing order scenarios. They find that the NSG is present at all dopings from 0.11 to 0.19 and the temperature at which it disappears correlates with T_c, at least on the overdoped side of the SC dome. However, the NSG also survives to surprisingly high magnetic fields and this is not obviously explained by the preformed pair (SC fluctuation) picture either (Biswas *et al.*, 2001; Kleefisch *et al.*, 2001; Yu *et al.*, 2006). In contrast, Shan *et al.* (2008b) reported that the NSG and the SC gap are distinct entities at all

dopings, which is consistent with the 'two-gap' scenario in the underdoped p-type cuprates.

Very few STM studies have been performed on the n-type compounds as compared to the extensive measurements on the hole-doped materials (Fischer *et al.*, 2007). Niestemski *et al.* (2007) reported reproducible high resolution STM measurements of $x = 0.12$ PLCCO ($T_c = 24$ K) (Fig. 27). The extremely inhomogeneous nature of doped transition metal oxides makes spatially resolved STM an essential tool for probing local energy scales. Statistics of the superconducting gap spatial variation were obtained through thousands of mappings in various regions of the sample. Previous STM measurements on NCCO gave gaps of 3.5 to 5 meV, but no obvious coherence peaks (Kashiwaya *et al.*, 1998). The linecut (Fig. 27a) shows spectra that vary from ones with sharp coherence peaks to a few with more pseudogap-like features and no coherence peaks. Although most measured samples at this doping (9 out of 13 mappings) gave gaps in the range of 6.5 - 7.0 meV, the average gap over all measured maps was 7.2 ± 1.2 meV, which gives a $2\Delta/k_B T_c$ ratio of 7.5, which is consistent with a strong coupling scenario. However, this ratio strongly differs with point contact (Shan *et al.*, 2008a) and SIS planar tunneling results Dagan and Greene (2007) as well as Raman scattering (Qazilbash *et al.*, 2005), which have given a $2\Delta/k_B T_c$ ratio of approximately 3.5 for PCCO at $x = 0.15$. This may be pointing to a $2\Delta/k_B T_c$ ratio that varies significantly with x as seen in the p-type compounds (Deutscher, 1999).

The STM spectra have a very notable 'V' shaped higher energy background. When this background is divided out a number of other features become visible. Similar to the hole-doped compounds (Fischer *et al.*, 2007), the claim is that features in the tunneling spectra can be related to an electron-bosonic mode coupling at energies of 10.5 ± 2.5 meV. This energy is consistent with an inferred magnetic resonance mode energy in PLCCO (Wilson *et al.*, 2006a) as measured by inelastic neutron scattering as well as low-energy acoustic phonon modes, but differs substantially from the oxygen vibrational mode identified *via* STM as coupling to charge in BSCCO(Lee *et al.*, 2006a). The analysis of Niestemski *et al.* (2007) of the variation of the local mode energy and intensity with the local gap energy scale was interpreted as being consistent with an electronic origin of the mode consistent with spin-excitations rather than phonons.

C. ARPES

The first angle resolved photoemission (ARPES) studies of the electron-doped cuprates appeared in adjoining 1993 Physical Review Letters (Anderson *et al.*, 1993; King *et al.*, 1993). Both reported the existence of a large Fermi surface centered around the (π, π) position in $Nd_{1.85}Ce_{0.15}CuO_4$. It had a volume that scaled approximately with the number of charge carriers thereby
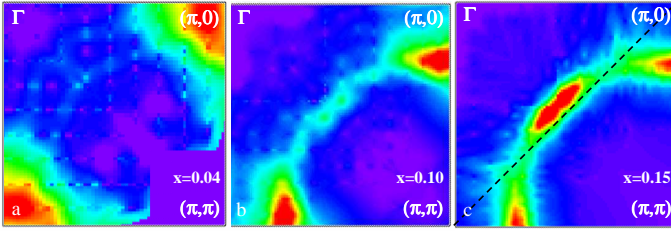
FIG. 28 (Color) Fermi surface plot: (a) $x = 0.04$,(b) $x = 0.10$, and (c) $x = 0.15$. EDCs integrated in a 60meV window (-40meV,+20meV) plotted as a function of $\vec{k}$. Data were typically taken in the displayed upper octant and symmetrized across the zone diagonal. Adapted from Armitage *et al.* (2003).

satisfying Luttinger's theorem and a shape similar to existing band structure calculations (Massidda *et al.*, 1989). It was pointed out by King *et al.* (1993) that the extended Van Hove states at the $(\pi, 0)$ point located at approximately 350 meV binding energy contrasted with the hole-doped case, where these states were located within tens of meV of E_F. It was speculated at that time that the lack of a large near-E_F density of states may be responsible for some of the very different hole and electron-doped compound properties. Subsequent calculations also emphasize this difference as a route to explaining the differences between electron- and hole-doped compounds (Manske *et al.*, 2001b).

Recently there have been a number of electron-doped ARPES studies which take advantage of dramatic advances in photoemission technology, including the vastly improved energy (< 10 meV) and momentum ($< 1\%$ of π/a for a typical cuprate) resolution as well as the utility provided by parallel angle scanning in *Scienta*-style detectors (Armitage *et al.*, 2001a,b, 2003, 2002; Matsui *et al.*, 2005a,b; Sato *et al.*, 2001). The contribution of ARPES to the study of the superconducting order parameter is detailed below in Sec. IV.A.4.

In studies concerning the overall electronic structure, the large Fermi surface around the (π, π) position was confirmed in the later high resolution studies by Armitage *et al.* (2001b), but it was also found that there are anomalous regions on the Fermi surface where the near E_F intensity is suppressed (Fig. 28(c)). A detailed look at the Energy Distribution Curves (EDCs) through the suppressed region of the Fermi surface reveals that the electronic peak initially approaches E_F, but then monotonically loses weight despite the fact that its maximum never comes closer than 100 meV to E_F. Such behavior with broad features and suppression of low-energy spectral weight is similar to the high-energy pseudogap seen in the extreme underdoped p-type materials (Marshall *et al.*, 1996), although in the present case it is observed to be maximum near $(0.65\pi, 0.3\pi)$ and not at $(\pi, 0)$, the maximum of the d-wave functional form.

As noted by Armitage (2001); Armitage *et al.* (2001b) these regions of momentum space with the unusual low-

energy behavior fall close to the intersection of the underlying FS with the antiferromagnetic Brillouin zone (AFBZ) boundary, as shown by the dashed lines in Fig. 28(c). This suppression of low-energy spectral weight and the large scattering rate in certain regions on the FS is reminiscent of various theoretical predictions that emphasize a coupling of charge carriers to a low-energy collective mode or order parameter with characteristic momentum (π, π). A simple phase space argument shows that it is those charge carriers which lie at the intersection of the FS with the AFBZ boundary that suffer the largest effect of anomalous (π, π) scattering as these are the only FS locations that can have low-energy coupling with $q \approx (\pi, \pi)$. These regions were those later inferred by Blumberg *et al.* (2002); Matsui *et al.* (2005b) to have the largest superconducting gap as well. Although it is the natural choice, due to the close proximity of antiferromagnetism and superconductivity, this low-energy scattering channel need not be antiferromagnetic for the role played by the AFBZ boundary to hold; other possibilities such as d-density wave exist (Chakravarty *et al.*, 2001). It is only necessary that its characteristic wave vector be (π, π). These heavily scattered regions of the FS have been referred to in the literature as "hot spots" (Hlubina and Rice, 1995). It has been suggested that the large backscattering felt by charge carriers in the hot spots is the origin of the pseudogap in the underdoped hole-type materials[14].

The gross features of the ARPES spectra in the optimally doped n-type compounds can be approximately described by a two band model exhibiting long range SDW order (Armitage, 2001; Matsui *et al.*, 2005a; Park *et al.*, 2007). Such a model reflects the folding of the underlying band structure across the AFBZ boundary and hybridization between bands *via* a potential $V_{\pi,\pi}$ (see Sec. IV.G below). It gives the two components (peak-dip-hump (PDH) structure) in the spectra near the $(\pi, 0)$ position (Armitage *et al.*, 2001a, 2003; Matsui *et al.*, 2005a; Sato *et al.*, 2001), the location of the hot spots, and perhaps more subtle features showing back folded sections of the FS. As will be discussed below in more detail, such a scenario does shed light on a number of other aspects of n-type compounds, including one long outstanding issue in transport where both hole and electron contributions to the Hall coefficient have been resolved (Dagan *et al.*, 2004; Fournier *et al.*, 1997; Gollnik and Naito, 1998; Wang *et al.*, 1991). Additionally, such a scenario

---

[14] We should mention that the observation of "hot-spots" has been disputed (Claesson *et al.*, 2004) in an ARPES study that used higher energy photons, thereby gaining marginally more bulk sensitivity over other measurements. It is unclear however, whether this study's relatively poor energy resolution (140 meV as compared to ≈ 10 meV in other studies) coupled with a large near-E_F integration window (136 meV) can realistically give any insight into this matter regarding low energy spectral suppression when the near E_F suppression is observed primarily at energies below 70 meV.
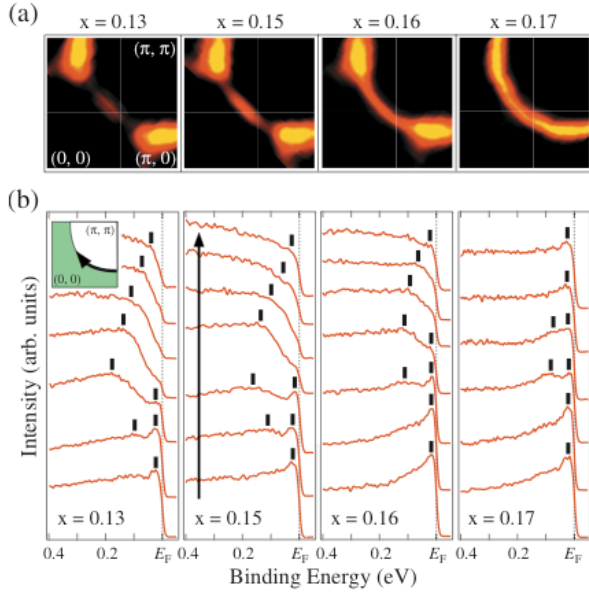
FIG. 29 (Color) (a) Doping dependence of the FS in NCCO, obtained by plotting the ARPES intensity integrated over ± 20 meV with respect to E_F as a function of momentum. The intensity is normalized to that at 400 meV binding energy and symmetrized with respect to the $(0,0)$ - (π, π) direction. (b) Doping dependence of a set of ARPES spectra measured at several k points around the FS at several dopings. From Matsui *et al.* (2007).

FIG. 30 Temperature dependence of the ARPES spectrum of NCCO (x = 0.13) measured in the "hot spot" (at the position on the Fermi surface shown by a circle in the inset) where the two component structure is observed clearly. The solid straight lines on the spectra show the linear fits to the high-energy region (0.20.5 eV) showing that it doesn't change with temperature. From Matsui *et al.* (2005a).

appears to be consistent with aspects of the optical data (Zimmers *et al.*, 2005).

Matsui *et al.* (2005a) found that the lineshape in these "hot-spots" in NCCO x=0.13 have a strong temperature dependence, giving more credence to the idea that this suppression is due to spin density wave formation (Matsui *et al.*, 2005a). As shown in Fig. 29, Matsui *et al.* (2007) also demonstrate that the hot-spot effect largely goes away by x=0.17 doping in NCCO, with the high-energy pseudogap filling in at the antiferromagnet-superconductor phase boundary. The magnitude (Δ_{PG}) and the temperature (T^*) at which the pseudogap fills in shows a close relation to the effective magnetic coupling energy (J_{eff}) and the spin-correlation length (ξ_{AF}), respectively again suggesting the magnetic origin of the pseudogap and hot-spot effect. As seen in Fig. 30, it was shown that the lowest energy sharp peak had largely disappeared by the Néel temperature $T_N = 110K$ for the $x = 0.13$ sample while the near-E_F spectral weight suppression persisted until a higher temperature scale. These authors also claimed that the overall k-space dependence of their data was best understood within a spin density wave model with a non-uniform SDW gap in k-space.

In contrast, Park *et al.* (2007) in a comprehensive BZ wide study on SCCO claim that it was not that the gap was non-uniform, but that there appeared to be remnant bands refl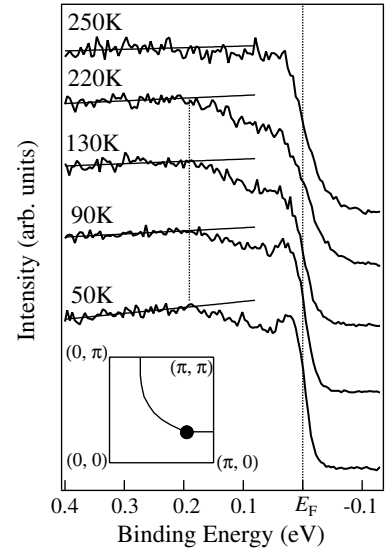ective of the bare band structure that dispersed uninterrupted through the AFBZ. Through a simple model they showed how this might be reflective of short-range magnetic ordering. Moreover, these authors showed that the hot-spot effect in SCCO is so strong that the zone diagonal states were actually pushed below E_F raising the possibility of nodeless d-wave superconductivity in this compound. This observation may shed light on reports of nodeless superconductivity found in PCCO films grown on buffered substrates (Kim *et al.*, 2003). Such effects had been theoretically anticipated (Das *et al.*, 2007; Yuan *et al.*, 2006a).

Richard *et al.* (2007) have made a detailed comparison of the ARPES spectra of as-grown and oxygen-reduced PCCO and PLCCO materials. They claim that to within their error bars (estimated by us to be approximately 1 %) neither the band filling nor the tight binding parameters are significantly affected by the reduction process in which a small amount of oxygen was removed ($\approx 1\%$). They demonstrated that the main observable effect of reduction was to remove an anisotropic leading edge gap around the Fermi surface.

Much recent discussion regarding ARPES spectra of the hole-doped cuprates has concerned a "kink" or mass renormalization in the electronic dispersion which has been found ubiquitously in the p-type materials (at $\approx$ 70 meV) (Bogdanov *et al.*, 2000; Lanzara *et al.*, 2001). Its origin is a matter of much current debate (Campuzano *et al.*, 2004; Damascelli *et al.*, 2003), with various phononic or magnetic scenarios being argued for or against. Its existence on the electron-doped side of the phase diagram has been controversial. Armitage *et al.*

(2003) claimed that there was no kink feature along the zone diagonal and that the zone diagonal was best characterized by a smooth concave downward dispersion. Although apparent mass renormalizations were found along the zone face (Armitage *et al.*, 2003; Matsui *et al.*, 2005a; Sato *et al.*, 2001), it was claimed these were related to the "hot spot" effect and therefore of different origin than the *p*-type kink[15]. More recently, it has been claimed that a weak kink around 60 - 70 meV in fact exists along both relevant symmetry directions in NCCO with even a stronger kink found in SCCO (Liu *et al.*, 2008; Park *et al.*, 2008; Schmitt *et al.*, 2008). Coupling constants are reported in the range of 0.2-0.8 which is a similar magnitude as in the hole doped compounds (Lanzara *et al.*, 2001). All these groups make the point that unlike the hole-doped compounds where magnetic modes and phonons exist at similar energies, in the electron-doped cuprates the magnetic resonance mode appears to be found at much lower energies (Wilson *et al.*, 2006a; Yu *et al.*, 2008; Zhao *et al.*, 2007). A kink has also been found in recent soft x-ray angle resolved photoemission (Tsunekawa *et al.*, 2008). As phonon anomalies associated with the oxygen half-breathing mode are found in the 60 meV energy range, the mass renormalization is reasonably associated with electron-phonon interaction. As discussed below (Sec. IV.D), this work gives additional evidence that the electron-phonon interaction is not so different on the two sides of the phase diagram.

Another item of recent interest in the photoemission spectra of cuprates is that of an almost universal 'high-energy kink' in the dispersion of the hole-doped cuprates that manifests as an almost vertical drop in the dispersion curve around 300 meV (Graf *et al.*, 2007; Meevasana *et al.*, 2007; Ronning *et al.*, 2005). Pan *et al.* (2006) found a similar anomaly in PLCCO at energies around 600 meV that they termed a quasiparticle coherence-incoherence crossover. Moritz *et al.* (2009) showed a drop in the dispersion of $x = 0.17$ NCCO around 600 meV that confirms a high energy kink in the electron-doped cuprates found at an energy approximately twice that of the hole-doped compounds. Pan *et al.* (2006) claimed that this result ruled out the super exchange interaction J as the driving interaction as the energy scales of the high energy kink were so different, yet the scale of J so similar between the two sides of the phase diagram. Through their quantum Monte Carlo calculations within the one band Hubbard model Moritz *et al.* (2009) assign the anomaly to a crossover when following the dispersion from a quasi-particle-like band at low binding energy near-E_F to an incoherent

Hubbard band-like features. These features are at higher energies in the electron-doped cuprates due to the presence of the charge transfer gap on the occupied side of the spectrum.

We should point out that although the general "hot-spot" phenomena are exhibited in all studied electron-doped cuprates close to optimal doping, the details can be considerably different. In NCCO (Matsui *et al.*, 2005a) and PLCCO (Matsui *et al.*, 2005b) there is an actual peak at E_F with greatly reduced spectral weight in the hot spot. In contrast in underdoped SCCO (Park *et al.*, 2007) and ECCO (Ikeda *et al.*, 2009b, 2007) there is a clear gap at the hot spot and no sign of near-E_F quasi-particle. These differences may be directly related to changes in chemical pressure caused by different rare earth ion radii and its effect on band structure parameters like the t'/t ratio or indirectly by chemical pressure by causing the extent of antiferromagnetism (and for instance the strength of $V_{\pi,\pi}$) to be different. Note that these differences may also be due to the differences in the optimal reduction conditions for different compounds, which are known to exist as one goes from PCCO to SCCO and ECCO. Ikeda *et al.* (2009b) performed a systematic ARPES study of the Nd, Sm, Eu series of rare earth substitutions, which due to decreasing ion size corresponds to increasing chemical pressure. In- and out-of-plane lattice constants as well as T_c decreases across this series (Markert *et al.*, 1990; Uzumaki *et al.*, 1991). Ikeda *et al.* found that the underlying Fermi surface shape changes considerably (Fig. 31) and exhibits significantly less curvature when going from Nd to Eu, which is consistent with a decreasing $|t'/t|$ ratio. Fitting to a tight bonding band structure with nearest and next-nearest neighbors they found $|-t'/t| = 0.40, 0.23$, and 0.21 for NCCO, SCCO, and ECCO, respectively[16]. The decreasing ratio was associated with a strong dependence on the in-plane lattice constant. The hot spot effects also change considerably within this series as seen by the increasing suppression of the near-E_F intensity in Fig. 31. Ikeda *et al.* attributed this to an increasing $V_{\pi,\pi}$, which was associated with the decreasing out-of-plane lattice constant and a strengthening of 3D antiferromagnetism. The $V_{\pi,\pi}$ undoubtedly increases across this series, however at least part of the differences in the hot-spot phenomena may be due to whether or not different $x = 0.15$ samples near the AF phase boundary exhibit long range SDW order or just strong fluctuations of it. One expects that a true gap forms at the hot spot only in the case of true long range order. These issues are discussed in more detail in

---

[15] Armitage *et al.* (2003) gave effective Fermi velocities that did not include the effects of any kinks, by using a $\omega \to 0$ extrapolation of a function fitted to the dispersion at higher energy ($\omega > 100$ meV). Analyzing the data in this fashion gives velocities of $\vec{v}_F^{0eff}(\omega \to 0) = 4.3 \times 10^5$ m/sec (2.3 eV·$a/\hbar\pi$) for the Γ-(π,π) FS crossing and $\vec{v}_F^{0eff}(\omega \to 0) = 3.4 \times 10^5$ m/sec (1.8 eV·$a/\hbar\pi$) for the $(\pi,0)$-(π,π) FS crossing.

[16] Note that, fitting not just to the FS positions, but also v_F Armitage (2008) find slightly different values for $x = 0.15$ NCCO. Using a dispersion relation $E_k = \mu + 2t(\cos k_x + \cos k_y) + 4t'(\cos k_x \cos k_y)$ he gets parameters $\mu = 0.081 \pm 0.02$, $t = -0.319 \pm 0.015$, and $t' = 0.099 \pm 0.01$ (all in eV) when one includes the mass renormalization from the kink and $\mu = 0.04 \pm 0.04$, $t = -0.31 \pm 0.01$, and $t' = 0.068 \pm 0.01$ when one does not.
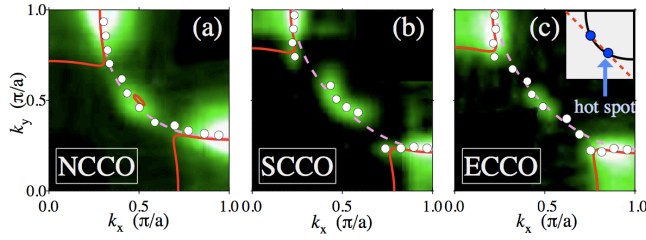
FIG. 31 (Color) ARPES intensity within ± 30 meV of E_F plotted in the BZ quandrant space for nominally $x = 0.15$ NCCO, SCCO, and ECCO. White circles show the peak positions of momentum distribution curves (MDCs) at E_F, indicating the underlying Fermi surface. Solid red curves and dashed pink curves show the Fermi surface obtained by tight-binding fit to the ARPES data assuming the AFM and para-magnetic band structures, respectively. The FS exhibit significantly less curvature in ECCO as compared to NCCO. Inset: Schematic diagram of the hot spot. Black curve and red dashed line represent the Fermi surface and the antiferro-magnetic Brillouin zone boundary, respectively. From Ikeda *et al.* (2009b).

Sec. IV.G below.

Finally, with regards to the doping dependence, Armitage *et al.* (2002) showed dramatic changes of the ARPES spectra as the undoped AF parent compound NCO is doped with electrons away from half filling towards the optimally doped metal as shown in Fig. 28. It was found that the spectral weight was lost from the charge transfer band (CTB) or lower Hubbard band feature observed by Ronning *et al.* (1998); Wells *et al.* (1995) and transferred to low energies as expected for a doped Mott insulator (Meinders *et al.*, 1993). One interesting feature about performing a photoemission study on an electron-doped material is that - in principle - the doping evolution of the Mott gap is observable due to it being below the chemical potential (See Fig. 4). In hole-doped compounds, such information is only available *via* inverse photoemission. At the lowest doping levels, $x = 0.04$, it was observed that the electrons reside in small 'Fermi' patches near the $(\pi,0)$ position, at an energy position near the bottom of the upper Hubbard band (as inferred from optics (Tokura *et al.*, 1990)). This is consistent with many models in which the lowest electron addition states to the insulator are found near $(\pi,0)$ (Tohyama, 2004). Importantly mid-gap spectral weight also develops. At higher dopings the band near $(\pi,0)$ becomes deeper and the midgap spectral weight becomes sharper and moves toward the chemical potential, eventually contacting the Fermi energy and forming the large Fermi surface observed in the highest-T_c compounds.

These observations showed for the very first time, at least phenomenologically, how the metallic state can develop out of the Mott insulator. Note that there was some evidence that the CT gap was renormalized to smaller energies upon electron doping as the energy from the CTB onset to the chemical potential (0.8 eV) is smaller than the energy onset of the optical gap in the undoped

compound. However, these data clearly showed that the CT gap does *not* collapse or close with electron addition (Kusko *et al.*, 2002) and instead 'fills in.' A gap that mostly fills in and does not collapse with doping is also consistent with optical experiments (Arima *et al.*, 1993; Onose *et al.*, 2004). Such behavior is reproduced within slave-boson approaches (Yuan *et al.*, 2005) as well as numerical calculations within the Hubbard model (Aichhorn *et al.*, 2006; Kancharla *et al.*, 2008; Macridin *et al.*, 2006; Senechal and Tremblay, 2004; Tohyama, 2004) that show most features of the FS development can be reproduced with a doping independent CT gap.

D. Optics

As in the hole-doped cuprates, optical and infrared spectroscopy has contributed greatly to our knowledge of electronic dynamics in the n-type materials. The first detailed comparison between electron- and hole-doped insulating parent compounds was reported by Tokura *et al.* (1990). Interestingly, they found an onset in the optical conductivity around 1 eV and a peak around 1.5 eV, which is about 0.5 eV smaller than that found in the analogous T phase La_2CuO_4. This optical gap was associated with a charge transfer (CT) gap of 1 - 1.5 eV in the T' structure compound Nd_2CuO_4. The smaller charge transfer gap energy was correlated with the lack of oxygen in the apical oxygen-free T' structure compound and its effect on the local Madelung potential.

In one of the first detailed studies of the optical spectra's doping dependence Arima *et al.* (1993) found in $Pr_{2-x}Ce_xCuO_4$ mid-gap states that grew in intensity with doping similar to, but slightly slower than the hole doped compounds. They also found a remnant of the CT band at doping levels almost as high as optimal doping. More recently the infrared and optical conductivity has been investigated by a number of groups (Homes *et al.*, 1997; Lupi *et al.*, 1999; Onose *et al.*, 1999, 2001, 2004; Singley *et al.*, 2001; Wang *et al.*, 2006a; Zimmers *et al.*, 2005). It is found generally, that upon rare earth substitution, a transfer of spectral weight from the CT band to lower frequencies takes place. A broad peak in the mid-infrared (4000-5000 cm^{-1} or approximately 0.6 eV) is first formed at low doping levels, with a Drude component emerging at higher dopings. Fig. 32 shows typical behavior. It bears a passing resemblance to the hole-doped compounds except that despite softening with Ce doping the mid-IR band can still be resolved as a distinct feature in the highest T_c samples (x=0.15).

Other important differences exist. For instance, Onose *et al.* (2001, 2004) found that this notable 'pseudogapped' mid-infrared feature ($\Delta_{pg} = 0.2 - 0.4$ eV) appeared directly in the optical conductivity spectrum for metallic but non-superconducting crystals of $Nd_{2-x}Ce_xCuO_4$ below a characteristic temperature T^*. They found that $\Delta_{pg} = 10k_BT^*$ and that both decrease with increasing doping. Moreover, the low temperature Δ_{pg} was
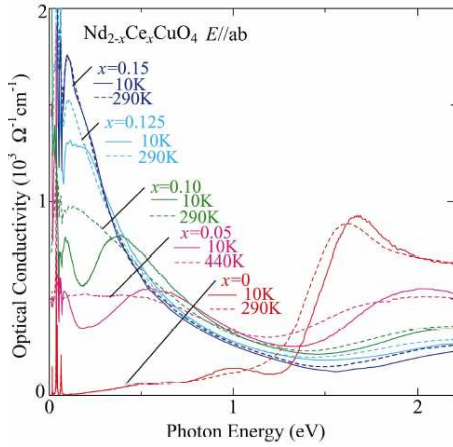
FIG. 32 (Color) Doping dependence of optical conductivity spectra for $Nd_{2-x}Ce_xCuO_4$ crystals with x=0 - 0.15 at 10 K and a sufficient high temperature (440 K) for the x=0.05 crystal and 290 K for the others. From Onose *et al.* (2004)

comparable to the magnitude of the pseudogap measured by Armitage *et al.* (2002) *via* photoemission spectroscopy, which indicates that the pseudogap appearing in the optical spectra is the same as that in photoemission. Such a distinct pseudogap (PG) in the optical spectrum is not found in underdoped *p*-type superconductors where instead only an onset in the frequency dependent scattering-rate $1/\tau(\omega)$ derived by an extended Drude model analysis is assigned to a PG (Puchkov *et al.*, 1996). Singley *et al.* (2001) found that the frequency dependent scattering rate in the electron-doped compounds is depressed below 650 cm^{-1}, which is similar to the behavior which has been ascribed to the pseudogap state in the hole-doped materials (Puchkov *et al.*, 1996). However, whereas in the underdoped *p*-type compounds the energy scales associated with the pseudogap and superconducting states can be quite similar, these authors showed that in $Nd_{1.85}Ce_{0.15}CuO_4$ the two scales differ by more than an order of magnitude. In this case, the origin of pseudogap formation was ascribed to the strong T-dependent evolution of antiferromagnetic correlations in the electron-doped cuprates. It has been claimed that it is actually the maximum in the scattering rate and not the visible gap in the optical conductivity that correlates with the ARPES gap best (Wang *et al.*, 2006a).

Zimmers *et al.* (2005) found that the magnitude of the PG Δ_{pg} extrapolates to zero at concentration of x = 0.17 in $Pr_{2-x}Ce_xCuO_4$ films, implying the coexistence of magnetism and superconductivity in the highest T_c samples and the existence of a quantum critical point around this doping. Moreover, they performed a detailed analysis of their optical spectra over an extended doping range and found that a simple spin density wave model similar to the one dicussed in the context of photoemission above with (π, π) commensurate order with frequency- and temperature-dependent self energies could describe many of the principal features of the data. Note however,

that Motoyama *et al.* (2007) gives convincing evidence the AF state terminates around $x = 0.134$ doping in NCCO. In this regard it is possible that the PG observed by Zimmers *et al.* (2005) and others corresponds to the buildup of appreciable AF correlations and not the occurrence of long-range anti-ferromagnetic behavior. For instance, Wang *et al.* (2006a)'s optical data clearly show the existence of a large pseudogap in underdoped samples at temperatures well above the Néel temperature.

Onose *et al.* (1999) found that although the temperature dependence for reduced superconducting crystals was weak, for unreduced $Nd_{1.85}Ce_{0.15}CuO_4$ the large pseudogap structure evolves around 0.3 eV, but also that activated infrared and Raman Cu-O phonon modes grew in intensity with decreasing temperature. This was interpreted as being due to a charge ordering instability promoted by a small amount of apical oxygen. Singley *et al.* (2001) also found a low energy peak in the in-plane charge response at $50-110$ cm^{-1} of even superconducting $Nd_{1.85}Ce_{0.15}CuO_4$ crystals, possibly indicative of residual charge localizing tendencies

Singley *et al.* (2001) also showed that in contrast to the *ab*-plane optical conductivity, the c-axis showed very little difference between reduced superconducting x=0.15 and as-grown samples. This is in contrast to the expectation for hole-doped cuprates where large changes in the c-axis response are observed below the pseudogap temperature (see Basov and Timusk (2005) and references therein). Since the matrix element for interlayer transport is believed to be largest near the $(\pi, 0)$ position and zero along the zone diagonal, interlayer transport ends up being a sensitive probe in changes of FS topology. The polarized c-axis results indicate that the biggest effects of oxygen reduction should be found along the zone diagonal. Using low frequency THz Pimenov *et al.* (2000) have shown that the out of plane low frequency conductivity closely follows the dependence of the in-plane. This is, again, likely the result of an interplane tunnelling matrix elements and the lack of a PG near $(\pi, 0)$. Using these techniques they also found that there was no apparent anomaly in the quasi-particle scattering rate at T_c, unlike in some hole-doped cuprates (Bonn and Hardy, 1996).

In the superconducting state of $Nd_{1.85}Ce_{0.15}CuO_4$ Singley *et al.* (2001) found that the c-axis spectral weight which collapses into the condensate peak, was drawn from an anomalously large energy range ($E > 8\Delta$) similar to that of the hole-doped cuprates. In contrast, Zimmers *et al.* (2004) claimed that the *in-plane* Ferrell-Glover-Tinkham spectral weight sum rule was satisfied in their $Pr_{2-x}Ce_xCuO_4$ thin films at a conventional energy scale $4\Delta_{max}$ much less than that of the hole-doped cuprates(Zimmers *et al.*, 2004). If true, the discrepancy between out-of- and in-plane sum rule 'violation' is unlike the *p*-type cuprates and is unexplained. It would be worthwhile to repeat these measurements on the same sample, perhaps with the benefit of higher accuracy far infrared ellipsometry.

Finally, Homes *et al.* (2006) has made the observa-

tion of a kink in the frequency dependent reflectivity of $Pr_{1.85}Ce_{0.15}CuO_4$ at T_c. This is interpreted as a signature of the superconducting gap whose presence in the optical spectra is consistent with their observation that scattering rate $1/\tau$ is bigger than 2Δ and hence that these materials are in the dirty limit. It was argued that the ability to see the gap is enhanced as consequence of its non-monotonic d-wave nature (see Sec. IV.A below). The extracted gap frequency $\Delta_0 \approx 35$ cm^{-1} (4.3 meV) gives a $2\Delta/k_B T_c$ ratio of approximately 5, which is in good agreement with other techniques such as tunnelling (Shan *et al.*, 2005). Schachinger *et al.* (2008) recently reanalyzed the data of Homes *et al.* (2006) as well as Zimmers *et al.* (2004, 2005) to generate a boson-electron coupling function $I^2\chi(\omega)$. They find that the optical conductivity can be modeled with a coupling function with peaks at 10 meV and 44 meV. They identified this lower peak with the magnetic resonance mode found by Wilson *et al.* (2006a) in PLCCO at 11 meV and draw attention to the correspondence of this energy scale with the 10.5 meV feature in STM (Niestemski *et al.*, 2007).

E. Raman spectroscopy

Raman spectroscopy has been extensively used for the investigation of both normal state and superconducting properties of the cuprate superconductors (Devereaux and Hackl, 2007). It is a sensitive probe of quasiparticle properties, phonon structure, superconducting order parameter symmetry, and charge order. In the electron-doped compounds, both phonons (Heyen *et al.*, 1991) and crystal-field excitations (Jandl *et al.*, 1996, 1993) were studied early.

Onose *et al.* (1999) found that activated infrared and Raman Cu-O phonon modes grew in intensity with decreasing temperature in unreduced crystals. This was interpreted in terms of a charge ordering instability induced by a minute amount of interstitial apical oxygen. Onose *et al.* (2004) found some of the most definitive evidence that antiferromagnetic correlations manifest themselves in transport anomalies and signatures in the charge spectra (ARPES, optics etc.). As shown in Fig. 33, the B_{1g} two-magnon peak, which is found at 2800 cm^{-1} in the x=0 compound (Sugai *et al.*, 1989), broadens and loses intensity with Ce doping. The peak energy itself shows little doping dependence. They found that the peak's integrated intensity shows a sudden onset below T* - the same temperature where the optical and ARPES pseudogaps develop and there is a crossover in the out-of-plane resistivity.

Koitzsch *et al.* (2003) specifically studied the pseudogap state of $Nd_{1.85}Ce_{0.15}CuO_4$. They observed the suppression of spectral weight below 850 cm^{-1} for the B_{2g} Raman response and identify it as an anisotropic PG in the vicinity of $(\pi/2, \pi/2)$ points of the BZ. This was consistent with a model of the pseudogap which originated in enhanced AF interactions in the hot spot region which
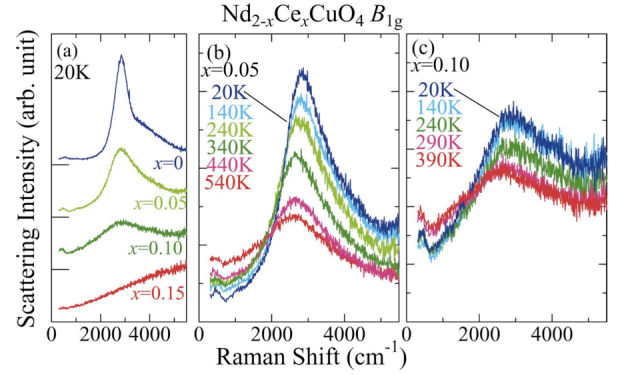

FIG. 33 (Color) (a) Doping dependence of the B_{1g} two-magnon peak Raman spectra at 20 K for crystals of $Nd_{2-x}Ce_xCuO_4$. (b),(c) Temperature variation of the B_{1g} Raman spectra for (b) $x = 0.05$ and (c) $x = 0.10$ crystals. From Onose *et al.* (2004).

are closer to the $(\pi/2, \pi/2)$ points in these materials than in the hole-doped compounds. They also observed a narrow Drude-like coherent peak in the B_{2g} channel in the pseudogap phase below T*, which reveals the emergence of long-lived excitations in the vicinity of the $(\pi/2, \pi/2)$ points. Interestingly these excitations do not seem to contribute to the optical conductivity, as it is the B_{1g} response (sensitive to the $(\pi, 0)$ region) which closely tracks the optical response.

Although the original Raman measurements of the superconducting gap (Stadlober *et al.*, 1995) found evidence for an s-wave order parameter, more recent measurements have been interpreted in terms of an d-wave order parameter, which is non-monotonic with angle around the FS(Blumberg *et al.*, 2002; Qazilbash *et al.*, 2005). This will be discussed in more detail in Sec. IV.A.3. In PCCO and NCCO, Qazilbash *et al.* (2005) have also determined both an effective upper critical field $H^*_{c2}(T, x)$ at which the superfluid stiffness vanishes and an $H^{2\Delta}_{c2}(T, x)$ at which the SC gap amplitude is suppressed. $H^{2\Delta}_{c2}(T, x)$ is larger than $H^*_{c2}(T, x)$ for all doping concentrations. The difference between the two quantities suggests the presence of phase fluctuations that are larger for $x < 0.15$. The ability of a magnetic field to suppress the Raman gap linearly at even small fields is unlike the hole-doped compounds (Blumberg *et al.*, 1997) or even conventional s-wave NbSe$_2$ (Sooryakumar and Klein, 1980, 1981) and may be related to the non-monotonic d-wave gap where points of maximum gap amplitude are close to each other in reciprocal space. From the doping dependence of $H^{2\Delta}_{c2}(T, x)$ Qazilbash *et al.* (2005) extracted the Ginzburg-Landau coherence length $\xi_{GL} = \sqrt{\Phi_0/2\pi H^{2\Delta}_{c2}(T, x)}$. ξ_{GL} is almost an order of magnitude larger than the p-doped compounds, giving $k_F\xi_{GL}$ values between 40 and 150 (or $E_F/\Delta \approx 6 - 24$). This larger Cooper pair size requires higher order pair interactions to be taken into account and supports the existence of the nonmonotonic d-wave

functional form.

F. Neutron scattering

1. Commensurate magnetism and doping dependence

Neutron scattering has been the central tool for investigating magnetic and lattice degrees of freedom in the cuprates (Bourges, 1999; Kastner *et al.*, 1998). In this section we concentrate on their contribution towards our understanding of the magnetism of the electron-doped cuprates. Their important contribution to the understanding of electron-phonon coupling in the n-type compounds (See for instance Braden *et al.* (2005)) will be discussed in Sec. IV.D.

It was found early on (Matsuda *et al.*, 1992; Thurston *et al.*, 1990) in doped, but not superconducting materials that the spin response of the n-type systems remained commensurate at (π, π) unlike the hole-doped compounds, which develop a large incommensurability. This commensurability is shared by all doped compounds in this material class. Doping also appears to preserve the unusual non-collinear c-axis spin arrangement (Sumarlin *et al.*, 1995). Due primarily to the lack of large superconducting single phase crystals, it wasn't until 1999 that Yamada *et al.* (1999) showed the existence of well-defined commensurate spin fluctuations in a reduced superconducting sample. The magnetic scattering intensity was peaked at (π, π) as in the as-grown antiferromagnetic materials, but with a broader q-width. It was suggested by Yamada *et al.* (2003) that the commensurate dynamic (> 4 meV) short range spin correlations in the SC phase of the n-type cuprate reflect an inhomogeneous distribution of doped electrons in the form of droplets/bubbles in the CuO_2 planes, rather than organizing into one-dimensional stripes as the doped holes may in many p-type cuprates. They estimated the low temperature (8 K) in-plane and out-of-plane dynamic magnetic correlation lengths to be $\xi_{ab} = 150$Å and $\xi_c = 80$ Å respectively for a $T_c = 25$ K sample.

It has been emphasized by Krüger *et al.* (2007) that within a fermiology approach the commensurate magnetic response of the doped compounds is even more at odds with their experimentally determined FS than a commensurate response would be for hole-doped compounds (which are actually incommensurate). They demonstrated that with a momentum independent Coulomb repulsion (which derives from the dominate hard core, local repulsion inherited from the microscopic Hubbard U) the magnetic spectrum will be strongly incommensurate[17]. Indeed based on the nesting wavevec-

tors between $(\pi, 0)$ regions of the Fermi surfaces (Armitage *et al.*, 2001b), one might expect that their magnetic response to be even *more incommensurate* than the hole-doped. The commensurability shows the central role that strong coupling and local interactions play in these compounds.

As mentioned in Sec. II.B, one approach to understanding the relatively robust extent of the antiferromagnetic phase in the n-type compounds has been to consider *spin-dilution models*. Keimer *et al.* (1992) showed that Zn doping into La_2CuO_4 reduces the Néel temperature at roughly the same rate as Ce doping in $Pr_{2-x}Ce_xCuO_{4\pm\delta}$. As Zn substitutes as a spinless impurity in d^{10} configuration and serves to dilute the spin system, this implies that Ce does a similar thing. Although this comparison of Ce with Zn doping is compelling it cannot be exact as the charge carriers added by Ce doping are itinerant and cannot decrease the spin stiffness as efficiently as localized Zn. Mang *et al.* (2004b) found in as grown non-superconducting $Nd_{2-x}Ce_xCuO_{4+\delta}$ that by looking at the instantaneous correlation length [obtained by integrating the dynamic structure factor $S(q_{2D}, \omega)$] the effects of itinerancy could apparently be mitigated. An almost quantitative agreement was found with quantum Monte Carlo calculations of the randomly site-diluted nearest-neighbor spin 1/2 square-lattice Heisenberg antiferromagnet.[18]

In NCCO's superconducting state, Yamada *et al.* (2003) showed that in addition to the commensurate elastic response, a gap-like feature opens up in the inelastic signal (Fig. 34). A similar spin gap with a magnitude of $6 - 7$ meV has also been reported in the p-type LSCO system near optimal doping. The maximum gap 2Δ behaves linearly with the SC temperature scale Ck_BT_c with $C \approx 2$ irrespective of carrier type. However, Yamada *et al.* (2003) claim that whereas the spin pseudo-gap behavior in the SC state of the p-type cuprates has a temperature independent gap energy and slowly "fills in" upon warming, in $x = 0.15$ NCCO the gap slowly closes from 4 meV as the temperature decreases from T_c to 2 K. 'Filling-in' behavior has been associated with phase separation and its absence argues against such phenomena in the n-type cuprates. Interestingly, Motoyama *et al.* (2006) found that the superconducting magnetic gap's magnetic field dependence shows an analogous trend as the temperature dependence when comparing hole- and electron-doping. Magnetic field causes a rigid shift to-

---

[17] In contrast, Ismer *et al.* (2007) have claimed that the magnetic spectrum can be fit well within a fermiology RPA approach. However they use a Coulomb repulsion $U(\vec{k})$ which is peaked strongly at (π, π), which essentially ensures the excellent fit. Li

---

et al. (2003) used a slave-boson mean-field approach to the $t - J$ model and include the antiferromagnetic spin fluctuations *via* the random-phase approximation. They claim that one does expect strong commensurate spin fluctuations in NCCO *via* nesting between FS sections near $(\pi/2, \pi/2)$ and symmetry related points

[18] However other observables showed worse agreement (for instance the ordered moment), pointing to the strong role that dynamics play and that fluctuations manifest themselves differently for different observables.
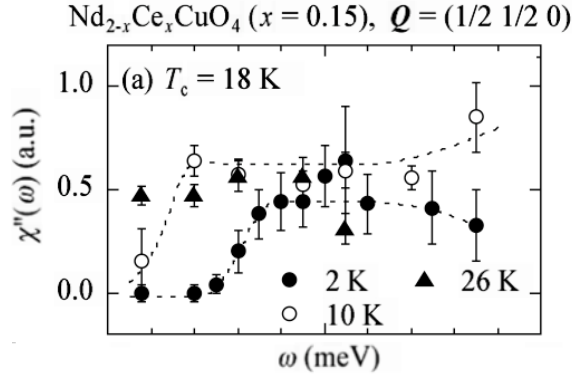
FIG. 34 Energy spectra of $\chi''(\omega)$ of NCCO obtained from the normal and SC phases (a) x=0.15, $T_c = 18$K. From (Yamada *et al.*, 2003).

FIG. 35 (Color)(a) Doping dependence of the spin stiffness ρ_s normalized to the AF superexchange ($J = 125$ meV for the undoped Mott insulator Nd_2CuO_4) as $2\pi\rho_s/J$ as well as the low-temperature spin correlation length ξ_0. The spin stiffness decreases smoothly with doping and reaches zero in an approximately linear fashion around $x_{AF} \approx 0.134$. The ground state for $x < x_{AF}$ has long-range AF order as indicated by the diverging ξ_0. (b) The apparent Néel temperature T_N, as determined from elastic scattering, as a function of doping given by the dotted curve. The dashed curve is the extrapolated contour of $\xi/a = 400$. Adapted from Motoyama *et al.* (2007).

wards lower energies of the n-type compound's gap. Such behavior contrasts with the case of optimally-doped and over-doped LSCO, in which an applied field induces in-gap states and the gap slowly fills in (Gilardi *et al.*, 2004; Lake *et al.*, 2001; Tranquada *et al.*, 2004a)[19].

With regards to a coexistence of antiferromagnetism and superconductivity, Motoyama *et al.* (2007) concluded *via* inelastic scattering that the spin stiffness ρ_s fell to zero at a doping level of approximately $x = 0.13$ (Fig. 35a) in NCCO which is close to the onset of superconductivity. They concluded that the actual antiferromagnetic phase boundary terminates at $x \approx 0.134$, and that the magnetic Bragg peaks observed at higher Ce concentrations originate from rare portions of the sample which were insufficiently oxygen reduced (Fig. 35b). This issue of the precise extent of antiferromagnetism, the presence of a quantum phase transition, and coexistence regimes will be dealt with in more detail below.

Wilson *et al.* (2006b) reported inelastic neutron scattering measurements on $Pr_{1.88}LaCe_{0.12}CuO_{4-\delta}$ in which they tracked the response from the long-range ordered antiferromagnet into the superconducting sample *via* oxygen annealing. This is along the δ axis in Fig. 7 (top). As discussed elsewhere (Sec. II.D.2), in general oxygen annealing creates an RE_2O_3 impurity phase in these systems. An advantage of PLCCO is that its impurity phase has a much weaker magnetic signal due to the small RE magnetic moment. They find that the spin gap of the antiferromagnet (finite in the insulator due to anisotropy) decreases rapidly with decreasing oxygen concentration, eventually resulting in a gapless low energy spectrum in this material. Note that superconducting PLCCO
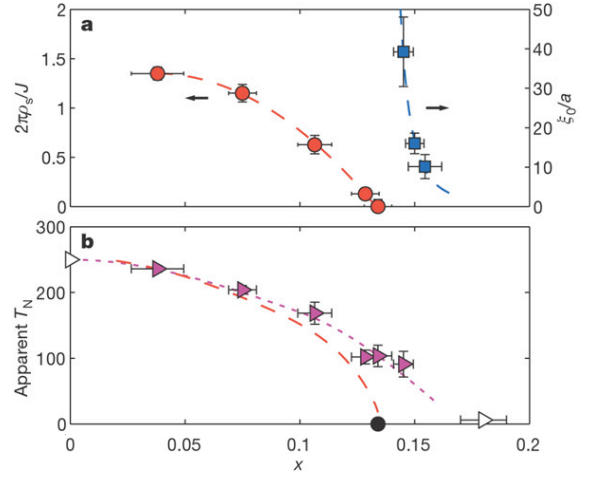
compounds do not exhibit a spin gap found in NCCO below T_c (Yamada *et al.*, 2003)[20]. The linewidths of the excitations broaden dramatically with doping, and thus the spin-stiffness effectively weakens as the system is tuned toward optimal doping. The low energy response of PLCCO is characterized by two regimes. At higher temperatures and frequencies, the dynamic spin susceptibility $\chi''(\omega, T)$ can be scaled as a function of $\frac{\omega}{T}$ at AF ordering wavevectors. The low energy cut-off of the scaling regime is connected to the onset of AF order. The fact that this energy scale comes down as the antiferromagnetic phase is suppressed leads to an association of this behavior with a QCP near optimal doping.

Fujita *et al.* (2008a) performed an inelastic study on PLCCO over a wide Ce doping range that spanned the antiferromagnetic ($x = 0.07$) to superconducting regimes ($x = 0.18$). For all concentrations measured, the low energy spectra were commensurate and centered at (π, π). Although they found a small coexistence regime between superconductivity and antiferromagnetism around $x = 0.11$, some characteristics, such as the relaxation rate and spin-stiffness decreases rapidly when one enters the

---

[19] As discussed below (Sec. III.F.2) Yu *et al.* (2008) have disputed the claim of an approximately 4 meV spin gap and claim that the spectra is better understood as an ≈ 6.4 meV spin gap and an ≈ 4.5 meV resonance. If true, this would necessitate a reinterpretation of some of the results presented above.

[20] We note that a spin gap was not observed in hole-doped LSCO crystals until sample quality improved sufficiently (Yamada *et al.*, 1995). Whether the lack of spin gap in PLCCO is due to the current sample quality of single crystals or is an intrinsic effect is unknown.

superconducting phase. The static AF response is absent at $x > 0.13$. The spin stiffness appears to extrapolate to zero around $x = 0.21$ when superconductivity disappears[21]. This indicates a close relation between spin fluctuations and the superconductivity in the electron-doped system. Interestingly other quantities, like the spectral weight (ω integration of $\chi''(\omega)$) do not show much doping dependence. This is unlike the p-type systems and was associated by these authors with a lack of phase separation in the n-type compounds.

In contrast to the hour-glass-type dispersion observed in hole-doped cuprates (Arai *et al.*, 1999; Tranquada *et al.*, 2004b), the dispersion at higher energies in optimally doped PLCCO $T_c = 21 - 25.5K$ looks like a more conventional spin wave response centered around the commensurate position, which disperses outward in a ring-like pattern at higher energy transfers (Fujita *et al.*, 2006; Wilson *et al.*, 2006b,c). It can be described in terms of three basic energy regimes (Wilson *et al.*, 2006a). At the lowest energies $\omega < 20$ meV the system shows the essentially over damped spin wave behavior discussed above with a small nearest neighbor spin coupling J_1 of approximately 29 ± 2.5 meV. At intermediate energies 50 meV $< \omega <$ 80 meV the excitations are broad and only weakly dispersing. At energies above 100 meV, the fluctuations are again spin wave like with a J_1 of 162 ± 13 meV. This is substantially larger than the undoped compounds (121 meV for PCO (Bourges *et al.*, 1997) and 104 meV for LCO (Coldea *et al.*, 2001)). A similar situation with a high energy response centered around the commensurate position has also been observed in overdoped PLCCO ($T_c = 16K$) (Fujita *et al.*, 2008b).

2. The magnetic 'resonance'

In the superconducting state, Wilson *et al.* (2006a) found an enhancement of peak in the inelastic neutron scattering response of PLCCO (Fig. 36) at approximately 11 meV at $(1/2,1/2,0)$ (equivalent to (π, π)) in the superconducting state. This was interpreted to be the much heralded 'resonance' peak (Rossat-Mignod *et al.*, 1991) found in many of the hole-doped cuprates, perhaps indicating that it is an essential part of superconductivity in all these compounds. They find that it has the same $E_r = 5.8k_BT_c$ relationship as other cuprates, but that it does not derive from incommensurate 'hour-glass' peaks that merge together as in YBCO and LSCO (Arai *et al.*, 1999; Tranquada *et al.*, 2004b). Instead it appears to rise out of the commensurate $(1/2,1/2,0)$ features found in the electron-doped systems (Yamada *et al.*, 1999). The inferred resonance energy also scales with the different

---

[21] Here the spin stiffness is defined as $\omega/\Delta q$ where Δq is the momentum width of a peak at a frequency ω, and is given by the slope of the Δq vs. ω relation. This is a different definition than that given by Motoyama *et al.* (2007).
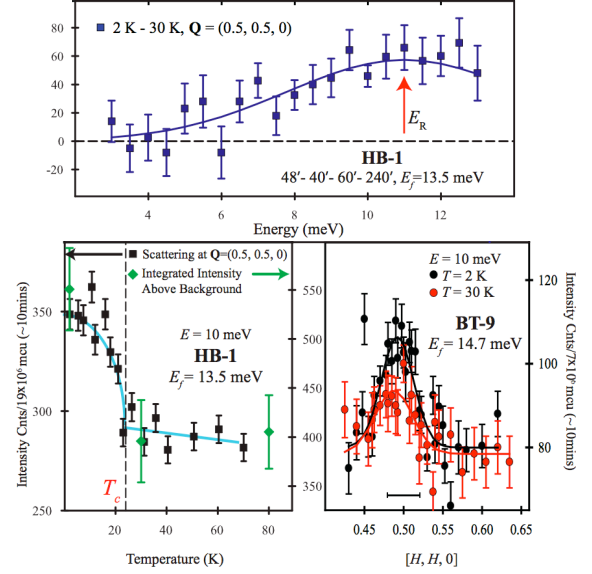

FIG. 36 (Color) (top) Temperature difference spectrum between 2 K and 30 K suggests a resonance-like enhancement at ~11 meV. (bottom left) Temperature dependence of the neutron intensity ($\sim$ 1 hour/point) at $(1/2, 1/2, 0)$ and 10 meV in black squares. Green diamonds are integrated intensity of the localized signal centered around Q= $(1/2, 1/2, 0)$ above backgrounds. (bottom right) Q-scans at $\omega = 10$ meV above and below the superconducting transitions. From Wilson *et al.* (2006a).

T_c's for different annealing conditions (Li *et al.*, 2008a). It is important to note that as mentioned above superconducting PLCCO spectra are essentially gapless below T_c (Yamada *et al.*, 2003) and in fact, except for the resonance, show very little temperature dependence at all below 30 K. Supporting evidence for this feature being 'the resonance' comes also from Niestemski *et al.* (2007) who have - as mentioned above - found signatures of a bosonic mode coupling to charge in their STM spectra at 10.5 meV $\pm$ 2.5 meV (Fig. 27) and Schachinger *et al.* (2008) who find a feature in the electron-boson coupling function $I^2\chi(\omega)$ extracted from the optical conductivity at 10 meV. Additionally Wilson *et al.* (2007) have shown that a magnetic field suppresses the superconducting condensation energy and this resonance feature in PLCCO in a remarkably similar way.

In continuing work Zhao *et al.* (2007) have claimed that optimally doped NCCO has a resonance at 9.5 meV, which also obeys the $E_r = 5.8k_BT_c$ relation. However, their assignment of this intensity enhancement has been disputed by Yu *et al.* (2008), who claim that their full ω scans show the spectra are better described by an inhomogeneity broadened spin gap at ≈ 6.4 meV and a sub gap resonance at the much smaller energy of ≈ 4.5 meV as shown in Fig. 37. This scenario has a number of appealing features. Both energy positions show sudden increases in intensity below T_c. Moreover, the spin gap they assign is to within error bars equal to the full

electronic gap maximum 2Δ (as measured by techniques like Raman scattering (Qazilbash *et al.*, 2005)), suggesting that - *unlike* the hole-doped cuprates - the commensurate response allows electronic features to be directly imaged in the magnetic scattering as (π,π) bridges these portions of the FS. *Like* the hole-doped cuprates the resonance they find is at energies less than the full superconducting gap, which is a reasonable condition for the stability of spin-exciton-like excitations. This interpretation is at odds with the original observation of the spin gap in NCCO by Yamada *et al.* (2003) and as the authors point out necessitates a reinterpretation of that data as well as some of their own previous work. These authors are careful to state that their result does not necessarily invalidate the claim of a resonance peak at the larger energy of 11 meV in PLCCO as the superconducting gap may be much larger in PLCCO (Niestemski *et al.*, 2007) and may allow a stable coherent excitation at this energy.
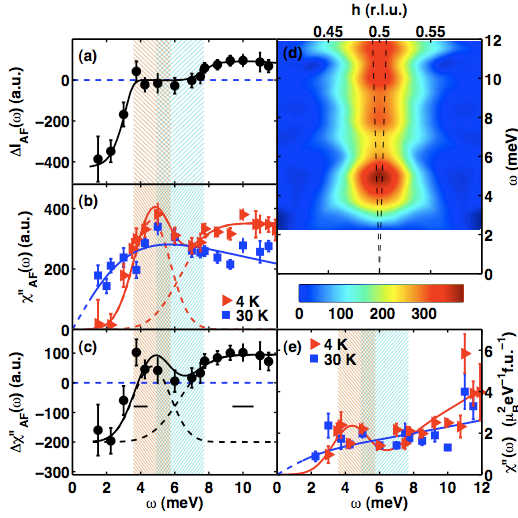

FIG. 37 (a) Change in scattering intensity between 4 K and 30 K at the antiferromagnetic wavevector $(1/2,1/2,0)$. (b) Dynamic susceptibility $\chi''(Q,\omega)$ which shows two peaks after correcting the measured intensity for the thermal factor. (c) Relative change from 30 K to 4 K in susceptibility at the AF wavevector. (d) Contour plot of $\chi''(Q,\omega)$ at 4K, made by interpolation of symmetrized momentum scans through the AF zone center with a constant background removed. (e) Local susceptibility in absolute units from the momentum-integral of the dynamic susceptibility by comparing with the measured intensity of acoustic phonons. The shaded vertical bands in (a) - (c) indicates the range of values of $2\Delta_{el}$ from Raman scattering (Qazilbash *et al.*, 2005) corresponding to the author's estimation of the distribution of gap sizes from chemical inhomogeneity. From Yu *et al.* (2008).

3. Magnetic field dependence

The dependence of the ordered spin structure on magnetic field of superconducting samples and the possibility of field induced antiferromagnetism has become of

intense interest. These studies parallel those on underdoped LSCO, where neutron scattering has shown that a c-axis-aligned magnetic field not only can suppress superconductivity but also creates a static incommensurate spin density wave order, thus implying that such an order directly competes with the superconducting state (Katano *et al.*, 2000; Khaykovich *et al.*, 2002; Lake *et al.*, 2001, 2002). The effect of field on n-type superconducting and reduced samples is a matter of some controversy. While experiments by Matsuda *et al.* (2002) found that a 10-T c-axis-aligned field has no effect on the AF signal in their superconducting NCCO x=0.14 samples, Kang *et al.* (2003a) demonstrated in similar x=0.15 samples antiferromagnetic related Bragg reflections such as $(1/2,1/2,0)$ grew in intensity until a field close to the critical field B_{c2} and then decreased. The experiments were interpreted as demonstrating that a quantum phase transition from the superconducting state to an antiferromagnetic state is induced at B_{c2}.

Although their raw data are similar to Kang *et al.* (2003a), this interpretation was disputed by Mang *et al.* (2003) who found that additional magnetic intensity comes from a secondary phase of $(Nd,Ce)_2O_3$. As noted above, a severe oxygen reduction procedure always has to be applied to as-grown crystals to induce superconductivity. Mang *et al.* (2003) discovered that the reduction process decomposes a small amount of NCCO (0.1 - 1.0 % by volume fraction). The resultant $(Nd,Ce)_2O_3$ secondary phase has a complex cubic bixbyite structure, with a lattice constant approximately $2\sqrt{2}$ times the planar lattice constant of tetragonal NCCO. The $(Nd,Ce)_2O_3$ impurity phase grows in epitaxial register with the host lattice in sheets on average five unit cells thick. Because of the simple $2\sqrt{2}$ relationship between the lattice constants of NCCO and $(Nd,Ce)_2O_3$ the structural reflections of the impurity phase - for instance the cubic $(2,0,0)_c$ - can be observed at the commensurate NCCO positions $(1/2,1/2,0)$. However the c axis is different and there is approximately a 10% mismatch between $(Nd,Ce)_2O_3$'s lattice constant and a_c of NCCO, and therefore the impurity phase's $(0,0,2)_c$ can be indexed as $(0,0,2.2)$. Moreover, Mang *et al.* (2004a) found that the field effects reported by Kang *et al.* (2003a) are observable in non-superconducting, but still oxygen-reduced, x=0.10 samples, both at the previously reported lattice positions and at positions unrelated to NCCO but equivalent in the cubic lattice of $(Nd,Ce)_2O_3$. Mang *et al.* (2004a) interpreted the non-monotonic field dependence of the scattering amplitude as a consequence of the two inequivalent crystalline sites of the Nd atoms in Nd_2O_3 and in accordance with such a model, showed that the intensity scales as a function of B/T as shown in Fig. 38.

Dai and coworkers subsequently confirmed the presence of a cubic impurity phase, but feel additional results support their original scenario. Kang *et al.* (2003b); Matsuura *et al.* (2003) pointed out, that while one would expect the field induced intensity of the impurity phase to be the same along all axis directions due to its cubic
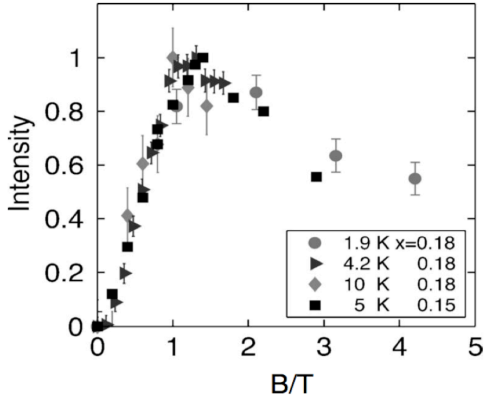
FIG. 38 Scaled scattering intensity at $(1/2,1/2,0)$ for a superconducting sample of NCCO ($x = 0.18$; $T_c = 20$ K), plotted as a function of B/T. Field direction is [0,0,1]. Data is compared with the results at $T = 5$ K of Kang *et al.* (2003a) ($x = 0.15$; $T_c = 25$ K). Adapted from Mang *et al.* (2004a).

symmetry, the effect at $(1/2,1/2,0)$ is much larger when B is parallel to the c-axis. This is consistent with the much smaller upper critical field along the c-axis. Moreover the $(1/2,1/2,3)$ peak has a z index which cannot be contaminated by the impurity phase and yet shows an induced antiferromagnetic component when the field is along the c-axis and hence superconductivity is strongly suppressed, but not when in-plane and superconductivity is only weakly affected. (Matsuura *et al.*, 2003).

It is difficult to draw generalized conclusions about the field dependence of the neutron scattering response in the electron-doped cuprates as important differences exist between the measurements of NCCO and PLCCO. Optimally doped PLCCO (Fujita *et al.*, 2004; Kang *et al.*, 2005) has no residual AF order (like LSCO (Kastner *et al.*, 1998)) while a 3D AF order has been inferred to coexist with superconductivity in NCCO even for optimally doped samples[22]. Additionally, the magnetic field of the maximum induced intensity in PLCCO is independent of temperature, in contrast to the peak position scaled by H/T in NCCO and in opposition to the impurity model proposed by Mang *et al.* (2003). A c-axis magnetic field enhances not only the scattering signal in optimally doped NCCO at $(1/2,1/2,0)$ but also at the 3D AF Bragg positions such as $(1/2,3/2,0)$ and $(1/2,1/2,3)$, whereas for underdoped PLCCO, there is no observable effect on $(1/2,3/2,0)$ (and related) 3D peaks up to 14 T (Kang *et al.*, 2005). At this point the effect of magnetic field on the SC state of the electron-doped compounds still has to be regarded as an open question.

---

[22] As noted above and discussed in more detail below, Motoyama *et al.* (2007) have concluded that true long-range order in NCCO terminates at $x = 0.13$ and that the Bragg peaks seen near optimal doping are due to insufficiently reduced portions of the sample.

G. Local magnetic probes: μSR and NMR

Nuclear Magnetic Resonance (NMR) (Asayama *et al.*, 1996) and muon spin resonance and rotation (μSR) (Luke *et al.*, 1990; Sonier *et al.*, 2000) measurements are sensitive probes of *local* magnetic structure and have been used widely in the cuprate superconductors. Using μSR on polycrystalline samples, Luke *et al.* (1990) first showed that the Mott insulating parent compound Nd_2CuO_4 has a Néel temperature (T_N) of approximately 250K, which decreases gradually upon substitution of Nd by Ce to reach a zero value close to optimal doping ($x \sim 0.15$). Fujita *et al.* (2003) performed a comprehensive μSR study, which established the phase diagram of PLCCO. They found bulk superconductivity from $x = 0.09$ to 0.2 and only a weak dependence of T_c on x for much of that range. The antiferromagnetic state was found to terminate right at the edge of the superconducting region, which was interpreted as a competitive relationship between the two phases. Only a very narrow coexistence regime was observed (≈ 0.01 wide). Although changes in the form of the muon relaxation were observed below a temperature T_{N1} where elastic neutron Bragg peaks have been observed (Fujita *et al.*, 2003), there was no evidence for a static internal field until a lower temperature T_{N2}. At the lowest temperatures, it was found that the magnitude of the internal field decreased upon electron doping, showing a continuous and apparently spatially uniform degradation of magnetism. This is in contrast to the hole-doped system where in the Néel state ($x < 0.02$) the internal field was constant (Borsa *et al.*, 1995; Harshman *et al.*, 1988), which has been taken as evidence for phase separation (Chou *et al.*, 1993; Matsuda *et al.*, 2002). Extensive NMR measurements have also been done by Bakharev *et al.* (2004); Williams *et al.* (2005); Zamborszky *et al.* (2004) that have given important information about inhomogeneity in these systems. These measurements are discussed in more detail in Sec. IV.E.

Zheng *et al.* (2003) showed that when the superconducting state was suppressed in $x = 0.11$ PLCCO with a large out-of-plane magnetic field the NMR spin relaxation rate obeyed the Fermi-liquid Korringa law $1/T_1 \propto T$ over 2 decades in temperature. We discuss this result in more detail below (Sec. IV.F). Zheng *et al.* (2003) also found no sign of a spin pseudogap opening up at temperatures much larger than T_c, which is a hallmark of NMR in the underdoped p-type cuprates. Here they found that above the superconducting T_c $1/T_1T$ showed only a weak increase, consistent with antiferromagnetic correlation.

Related to the neutron scattering studies in field detailed above, under a weak perpendicular field Sonier *et al.* (2003) observed *via* μSR the onset of a substantial magnetic order signal (Knight shift) which was static on the μSR time scales in the superconducting state of optimally doped PCCO single crystals. The data was consistent with moments as large as 0.4μ being induced by fields as small as 90 Oe. There was evidence that

the antiferromagnetism was not confined to the vortex cores, since nearly all the muons saw an increase in the internal field and the vortex density was so low and so again the magnetism looked uniform. It has been argued however that this study overestimated the induced Cu moments by not explicitly taking into account the superexchange coupling between Pr and Cu ions as well as an unconventional hyperfine interaction between the Pr ions and the muons (Kadono *et al.*, 2004b, 2005). Kadono *et al.* (2004b, 2005) have interpreted their measurements as then consistent with only a weak field induced Cu magnetism in $x = 0.11$ PLCCO (near the AF boundary of $x \approx 0.10$) which becomes even smaller at $x = 0.15$.

Overall μSR results in the field applied state of the electron-doped cuprates appear to show substantial differences from the p-type compounds. At the onset of superconductivity, there is a well-defined Knight shift whereas in the hole-doped materials, superconductivity under applied field only evinces from an enhancement in the spin relaxation rate (Kakuyanagi *et al.*, 2002; Mitrovic *et al.*, 2001; Savici *et al.*, 2005) or changes in the field profile of the vortex cores (Kadono *et al.*, 2004a; Miller *et al.*, 2002). This again indicates that the induced polarization of Cu ions in the electron-doped compounds appears to be relatively uniform over the sample volume, whereas it appears to be more localized to the vortex cores in the hole-doped materials.

IV. DISCUSSION

A. Symmetry of the superconducting order parameter

There is a consensus picture emerging for the order parameter symmetry for the n-type cuprates. The original generation of measurements on polycrystals, single crystals and thin films seemed to favor s-wave symmetry, but experiments on improved samples including tricrystal measurements(Tsuei and Kirtley, 2000b), penetration depth(Côté *et al.*, 2008; Kokales *et al.*, 2000; Prozorov *et al.*, 2000), ARPES(Armitage *et al.*, 2001a; Matsui *et al.*, 2005a; Sato *et al.*, 2001), and others favor a $d_{x^2-y^2}$ symmetry over most of the phase diagram, albeit with an interesting non-monotonic functional form. Below, we give an overview of the main results of their order parameter and discuss similarities and differences with respect to the hole-doped cuprates. This is a subject that deserves a comprehensive review that sorts through the multitude of experiments. We give only a comparatively brief overview here.

1. Penetration depth

In the mid 90's, penetration depth λ measurements on high quality $YBa_2Cu_3O_7$ crystals gave some of the first clear signatures for an anomalous order parameter in the cuprates. The linear temperature dependence of $\Delta\lambda(T)$ (related to the superfluid density) was a clear demonstra-

tion that the density of states of this material was linear for sub-gap energies ($E < 20$ meV), in agreement with the behavior expected from a d-wave symmetry of the order parameter with nodes (Hardy *et al.*, 1993).

Early $\Delta\lambda(T)$ data obtained on single crystals and thin films of optimally doped NCCO showed no such temperature dependence(Andreone *et al.*, 1994; Anlage *et al.*, 1994; Schneider *et al.*, 1994; Wu *et al.*, 1993), not even the expected dirty d-wave behavior characterized by a $\Delta\lambda \propto T^2$ dependence at low temperature(Hirschfeld and Goldenfeld, 1993) seen for example in thin films of $YBa_2Cu_3O_7$(Ma *et al.*, 1993). The NCCO data was best fit to a BCS s-wave-like temperature dependence down to $T/T_c \sim 0.1$ with unusually small values of $2\Delta_o/k_BT_c \sim 1.5 - 2.5$. Later, Cooper proposed that the temperature dependence of the superfluid density measured with these techniques had been masked by the strong Nd magnetic response (see Section II.E) at low T (Cooper, 1996). Using the data of Wu *et al.* (1993) and correcting for the contribution of the low temperature magnetic permeability $\mu_{DC}(T)$ in NCCO (Dalichaouch *et al.*, 1993), he reached the conclusion that the real temperature dependence of $\Delta\lambda(T)$ could be close to T^2 at low temperature.

To circumvent the inherent magnetism of Nd ions in NCCO, slightly different experimental probes were used by Kokales *et al.* (2000) and Prozorov *et al.* (2000) to evaluate $\Delta\lambda(T)$ and the superfluid density (Fig. 39) in $Pr_{1.85}Ce_{0.15}CuO_4$ single crystals which has much weaker RE magnetism. Both experiments showed for the first time that $\Delta\lambda(T)$ follows a $\sim T^2$ behavior at low temperatures in PCCO, in agreement with the dirty d-wave scenario. Moreover, by extending the temperature range of the measurements for NCCO, they showed the presence of an upturn in the magnetic response due to Nd residual magnetism, confirming Cooper's interpretation.
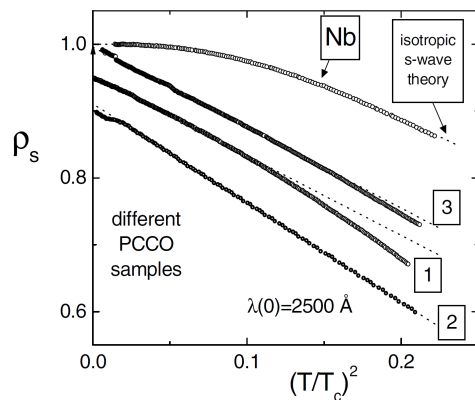

FIG. 39 Tunnel-diode driven LC resonator data for three different PCCO single crystals showing power law behavior of the superfluid density. From Prozorov *et al.* (2000).

More recent reports targeting the doping dependence of the superfluid density on certain specifically prepared thin films give a still controversial picture however.

Skinta *et al.* (2002) observed that the temperature dependence of $\Delta\lambda(T)$ evolves with increasing cerium doping. Using PCCO and LCCO thin films grown by Molecular Beam Epitaxy (MBE) (Naito *et al.*, 2002), the low temperature data present the gradual development of a gapped-like behavior for increasing doping(Skinta *et al.*, 2002) observed as a flattening of $\Delta\lambda(T)$ at low temperature. The growth of this T-independent s-wave-like behavior was interpreted as a possible signature of a transition from a pure d-wave symmetry on the underdoped regime to a $d-$ and $s-$wave admixture on the overdoped regime. A similar trend was also deduced by Pronin *et al.* (2003) from a quasioptical transmission measurement of $\Delta\lambda(T)$ at millimeter wavelengths (far-infrared). Another report (Kim *et al.*, 2003) on MBE-grown buffered PCCO thin films from under- to overdoping range claimed that $\lambda(T)$ can only be explained with a fully gapped density of states with a $d+is$-wave admixture for all doping. In contrast, Snezhko *et al.* (2004) showed that the T^2 behavior of thin films grown by pulsed-laser ablation deposition (PLD) is preserved even in the overdoped regime. These very conflicting results have yet to be explained, but the answers may lie partly in the different growth techniques, the quality of films, the presence of parasitic phases (Section II.D) and the differences in the experimental probes. It has been proposed that the presence of electron and hole Fermi surface pockets, as observed by ARPES (Section III.C) and confirmed by electrical transport (Section III.A.1), could result in an s-wave-like contribution despite that the dominant pairing channel has a $d_{x^2-y^2}$ symmetry(Luo and Xiang, 2005). The variability between different kinds of samples may reflect the influence of different oxygen content on the presence and the contribution of these pockets (arcs) as shown by ARPES(Richard *et al.*, 2007).

As a possible demonstration of other material-related issues, Côté *et al.* (2008) recently compared the penetration depth measurements by the microwave perturbation technique of optimally doped PCCO thin films grown by PLD with very similar T_c's but with different quality as characterized by their different normal-state resistivity close to T_c. They found that lower quality films show a flat $\lambda_1(T)$ at low temperature, showing that oxygen reduction and the presence of defects may be of crucial importance in determining the actual symmetry using penetration depth measurements.

Another avenue for the estimation of the temperature dependence of the penetration depth relies on the properties of grain boundary junctions (GBJ) made on $SrTiO_3$ bicrystal substrates(Hilgenkamp and Mannhart, 2002). Using the maximum critical current density J_c of small Josephson junctions, Alff *et al.* (1999) estimated $\Delta\lambda_{ab}/\lambda_{ab}$ as a function of temperature for both NCCO and PCCO GBJ's using thin films made by MBE. This scheme assumes that $J_c \propto n_s$, thus $\lambda_{ab} \propto 1/\sqrt{n_s} \propto 1/\sqrt{J_c}$. The striking aspect of this data is the upturn of the estimated effective λ_{ab} for NCCO due to Nd magnetism. Using the same correction scheme as that pro-

posed by Cooper (1996), the NCCO data could be superimposed on top of the PCCO GBJ data(Alff *et al.*, 1999). However, it was concluded that the penetration depth followed an s-wave-like exponential temperature dependence with $2\Delta_o/k_BT_c \sim 3$, in agreement with the initial penetration depth measurements and indicating a nodeless gap. This result together with the unresolved doping dependence controversy mentioned above may arise from the different sample preparations leading to many superimposed extrinsic contributions.

2. Tunnelling spectroscopy

There are two main signatures in tunnelling spectroscopy that can reveal the presence of d-wave symmetry. The first is related to their 'V-shaped' density of states. Unlike the conductance characteristic observed for tunnelling between a metal and a conventional s-wave superconductor at T = 0, which shows zero conductance until a threshold voltage $V = \Delta_o/e$ is reached(Tinkham, 1996), tunnelling into d-wave superconductors reveals substantial conductance at subgap energies even at T→0. The second signature, a zero-bias conductance peak (ZBCP), reveals the presence of an Andreev quasiparticle bound state (ABS) at the interface of a d-wave superconductor arising from the phase change of the order parameter as a function of angle in $\vec{k}$-space(Deutscher, 2005; Hu, 1994; Kashiwaya *et al.*, 1995; Lofwander *et al.*, 2001). This bound state occurs for all interface orientations with projection on the (110) direction. The ZBCP can also split under an increasing magnetic field(Beck *et al.*, 2004; Deutscher, 2005) and, in some instances, it is reported to even show splitting at zero magnetic field in the holed doped cuprates.(Covington *et al.*, 1997; Deutscher, 2005; Fogelström *et al.*, 1997).

As discussed above in Sec. III.B, tunnelling experiments on $n-$doped cuprates have been particularly difficult, which is presumably related to difficulties in preparing high quality tunnel junctions. Typical quasiparticle conductance G(V)=dI/dV spectra on optimaldoped NCCO (Shan *et al.*, 2005) are shown in Figure 26. Similar spectra are found for Pb/I/PCCO (where I is a natural barrier) (Dagan *et al.*, 2005b), and GB junctions (Alff *et al.*, 1998a; Chesca *et al.*, 2005). The main features of the $n-$doped tunnel spectra are: prominent coherence peaks which reveal an energy gap of order 4 meV at 1.8K for optimal doping, an asymmetric linear background G(V) for voltage well above the energy gap, a characteristic 'V' shape, coherence peaks which disappear completely by $T \approx T_c$ at H=0 (and by $H \approx H_{c2}$ for T=1.8K), and typically the absence of a zero bias conductance peak (ZBCP) at V=0.

Tunneling has given conflicting views of the pairing symmetry in $n-$doped cuprates. The characteristic 'V' shape of G(V) cannot be fit by an isotropic s-wave BCS behavior and closely resembles that of d-wave hole-doped

cuprates (Fischer *et al.*, 2007). On the other hand the ZBCP has been observed only sporadically (Biswas *et al.*, 2002; Chesca *et al.*, 2005; Qazilbash *et al.*, 2003; Wagenknecht *et al.*, 2008). Its absence in most spectra of tunnel junctions with large barriers may be the consequence of the coherence length ($\sim$ 50Å) being comparable to the mean free path (Biswas *et al.*, 2002) similar to the effect observed in YBCO (Aprili *et al.*, 1998). Its absence has also been attributed to the coexistence of AFM and SC orders (Liu and Wu, 2007).

Point contact spectroscopy data have shown a ZBCP in underdoped (x = 0.13) PCCO films, while it is absent for optimal and overdoped compositions (Biswas *et al.*, 2002; Qazilbash *et al.*, 2003). Combined with an analysis of the G(V) data based on Blonder-Tinkham-Klapwijk theory (Blonder *et al.*, 1982; Tanaka and Kashiwaya, 1995), this result has been interpreted as a signature of a *d*- to *s*-wave symmetry transition with increasing doping. However, there has been a more recent claim that all such tunneling spectra are better fit with a non-monotonic *d*-wave functional form (Dagan and Greene, 2007) over the entire doping range of superconductivity. This may explain in part the many reports claiming that the tunnelling spectra from several experimental configurations can not be fit with either pure *d*-wave or *s*-wave gaps [see for example Alff *et al.* (1998b); Kashiwaya *et al.* (1998); Shan *et al.* (2005)]. The SIS planar tunnelling work of Dagan and Greene (2007) and a detailed point contact tunnelling study as a function of doping of Shan *et al.* (2008a) also provide strong evidence that the $n-$doped cuprates are weak coupling, *d*-wave BCS superconductors over the whole phase diagram. This is in agreement with other techniques including Raman scattering (Qazilbash *et al.*, 2005).

As discussed above (Sec. III.B) Niestemski *et al.* (2007) reported the first reproducible high resolution STM measurements of PLCCO (T_c = 24 K) (Fig. 27). The linecut (Fig. 27a) shows spectra that vary from ones with sharp coherence peaks to a few with more pseudogaplike features and no coherence peaks. However almost all spectra show the very notable 'V' shaped higher energy background, which is consistent with *d*-wave symmetry.

Chesca *et al.* (2005) used a bicrystal GBJ with optimal doped LCCO films (a SIS junction) and measured both Josephson tunnelling and quasiparticle tunnelling below $T_c \sim 29$K. A ZBCP was clearly seen in their quasiparticle tunnelling spectrum and it has the magnetic field and temperature dependence expected for a *d*-wave symmetry, ABS-induced, zero energy peak. These authors argue that it requires extremely high-quality GB junctions– to reduce disorder at the barrier and to have a large enough critical current– in order to observe the ZBCP. Given the sporadic observations of a ZBCP in $n-$doped cuprates [Shan *et al.* (2005) and references therein], the authors suggest that perhaps the observation of a ZBCP rather than its absence should be regarded as a true test of the pairing symmetry.

Finally, similar GB junctions of LCCO have also re-

vealed an intriguing behavior with the observation of a ZBCP for magnetic field much larger than the usual upper critical field measured on the same film using in-plane resistivity (Wagenknecht *et al.*, 2008). With increasing temperature T, they find that the ZBCP vanishes at the critical temperature T_c = 29K if B = 0, and at T = 12K for B = 16T. These observations may suggest that the real upper critical field is larger than the one inferred from transport. They estimate $H_{c2} \approx 25$ T at T=0. However, this is in complete disagreement with the bulk upper critical field that has been estimated to remain below 10T at 2K for all dopings using specific heat(Balci and Greene, 2004) and the Nernst effect(Balci *et al.*, 2003; Li and Greene, 2007). These differences are not yet explained.

3. Low-energy spectroscopy using Raman scattering

Raman scattering is sensitive to the anisotropy of the superconducting gap, as particular polarization configurations probe specific regions of momentum space. It is possible to isolate signatures related to the superconducting gap, and in particular demonstrate anisotropy and zeros in the gap function (Devereaux *et al.*, 1994; Devereaux and Hackl, 2007). As observed in hole-doped cuprates (Stadlober *et al.*, 1995), peaks related to the magnitude of the gap are extracted in two specific polarization configurations, B_{1g} and B_{2g}. With a *d*-wave gap anisotropy, these peaks are expected to be found at different frequencies in different polarizations. Moreover, the presence of low-energy excitations below the maximum gap value (down to zero energy in the case of lines of nodes for *d*-wave symmetry) implies that the Raman response follows very specific power law frequency dependencies for these various polarizations (Devereaux *et al.*, 1994; Devereaux and Hackl, 2007). In the original Raman work on NCCO's order parameter, Stadlober *et al.* (1995) showed that the peaks in the B_{1g} and B_{2g} channels were positioned at close to the same energy, much like older works on s-wave classical superconductors like Nb_3Sn (Dierker *et al.*, 1983).

However, more recent experiments on single crystals and thin films reveal a more complicated picture. The low-frequency behavior of the B_{1g} and B_{2g} channels approach power laws consistent with the presence of lines of nodes in the gap function(Kendziora *et al.*, 2001). These power laws, although not perfect, indicate the presence of low energy excitations. Moreover, in some instances, the peak energy values in the B_{1g} and B_{2g} channels can be different(Kendziora *et al.*, 2001), and in some others, they are virtually identical (Blumberg *et al.*, 2002; Qazilbash *et al.*, 2005). In all these recent data however, the low energy spectrum continues to follow the expected power laws for lines of nodes. To reconcile the fact that these power laws are always observed and that some samples present peaks at identical energies in both channels, Blumberg *et al.* (2002) first proposed that a

non-monotonic d-wave gap function could explain this anomalous response (Blumberg *et al.*, 2002; Qazilbash *et al.*, 2005). In Fig. 40, we show a representative dataset in the B_{1g}, B_{2g} and A_{1g} channels, together with the non-monotonic gap function proposed by Blumberg *et al.* (2002). In this picture, the maximum value of the gap function ($\Delta_{max} \sim 4$ meV) coincides with the 'hot spots' on the Fermi surface (**HS** in Fig. 40), namely the position in $\vec{k}$-space where the Fermi surface crosses the AFBZ as found by Armitage *et al.* (2001b). At the zone boundary (ZB in Fig. 40), the gap value drops to $\sim$3 meV[23]. The non-monotonic gap has been found to be consistent with recent ARPES and tunneling results (Dagan and Greene, 2007; Matsui *et al.*, 2005b).
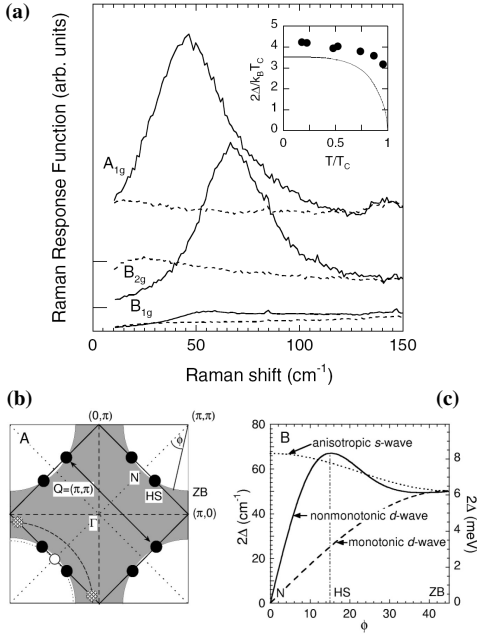

FIG. 40 (a) Electronic Raman scattering results comparing the response above (35K - dashed line) and below (11K - solid line) the critical temperature in the B_{1g}, the B_{2g} and the A_{1g} configurations; (b) a sketch of the position of the hot spots (HS) on the Fermi surface where the gap maximum also occurs; (c) a comparison of the angular dependence of the non-monotonic d-wave gap (solid line) with monotonic d-wave (dashed line) and anisotropic s-wave gap (dotted line). From Blumberg *et al.* (2002).

Venturini *et al.* (2003) countered that the basis for the conclusion of Blumberg *et al.* (2002) was insufficient and so an s-wave form can still not be ruled out. They argued that since the Raman scattering amplitudes are finite at the maximum of the proposed gap function for all

---

[23] It has been argued recently that the non-monotonic gap proposed by Blumberg *et al.* (2002) and others is not purely the superconducting one, but in fact reflects a coexistence of antiferromagnetic and superconducting orders (Yuan *et al.*, 2006b)

symmetries, the spectra in all these symmetries should exhibit multiple structures at the same energies in the limit of low damping as opposed to simply different size gaps in the different geometries (i.e. peaks should appear for energies corresponding to $\partial\Delta/\partial\phi = 0$). Blumberg *et al.* (2003) stand by their original interpretation and replied that no sharp threshold gap structures had ever been observed in any electron-doped cuprates even at the lowest temperature and frequencies and therefore irrespective of any other arguments an s wave symmetry can be definitively ruled out.

A very detailed study on single crystals and thin films has been reported by Qazilbash *et al.* (2005) who followed the doping dependence of PCCO and NCCO's Raman response. The authors extracted the magnitude of the gap as a function of doping and concluded that the smooth continuous decrease of the Raman response below the gap signatures (coherence peaks) is a sign that the superconducting gap preserves its lines of nodes throughout the whole doping range from under- to overdoping. Obviously, this non-monotonic d-wave gap function should have a definite impact on properties sensitive to the low energy spectrum.

4. ARPES

ARPES provided some of the first dramatic evidence for an anisotropic superconducting gap in the hole-doped cuprates (Shen *et al.*, 1993). Comparing the photoemission response close to the Fermi energy on the same sample for temperatures above and below T_c, one can clearly distinguish a shift of the intensity in the spectral function for momentum regions near $(\pi, 0)$. This "leading-edge" shift gets its origin from the opening of the superconducting gap and one can then map it as a function of $\vec{k}$ on the Fermi surface in the Brillouin zone (BZ). In the case of hole-doped cuprates, the first $\Delta(\vec{k})$ mapping was obtained with $Bi_2Sr_2CaCu_2O_{8+\delta}$ (Shen *et al.*, 1993), which is easily cleaved due to its weakly coupled Bi-O planes. Gap values consistent with zero were observed along the diagonal directions in the BZ, i.e. along the (0,0) to (π,π) line (Ding *et al.*, 1996). Away from the zone diagonal, the magnitude of the gap tracks the $\vec{k}$-dependence of the monotonic d-wave functional form.

Until modern advances in the technology, the smaller energy gap of the electron-doped cuprates, on the order of 5 meV for optimal doping, was at the limit of ARPES resolution. The first reports of a measured superconducting gap in NCCO were presented by Armitage *et al.* (2001a) and reported independently by Sato *et al.* (2001) and are shown in Fig. 41. They found an gap anisotropy with a negligible gap value along the zone diagonal directions and a leading-edge shift of $\sim$ 2-3 meV along the Cu-O bond directions (Armitage *et al.*, 2001a; Sato *et al.*, 2001). Such behavior was consistent with an order parameter of d-wave symmetry. Using a model taking into account thermal broadening and the finite energy resolu-

tion, Sato *et al.* estimated the maximum gap value to be on the order of 4 to 5 meV, in close agreement with the values observed by tunnelling (see Section IV.A.2) and Raman Sec. IV.A.3.
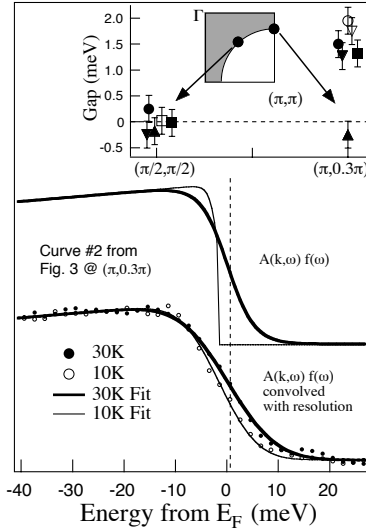

FIG. 41 Bottom curves are near E_F ARPES EDCs of optimally doped NCCO from $\vec{k}_F$ close to $(\pi,0.3\pi)$. Open and solid circles are the experimental data at 10 and 30K respectively, while solid lines are fits. Upper curves are the experimental fits without resolution convolution. "Curve #2 from Fig. 3" refers to figures in Armitage *et al.* (2001a). Upper panel: Gap values extracted from fits at the two $\vec{k}$-space positions using the difference between the 10 and 30K data. Different symbols are for different samples. From Armitage *et al.* (2001a).

In these early studies, the limited number of momentum space positions measured could not give the explicit shape of the gap function. Matsui *et al.* followed a few years later with more comprehensive results on $Pr_{0.89}LaCe_{0.11}CuO_4$ (PLCCO) that mapped out the explicit momentum dependence of the superconducting gap. Their data, shown in Fig. 42, confirm the presence of a very anisotropic gap function with zeros along the diagonal directions (Matsui *et al.*, 2005b) as in BSCCO. They also concluded that the gap function is non-monotonic as found by Blumberg *et al.* (2002) *via* Raman, with the maximum gap value coinciding with the position of the hot spots in the BZ. Matsui *et al.* fit their data with the function: $\Delta = \Delta_o[1.43\cos 2\phi - 0.43\cos 6\phi]$, with $\Delta_o = 1.9$ meV . Intriguingly, the maximum value of the gap extracted from the ARPES data ($\Delta_{max} \sim 2.5$ meV) seems to fall short from the values obtained from other experiments, in particular in comparison to the data of Blumberg *et al.* in Fig. 40, but also tunnelling data giving a maximum gap value of 4 meV for optimal doping (see Section IV.A.2). This could be related to the worse resolution of ARPES, but perhaps also the different materials used for the separate experiments (NCCO vs PLCCO) present slightly different properties. The possibility also

exists that the non-monotonic gap reflects a superposition of superconducting and antiferromagnetic order parameter gaps (Yuan *et al.*, 2006b).
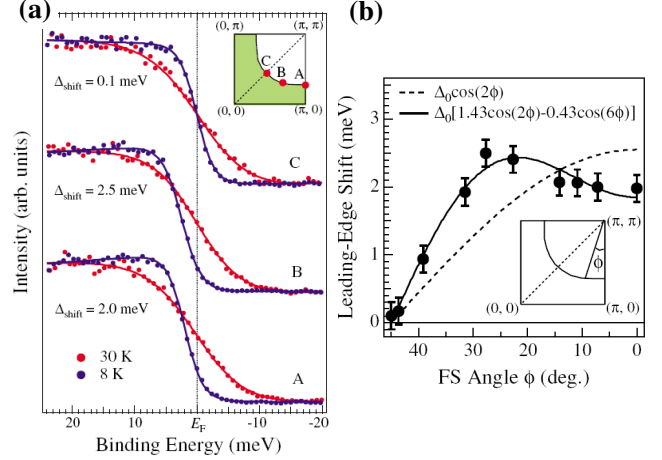

FIG. 42 (a) EDCs from ARPES measurements for temperatures above (30K : red) and below (8K : blue) the transition temperature for $Pr_{0.89}LaCe_{0.11}CuO_4$ single crystals at three distinct points in k-space on the Fermi surface; (b) Leading-edge shift determined as a function of position (angle) on the Fermi surface showing that it fits a non-monotonic *d*-wave symmetry. From Matsui *et al.* (2005b).

5. Specific heat

Specific heat measurements probe the low energy excitations of the bulk and are not sensitive to surface quality. Its temperature and field dependencies away from T_c and H_{c2} in hole-doped cuprates are sensitive to the energy dependence of the density of states below the gap energy. The specific heat for a pure *d*-wave superconductor with line nodes and a linear density of states should have an electronic contribution given by $c_{el}(T) = \gamma_n T^2/T_c$ where $\gamma_n T$ is the expected normal state electronic contribution to the specific heat(Scalapino, 1995; Volovik, 1993). In the presence of a magnetic field at fixed temperature, this electronic contribution should grow as $c_{el}(H) \propto \sqrt{H}$. This is the so-called 'Volovik effect' (Volovik, 1993) for a clean *d*-wave superconductor. Moler *et al.* showed that the electronic specific heat of YBCO, has the expected square root dependence on magnetic field. The temperature dependence exhibited a non-zero *linear* (not T^2) term down to zero temperature (Moler *et al.*, 1994, 1997), which is consistent with various 'dirty *d*-wave' scenarios.

For the electron-doped cuprates, extracting similar information about the electronic contribution to the specific heat is challenging because of its relatively small magnitude with respect to the phonon contribution(Marcenat *et al.*, 1993, 1994), the magnitude of T_c and the relatively small value for $H_{c2} \sim 10T$ [see Refs.

(Balci *et al.*, 2003; Fournier and Greene, 2003; Qazilbash *et al.*, 2005) and references therein]. Moreover, rare-earth magnetism gives rise to additional anomalies at low temperature that makes it difficult to extract the electronic contribution. For this reason, most recent studies of the electronic specific heat to unravel the symmetry of the gap have been performed with PCCO single crystals(Balci and Greene, 2004; Balci *et al.*, 2002; Yu *et al.*, 2005) with its weaker RE magnetism (Sect. II.E). The most recent results demonstrate that the field dependence follows very closely the expected $\gamma(H) \propto \sqrt{H}$ for all superconducting dopant concentrations(Balci and Greene, 2004; Balci *et al.*, 2002; Yu *et al.*, 2005).

The initial measurements on optimally doped PCCO (x = 0.15) showed a large non-zero linear in temperature electronic contribution down to the lowest temperature ($T/T_c \sim 0.1$) very similar to YBCO(Moler *et al.*, 1994, 1997). Furthermore, it presented a magnetic field dependence approaching $\sqrt{H}$ over a 2 - 7K temperature range as long as the field was well below H_{c2}(Balci *et al.*, 2002). Similar to hole-doped cuprates, these features were interpreted as evidence for line nodes in the gap function. However, a subsequent study from the same group seemed to reveal that the temperature range over which $c_{el}(H) \propto \sqrt{H}$ is limited to high temperatures, and that a possible transition (from *d*- to *s*-wave) is observed as the temperature is lowered(Balci and Greene, 2004). However, a different measurement scheme that removes the vortex pinning contribution through field cooling reveals (Fig. 43) that the anomalies interpreted as a possible *d*- to *s*-wave transition are actually resulting from the thermo-magnetic history of the samples (Yu *et al.*, 2005). Thus, the $c_{el}(H) \propto \sqrt{H}$ behavior is preserved down to the lowest temperatures for all dopant concentrations. It extends over a limited field region followed by a saturation at approximately $\mu_o H \sim 6$T interpreted as a value close to the bulk upper critical field. From a quantitative point of view, the analysis of the field dependence using a clean *d*-wave scenario according to $c_{el}/T \equiv \gamma(H) = \gamma_o + A\sqrt{H}$ yields $A \sim 1.92$ mJ/mol K^2 T$^{1/2}$. In the clean limit, this A parameter can be related to the normal state electronic specific heat measured at high magnetic fields leading to $A = \gamma_n \left(8a^2/\pi H_{c2}\right)^{1/2}$(Wang *et al.*, 2001) where a is a constant approaching 0.7. With $H_{c2} \sim 6$T, one gets $\gamma_n \sim 4.1$ mJ/mol K^2 and $\gamma_o + \gamma_n \sim 5.7$ mJ/mol K^2 approaching the normal state Sommerfeld constant measured at 6T. These results confirm that the bulk of the electron-doped cuprates presents specific heat behaviors in full agreement with a dominant *d*-wave symmetry over the whole range of doping at all temperatures explored.

6. Thermal conductivity

Thermal conductivity at very low temperatures is a sensitive probe of the very lowest energy excitations of a system (Durst and Lee, 2000). The electronic contribution to the thermal conductivity given usually by
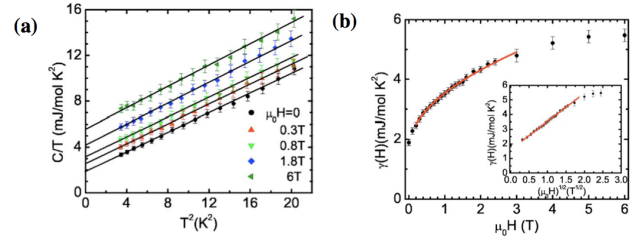

FIG. 43 Specific heat data from Yu *et al.* (2005) on a single crystal of $Pr_{1.85}Ce_{0.15}CuO_4$. In (a), the temperature dependence at various magnetic fields is used to extract the linear-T electronic contribution. (b) Field dependence of the linear in T coefficient that shows close to $\sqrt{H}$ dependence in a magnetic field range considerably below H_{c2}. The red line is a fit to $\gamma(H) = \gamma_o + A\sqrt{H}$. These data show also the saturation of the electronic specific heat at roughly 6T interpreted as the bulk upper critical field.

$\kappa_{el} = \frac{1}{3}c_{el}v_F l$ (where c_{el} is the electronic specific heat, v_F is the Fermi velocity and l is the mean-free path of the carriers) becomes a very sensitive test of the presence of zeroes in the gap function. In the case of conventional BCS s-wave superconductor, the fully gapped Fermi surface leads to an exponentially suppressed number of electronic thermal excitations as $T \to 0$. On the contrary, a non-zero electronic contribution is expected down to the lowest temperatures in a *d*-wave superconductor with line nodes. To extract this part from the total thermal conductivity that includes also a phonon contribution, a plot of κ/T as a function of T^2 yields a non-zero intercept at $T = 0$ (Taillefer *et al.*, 1997). Assuming that $\kappa = \kappa_{el} + \kappa_{ph} = AT + CT^3$, one can compare the measured value of A to the theoretical predictions that relates it to the slope of the gap function at the nodes $[S \equiv \left(\frac{d\Delta}{d\phi}\right)_{node}]$, i.e. its angular dependence along the Fermi surface. Durst and Lee (2000) showed that the electronic part is given by :

$$\frac{\kappa_{el}}{T} = \frac{k_B^2}{3\hbar}\frac{n}{d}\left(\frac{v_F}{v_2} + \frac{v_2}{v_F}\right) \quad (1)$$

where $\frac{d}{n}$ is the average distance between CuO_2 planes. The first term of Eq. 1 is expected to give the primary contribution (for example, $\frac{v_F}{v_2} \sim 14$ in YBCO (Chiao *et al.*, 2000)), such that $\kappa_{el}/T \approx \frac{k_B^2}{3\hbar}\frac{n}{d}\left(\frac{v_F}{v_2}\right)$ where $v_2 = S/\hbar k_F$. For a monotonic *d*-wave gap function, $\Delta = \Delta_o \cos(2\phi)$ such that $\kappa_{el}/T \propto 1/S \propto 1/\Delta_o$. This linear temperature dependence and its link to v_F/v_2 (which is sample-dependent) were confirmed in hole-doped cuprates by Chiao *et al.* (2000) for example. Similar to the specific heat, the Volovik effect should give rise also to $\kappa_{el}(H) \propto \sqrt{H}$ as was observed in YBCO (Chiao *et al.*, 1999).

In the case of the electron-doped cuprates, the low temperature data obtained by Hill *et al.* (2001) show a significant phonon contribution at low temperature as ob-

served in a plot of κ/T as a function of T^2 as evinced by the straight lines in Figure 44. Moreover, a substantial increase of thermal conductivity with the magnetic field confirms the presence of a large electronic contribution growing towards saturation at large fields (roughly 8T), in agreement with the above mentioned specific heat data. However, as demonstrated by the lack of a y-intercept the observed electronic contribution does not extend down to the lowest temperatures as in YBCO(Chiao $et~al.$, 1999). Instead a clear downturn is observed below 200mK that has recently been attributed to thermal decoupling of the charge carriers and the phonons(Smith $et~al.$, 2005). The electrons and the phonons that carry heat are not reaching thermal equilibrium at low temperature because of a poor electron-phonon coupling. This decoupling is obviously a major drawback for a direct extraction of the electronic contribution without the use of a theory(Smith $et~al.$, 2005) and makes it difficult to confirm the presence of a non-zero value at zero field in the electron-doped cuprates.

One can make a crude estimate of the expected linear coefficient of the specific heat A parameter (discussed in Sec. IV.A.5) using $v_F \sim 270$ km/s (Park $et~al.$, 2008; Schmitt $et~al.$, 2008) for nodal quasipartil/k0cle excitations and $v_2 = 2\Delta_o/\hbar k_F$ assuming a monotonic d-wave gap with the tunnelling maximum value of $\Delta_o \sim 4$ meV for optimal doping(Biswas $et~al.$, 2002). This gives $v_F/v_2 \sim 96$ and a $\kappa_{el}/T \approx 0.96$ mW/K^2-cm, which is shown as a blue circle in Fig. 44. Assuming instead a non-monotonic d-wave gap with $\Delta = \Delta_o[1.43\cos 2\phi - 0.43\cos 6\phi$(Matsui $et~al.$, 2005a), with $\Delta_o = 3$ meV (Blumberg $et~al.$, 2002; Qazilbash $et~al.$, 2005) leads to $v_F/v_2 \sim 47$, and $\kappa_{el}/T \approx 0.47$ mW/K^2-cm, which is shown as the red circle in Fig. 44[24]. In Figure 44, an unpublished analysis of the thermal conductivity (courtesy of L. Taillefer) of an optimally doped PCCO sample allows one to isolate the linear term at low temperature as $\kappa_{el}/T \approx 0.60$ mW/K^2-cm by taking into account the thermal decoupling of the charge carriers and the phonons mentioned above(Smith $et~al.$, 2005). This value is intermediate to the estimates given above for monotonic and non-monotonic d-wave superconductors (red and blue dots of Fig. 44). In Fig. 44 one can see the clear downturn from electron-phonon decoupling around 300 mK, which prevents the explicit measurement of κ/T.
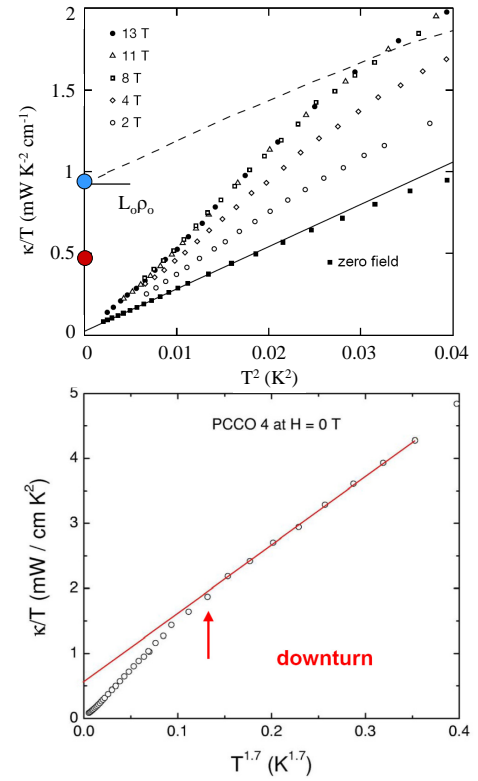
---

[24] Note that we have used the non-monotonic gap function from Matsui $et~al.$ (2005a) but the maximum gap values obtained by Blumberg $et~al.$ (2002); Qazilbash $et~al.$ (2005) to evaluate v_F/v_2. This takes into account the inconsistency between the absolute values of the gap maximum measured by various probes as discussed in section IV.A.3.

FIG. 44 (top) Thermal conductivity of PCCO for a heat current in the basal plane, plotted as κ/T versus T^2, at different values of the magnetic field applied normal to the plane. The solid line is a linear fit to the zero-field data below 130 mK. The dashed line shows the behaviour of a Fermi liquid consisting of the expected electronic part extracted from the Wiedemann-Franz law using the residual resistivity ρ_o for this sample obtained at high magnetic and a phonon contribution given by the solid line (zero-field data). From Hill $et~al.$ (2001). The blue (near (0,1)) and red (near 0,0.5) dots are estimates for the coefficient of the electronic contribution for monotonic and non-monotonic gap functions as given in the text. The experimental data show a zero y-intercept because of electron-phonon decoupling at low temperature. (bottom) Thermal conductivity of an optimal PCCO single crystal for a heat current in the basal plane, plotted as κ/T versus $T^{1.7}$. These data show the downturn to the decoupling of the electron and phonons. Note that the data above the downturn goes as a power of 1.7 and not 2. Courtesy of L. Taillefer.

7. Nuclear Magnetic Resonance

Measuring the nuclear magnetic resonance (NMR) response of electron-doped cuprates is also a difficult task because of the large magnetic contribution of the rare earth ions. It leads to dipolar and quadripolar local field that makes interpretation difficult. For this reason, only measurements with Pr and La (and eventually Eu) as the rare earth atoms have been of real interest to extract the symmetry of the order parameter. Zheng $et~al.$ (2003) have shown explicitly that the spin relaxation rate $1/T_1$ of ^{63}Cu in x=0.11 PLCCO falls dramatically in the super-

conducting state over some temperature range following a power law close to T^3 as shown in Figure 45. This temperature dependence is consistent with the existence of line nodes and a d-wave superconducting order parameter as was observed in hole-doped cuprates(Asayama et al., 1996). At the lowest temperatures the relaxation rate deviates from T^3 behavior which was interpreted by Zheng et al. (2003) as a consequence of disorder scattering. Also consistent with d-wave, there was no sign of a Hebel-Schlicter peak just below T_c (see also Fig. 45) which is a signature of class II coherence factors and s-wave superconductivity. A comparison of the data with calculation using a $d_{x^2-y^2}$ order parameter reveals a superconducting gap $2\Delta_0 = 3.8\ k_B T_c$, which is consistent with many other probes.
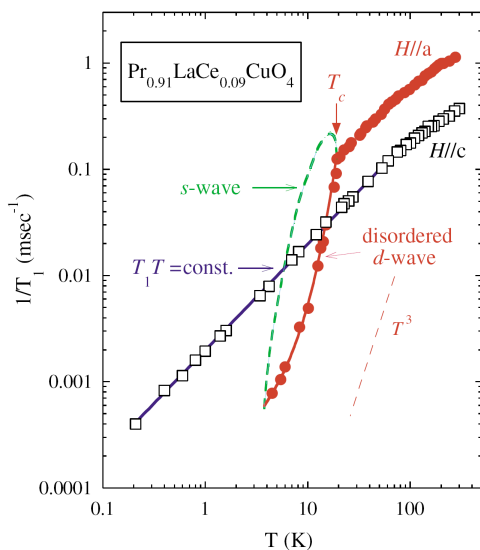

FIG. 45 ^{63}Cu spin relaxation rate $1/T_1$ as a function of temperature in the superconducting and the normal states of a $Pr_{0.91}LaCe_{0.09}CuO_{4-y}$ single crystal. Red solid circles: data in the superconducting state measured with a magnetic field of 6.2T parallel to the CuO_2 planes. Open black circles : data in the normal state measured with an out-of-plane magnetic field of 15.3T. The red solid line is a fit using a $d_{x^2-y^2}$ order parameter leading with $2\Delta_0 = 3.8\ k_B T_c$. The solid line is a fit to the Korringa law, which is consistent with Fermi liquid behavior. From Zheng et al. (2003).

8. Neutron scattering

As discussed above in III.F.2, in the inelastic neutron scattering response of PLCCO Wilson et al. (2006a) found an enhancement of the intensity (Fig. 36) at approximately 11 meV at $(1/2,1/2,0)$ (equivalent to (π,π) in the superconducting state. This was interpreted as being the analog of the much heralded 'resonance' peak

(Rossat-Mignod et al., 1991) found in many of the hole-doped compounds. Zhao et al. (2007) has claimed that optimally doped NCCO has a similar resonance at 9.5 meV although this has been disputed by Yu et al. (2008), who claim that a sub gap resonance is found at the much smaller energy of ≈ 4.5 meV as shown in Fig. 37. Irrespective of where exactly this peak is found, the observation is strong evidence for d-wave superconductivity, as the superconducting coherence factors impose that a (π,π) excitation can only exist in the superconducting state if the OP changes sign under this momentum translation (Bulut and Scalapino, 1996; Manske et al., 2001a). The resonance feature in the n-type compounds appears to turn on at T_c as seen in Fig. 36.

9. Phase sensitive measurements

Some of the most convincing and definitive experiments to demonstrate the d-wave pairing symmetry in the hole-doped cuprates measure the phase of the order parameter directly instead of its magnitude. Such techniques are sensitive to changes in the sign of the pair wave-function in momentum space. Most are based on the fact that the current flowing through a Josephson junction is sensitive to the phase difference between superconducting electrodes(Tinkham, 1996). By designing very special geometries of junctions and SQUIDs (Superconducting Quantum Interference Devices) that incorporate high-T_c and possibly conventional superconductors, one can demonstrate the presence of the sign change in the order parameter(van Harlingen, 1995; Tsuei and Kirtley, 2000a). Quasiparticle tunnelling can also be sensitive to the sign change. The presence of the so-called Andreev bound states at the interface of normal-insulator-superconductor (N-I-S) tunnel junctions is a direct consequence of the particular symmetry of the high-T_c cuprates.

The most convincing phase sensitive measurement for the electron-doped cuprates has been reported by Tsuei and Kirtley (2000b) who observed a spontaneous half flux quantum $(\phi_o/2)$ trapped at the intersection of a tricrystal thin film. This epitaxial thin-film-based experiment has been used extensively by the same authors to demonstrate the universality of the d-wave order parameter for hole-doped cuprates(Tsuei and Kirtley, 2000a). It relies on the measurement of the magnetic flux threading a thin film using a scanning SQUID microscope. When the epitaxial thin film is deposited on a tri-crystal substrate with carefully chosen geometry as in Figure 46(a), Josephson junctions are formed in the films at the grain boundaries of the substrates(Hilgenkamp and Mannhart, 2002). The presence of spontaneous currents induced by phase frustration at the tri-crystal junction point is a definitive test of a sign change in the order parameter.

In the case of the electron-doped cuprates, Tsuei and Kirtley (2000b) showed using a fit of the magnetic field (Kirtley et al., 1996) as a function of position that the

magnetic flux at the tri-crystal junction in Fig. 46(b) corresponds to half a flux quantum (Tsuei and Kirtley, 2000b). This observation was made despite very small critical current densities for the junctions along the grain boundaries, implying very weak coupling and very long penetration depth of the field along the grain boundary junctions. Similar to hole-doped cuprates (van Harlingen, 1995; Tsuei and Kirtley, 2000a), this observation is consistent with pure d-wave pairing symmetry.
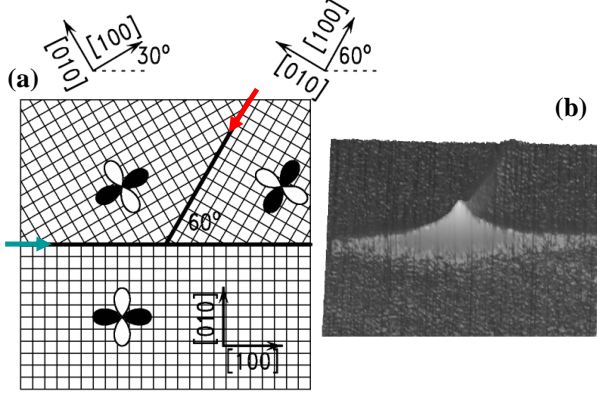

FIG. 46 (a) Tri-crystal geometry used to force phase frustration and spontaneous generation of a half-flux quantum at the tri-crystal junction point. The red and the blue arrows indicate the diagonal and horizontal grain boundaries respectively; (b) 3D image of the flux threading the film. Adapted from Ref. (Tsuei and Kirtley, 2000b).

FIG. 47 Zigzag ramp-edge Josephson junctions made of $Nd_{2-x}Ce_xCuO_4$ and conventional s-wave Nb. (a) Top view of the zigzag design; (b) Cross-section view of a ramp-edge junction including a thin interlayer of NCCO. Examples of anomalous field modulations of the critical current arising from the d-wave symmetry for devices made of (c) 8 facets of $25\mu m$ width and (d) 80 facets of $5\mu m$ width. From Ariando *et al.* (2005).

Ariando *et al.* (2005) fabricated ramp-edge junctions between NCCO (x = 0.15 and 0.165) and Nb in a special zigzag geometry as shown in Figure 47. Since the critical current density of the NCCO/Au/Nb ramp-edge junctions is very small ($J_c \sim 30$ A/cm^2), the zigzag geometry presented by Ariando *et al.* is in the small junction limit and one expects an anomalous magnetic field dependence in the d-wave case. For instance, one can note that the critical current density of this zigzag junction is suppressed at zero field. As one applies a small magnetic field to this junction, the critical current grows and then oscillates as the first quanta of flux penetrate the zigzag junction. Ariando *et al.* demonstrate an order parameter consistent with d-wave symmetry. In a similar experiment Chesca *et al.* (2003) patterned a $500\mu m$ thick LCCO film made by MBE on a tetracrystal substrate to create a π-SQUID at the junction point. The minimum in critical current at zero field for the π-design is consistent with d-wave pairing symmetry(Chesca *et al.*, 2003).

10. Order parameter of the infinite layer compounds

Although measurements of the normal state properties of the infinite layer compound SLCO are rare, there have
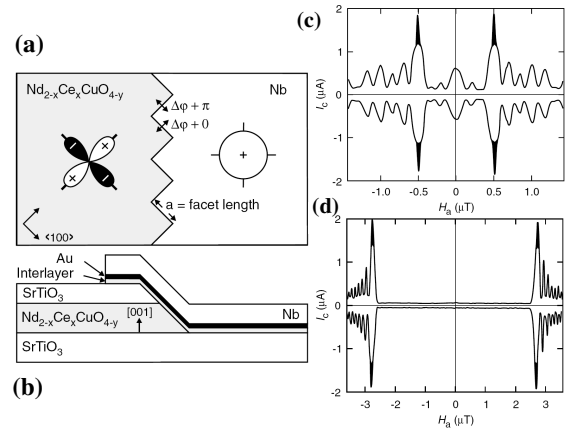
been a few experiments on their pairing symmetry. In general, measurements on the infinite layer compounds have been hampered by a lack of single crystals or thin films and give conflicting conclusions. The spatial independence of the STM spectra observed when performing a line scan across many randomly oriented grains on a polycrystalline sample has, along with the lack of ZBCP, been interpreted as being consistent with an s-wave symmetry(Chen *et al.*, 2002). Low temperature specific heat (Liu *et al.*, 2005) also suggests a conventional s-wave pairing symmetry while NMR suggests an unconventional, non s-wave, symmetry (Imai *et al.*, 1995). Stronger suppression of T_c by the magnetic impurity Ni than the nonmagnetic impurity Zn is indirect supporting evidence for s-wave (Jung *et al.*, 2002). Chen *et al.* (2002) also concluded in their STM study that the suppression of their tunneling coherence peaks with Ni doping, in contrast to the much smaller effect with Zn doping, was consistent with an s-wave symmetry. This is a system that certainly needs further investigation, both on the materials side as well as high quality experimentation. Measurements like μSR have not been able to measure the T dependence of the penetration depth to determine the pairing symmetry as they require single crystal (Shengelaya *et al.*, 2005).

B. Position of the chemical potential and midgap states

One long outstanding issue in the cuprates is the position of the chemical potential μ upon doping. In the case that the cuprates are in fact described by some Mott-Hubbard-like model, the simplest scenario is that the

chemical potential shifts into the lower Hubbard band (or CTB) upon hole doping and into the upper Hubbard band upon electron doping (see Fig. 4). This is the exact result for the one dimensional Hubbard model (Woynarovich, 1982). In contrast, dynamic mean field theory (DMFT) calculations show that, at least for infinitely coordinated Mott-Hubbard system, for doped systems μ lies in coherent mid-gap states (Fisher *et al.*, 1995). In a similar fashion, systems which have a tendency towards phase separation and inhomogeneity will generically generate mid-gap states in which the chemical potential will reside (Emery and Kivelson, 1992). The position of the chemical potential and its movement upon doping is an absolutely central issue, as its resolution will shed light on the local character of the states involved in superconductivity, the issue of whether or not the physics of these materials can in fact be captured by Mott-Hubbard like models, and the fundamental problem of how the electronic structure evolves from that of a Mott insulator to a metal with a large Luttinger theorem (Luttinger, 1960) respecting Fermi surface.

In the first detailed photoemission measurements of the *n*-type cuprates, Allen *et al.* (1990) claimed that μ did not cross the insulator's gap upon going from hole to electron doping and lies in states that fill the gap. This inference was based on a comparison of the angle integrated valence band resonant photoemission spectra of $Nd_{2-x}Ce_xCuO_4$ at x=0 and 0.15 with $La_{2-x}Sr_xCuO_4$ which showed that the Fermi level lies at nearly the same energy in both cases as compared to the valence band maximum. Similar conclusions based on x-ray photoemission have been reached by other authors (Matsuyama *et al.*, 1989; Namatame *et al.*, 1990). However, these results have been called into question by Steeneken *et al.* (2003) who showed that due to the large $4f$ electron occupation of $Nd_{2-x}Ce_xCuO_{4-y}$ (not to mention the crystal structure differences) the valence band maximum in NCCO is dominated by $4f$ electrons, making it a poor energy reference for the chemical potential. They proposed instead that the appropriate reference for the internal energies of the copper oxygen plane across material classes was the peak at the $3d^8$ final states of the photoemission process, which represents configurations where the hole left from electron removal has its majority weight on the copper site instead of an oxygen (a $3d^9\underline{L}$ configuration).

These $3d^9 \rightarrow 3d^8$ electron removal states are expected to be found at an energy approximately U (the microscopic onsite Hubbard interaction energy) below the $3d^{10} \rightarrow 3d^9$ states and so give a good energy reference that refers directly to the electronic structure of the CuO_2 plane. $3d^{10}$ initial states are assumed to be the primary result of electron doping, as electrons are believed to mostly be doped to Cu orbitals. Lining up valence band spectra to the $3d^8$ states (see Fig. 48), Steeneken *et al.* (2003) found that both Nd_2CuO_4, La_2CuO_4, and $La_{1.85}Sr_{0.15}CuO_4$ showed a spectral weight onset at the same energy (approximately 13 eV above the $3d^8$ reference), which was presumably the CTB. However,
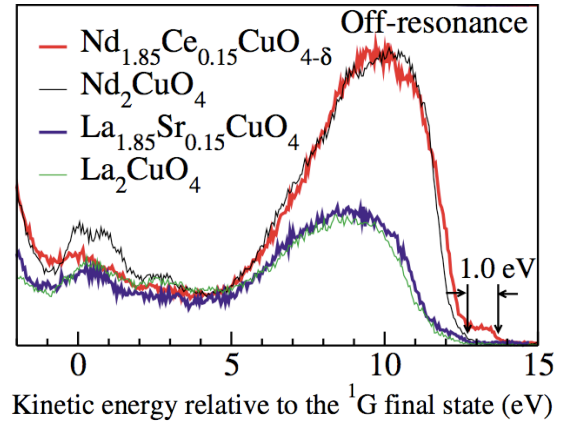

FIG. 48 (color) Photoemission valence band spectra of $Nd_{1.85}Ce_{0.15}CuO_{4-\delta}$, Nd_2CuO_4, La_2CuO_4, and $La_{1.85}Sr_{0.15}CuO_4$ taken 5eV below the Cu L_3 edge. Energies of the spectra are aligned with respect to the Cu $3d^8$ ^1G final states. From Steeneken *et al.* (2003).

$Nd_{1.85}Ce_{0.15}CuO_{4-\delta}$ showed an onset approximately 1eV higher and so it was concluded that the chemical potential shifts by approximately this amount (across the charge transfer gap) going from lightly hole- to electron-doped materials. As the onset in the optical charge transfer gap is of this order (1 -1.5 eV (Tokura *et al.*, 1990)), it was concluded that μ lies near the bottom of the conduction band (presumably the upper Hubbard band) of the Ce doped system and near the top of the valence band (presumably the primarily oxygen derived CTB) for the Sr doped system. A similar conclusion was reached in hard x-ray photoemission (Taguchi *et al.*, 2005), which is more bulk sensitive. The study of Steeneken *et al.* (2003) also concluded that the local character of the $3d^{10}$ near E_F states was singlet.

This conclusion with respect to hole doping is different than was inferred from ARPES studies on $La_{2-x}Sr_xCuO_4$, which posited that μ was found in mid-gap states derived from inhomogeneities (Ino *et al.*, 2000). It is however consistent with work on the $Na_{2-x}Ca_xCuO_2Cl_2$ system which finds that with light hole doping the chemical potential is always found near the top of the valence band (Ronning *et al.*, 2003; Shen *et al.*, 2004). It is also consistent with the ARPES work of Armitage *et al.* (2002) who found that for lightly electron-doped $Nd_{1.86}Ce_{0.04}CuO_4$ the chemical potential sat an energy approximately 1 eV above the onset of the CTB (which could be imaged simultaneously). As discussed above, there was evidence for in-gap states, but these filled in the gap at energies below E_F. Additionally at this low doping, the near E_F states formed a Fermi pocket at $(\pi, 0)$, which is the expectation upon electron doping for many Hubbard-like models (see for instance (Tohyama, 2004) and references therein). Note that the studies of Steeneken *et al.* (2003) and Armitage *et al.* (2002) do not rule out scenarios where the chemical po-

tential lies pinned in doping induced in-gap states. They only show that this pinning does not take the chemical potential very far from the band edges. The scenario proposed by Taguchi *et al.* (2005) is shown in Fig. 49.
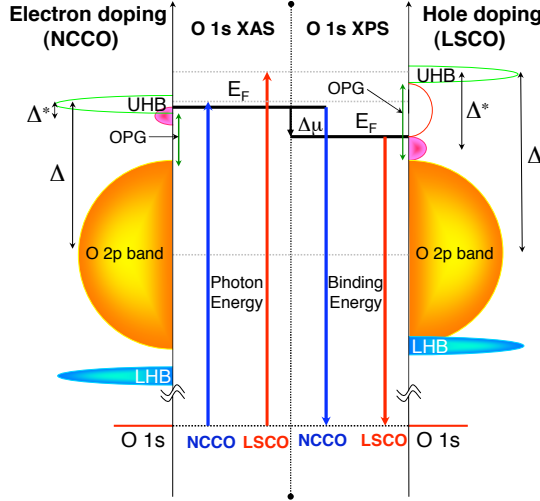

FIG. 49 (Color) Schematic illustration of the energy levels of LSCO and NCCO obtained from Anderson impurity model calculations and x-ray photoemission. OPG is the optical gap from undoped materials. Shaded regions represent occupied density of states. The manifold of O 2p bands are found to be displaced relative to the primarily Cu derived Hubbard-like bands between LSCO and NCCO. This explains the very small shift in the O 1s core level data when comparing hole- and electron-doped data. From Taguchi *et al.* (2005).

C. How do we even know for sure it is n-type?

Related to the issue of the position of the chemical potential is the even more basic issue of whether these materials can even be considered truly n-type. It is usually assumed (and been assumed throughout this review) that these compounds are the electron-doped analog of the more commonly studied hole-doped compound. However, there is no reason to believe *a priori* that the class of $RE_{2-x}Ce_xCuO_4$ compounds must be understood in this fashion. The effects of Ce doping could be of a completely different nature. For instance, an analysis based on the aqueous chemical redox potentials shows that Ce^{+3} may have difficulty reducing Cu^{+2} to Cu^{+1} (Cummins and Egdell, 1993). And even if electrons are actually introduced to the CuO_2 plane by Ce substitution, there is no guarantee that the correct way to think about its effects is by adding electrons into an upper Hubbard band in a fashion exactly analogous to adding holes to an effective lower Hubbard band. There have been been suggestions for instance that due to structural considerations the effect of Ce doping is to liberate holes (Billinge and Egami, 1993; Hirsch, 1995), or that doped electrons instead go into a band formed of extended relatively uncorrelated

Cu 4s states (Okada *et al.*, 1990) or an impurity band (Tan *et al.*, 1990). Meanwhile there is also the evidence discussed extensively above for simultaneous electron and hole contributions to transport (Fournier *et al.*, 1997; Gollnik and Naito, 1998; Wang *et al.*, 1991) and claims that these compounds have a 'negative charge transfer gap' (Cummins and Egdell, 1993). Are these compounds really n-type/electron-doped? There are a few different ways to phrase and answer this question.

Do the CuO_2 planes of the doped compounds have local charge densities greater than the insulator? - This is perhaps the most basic definition of electron doping. In principle high energy spectroscopies like x-ray core level photoemission (XPS), x-ray absorption (XAS) and electron energy loss spectroscopy (EELS) can probe the valence state of local orbitals (See Ignatov *et al.* (1998) for a good overview). As discussed above, naively one expects that electrons liberated from doped Ce will reside primarily in $3d$ orbitals nominally giving Cu $3d^{10}$. This appears to be the case.

The first Cu K-edge x-ray absorption study from Tranquada *et al.* (1989) concluded that $3d^{10}$ states formed upon Ce substitution, however a number of other early studies gave conflicting results (Fujimori *et al.*, 1990; Ishii *et al.*, 1989; Nücker *et al.*, 1989). Note that in general, most of these kind of spectroscopies suffer from a strong sensitivity to surface quality. In many of these measurements surfaces were prepared by scraping poly-crystalline ceramics (resulting in significant contamination signal as judged by the appearance of a shoulder on the high energy side of the main O 1s peak) or by high-temperature annealing which undoubtedly changes the surface composition (Cummins and Egdell, 1993). In contrast, in most of the measurements emphasized here, surfaces were prepared by breaking single crystals open in vacuum or the technique was inherently bulk sensitive (EELS or XAS in transmission or fluorescence yield mode for example).

Via Ce core level photoemission Cummins and Egdell (1993) demonstrated that Ce substitutes as Ce^{+4} rather than Ce^{+3} across the full doping range showing that the effects of Ce subsitution is electron donation. With EELS Alexander *et al.* (1991) observed that Th doping into $Nd_{1.85}Th_{0.15}CuO_4$ caused a 14% reduction in the relative intensity of the Cu $2p_{3/2}$ excitonic feature and only minor changes to the O $2p$ states, which is consistent with doping the Cu sites. Similarly, Liang *et al.* (1995) found that across the family of $RE_{2-x}Th_xCuO_4$ (RE = Pr, Nd, Sm, Edu, and Gd) that Cu $3d^{10}$ features in the XAS Cu K edge spectra increases linearly with Ce doping as shown in Fig 50. A similar picture was arrived at by Pellegrin *et al.* (1993). In x-ray core level photoemission Steeneken *et al.* (2003) observed that the $2p3d^9$ "satellites" decreased in intensity with increasing Ce content, while new structures like $2p3d^{10}$ appear (where $2p$ denotes a photoemission final state with a Cu core hole). Additionally they found that the Cu L_3 x-ray absorption spectra intensity decreases with Ce doping. As this absorption is dominated by the transition

$3d^9 + h\nu \rightarrow \underline{2p}3d^{10}$, these results also imply that Ce doping results in a decrease of the Cu^{+2} and increase in Cu^{+1} content. The nominal $3d^{10}$ configuration of an added electron has also been confirmed *via* a number of resonant photoemission studies which show a Cu $3d$ character at the Fermi level (Allen *et al.*, 1990; Sakisaka *et al.*, 1990). All these studies provide strong support for the expected increase in the mean $3d^{10}$ electron count with Ce doping[25].

As discussed above, in neutron scattering, Mang *et al.* (2004b) found that the *instantaneous* AF correlation length of doped unreduced NCCO can be described by a quantum Monte Carlo calculations for the randomly site-diluted nearest-neighbor spin 1/2 square-lattice Heisenberg antiferromagnet. Setting the number of non-magnetic sites to within $\Delta x \approx 0.02$ of the nominal Ce concentration gave quantitative agreement with their calculation. This also shows that every Ce atom donates approximately one electron to the CuO_2 planes.
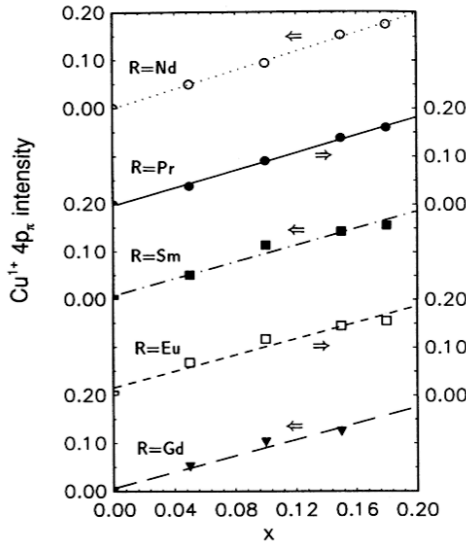

FIG. 50 Peak height of the Cu^{+1} $4p_\pi$ spectral feature in the Cu K-edge XAS spectra as a function of Ce concentration for various (RE)CCO compounds. Its intensity is approximately proportional to the $3d^{10}$ occupation. From Liang *et al.* (1995).

Does the enclosed volume of the FS reflect a metallic band that is greater than half-filled? - This is an equivalent question to the one immediately above if one agrees that there is a single metallic band that crosses E_F which is formed out of Cu $d_{x^2-y^2}$ and O $2p_{x,y}$ states. However,

this specific issue can be addressed in a different, but very direct fashion from the area of the FS as measured by ARPES. If one neglects the issue of 'hot-spots' and speaks only of the underlying FS the Luttinger sum rule appears to be approximately obeyed (King *et al.*, 1993). Armitage *et al.* (2001b) found that in NCCO the enclosed volume is 1.09 for a nominally $x = 0.15$ NCCO sample. Others have found FS volumes closer to that expected (Park *et al.*, 2007; Santander-Syro *et al.*, 2009), but in all cases the Luttinger sum rule is consistent with a band greater than half-filling (approximately $1 + x$). As hole-doped systems seem to have a Luttinger volume which closely reflects the number of doped holes $1 - x$ (Kordyuk *et al.*, 2002), in this sense also (RE)CCO systems can be regarded as electron-doped.

What is the nature of charge carriers from transport? - It was pointed out early on that there are both hole and electron contributions to transport (Fournier *et al.*, 1997; Gollnik and Naito, 1998; Wang *et al.*, 1991). At low concentrations an electron contribution is naively expected within a model of electrons being doped into a semiconductor. At higher dopings these observations were at odds with the shape of the experimentally determined FS, which King *et al.* (1993) had found to be a large hole pocket centered at (π,π). Later, it was found by Armitage *et al.* (2001b, 2002) that at low dopings the FS was a small electron pocket around the $(\pi,0)$ position. At higher dopings there is a rearrangement of the electronic structure and a large Fermi surface is developed, which derives from electron- and hole-like sections of the FS and may retain remnant signatures of them. Therefore the hole-like experimental signatures may result from electron doping itself. These issues are discussed in more detail above in Sec. III.A.1 and III.C.

Do doped electrons occupy electronic states analogous to those occupied by holes in the p-type compounds? - As discussed in a number of places in this review (see Section II.B), although the local orbital character of doped electrons is undoubtedly different than doped holes within certain models, under certain circumstances one can map the hole and electron addition states to an effective Hubbard model with an approximate electron-hole symmetry. Although mid-gap states are undoubtedly also created upon doping, it appears (Sec. IV.B) that the chemical potential crosses the effective Hubbard gap (formally the CT gap) upon moving from hole to electron doping. Additional evidence for the existence of an effective upper Hubbard band in NCO comes from Alexander *et al.* (1991) who found the same prepeak in undoped (RE)CO and doped (RE)CCO O $1s \rightarrow 2p$ EELS absorption spectra as found in LCO. To first approximation this absorption probes the local unoccupied O density of states. Here however this prepeak is not interpreted as holes in a nominally filled $2p^6$ local configuration and instead has been interpreted as excitations into a Hubbard band of predominantly Cu $3d$ character with a small O $2p$ admixture as expected. In this way Ce doping may be described as the addition of electrons to an effective

---

[25] Similar studies on the hole-doped compounds in contrast give no evidence for $3d^{10}$ occupation and instead signatures of O $2p$ holes are found, which is consistent with the picture presented above in which doped holes reside primarily on the in-plane oxygen atoms. See for instance, Alp *et al.* (1987); Kuiper *et al.* (1988) and references therein.

upper Hubbard band, just as hole doping is the addition of holes to an effective lower Hubbard band. In this sense also these systems may be considered as electron-doped.

D. Electron-phonon interaction

There has been increasing discussion on the subject of strong electron-phonon coupling in the cuprate high temperature superconductors. This has been inferred from both possible phonon signatures in the charge spectra (Lanzara *et al.*, 2001; Lee *et al.*, 2006a), as well as directly in the doping induced softening of a number of high-frequency oxygen bond-stretching modes in many $p-$type cuprates as observed by neutron and x-ray scattering (Fukuda *et al.*, 2005; McQueeney *et al.*, 1999, 2001; Pintschovius and Braden, 1999; Pintschovius *et al.*, 2006; Uchiyama *et al.*, 2004).

In NCCO Kang *et al.* (2002) did find changes with doping in the generalized phonon density of states around ≈ 70 meV by neutron scattering. Although this is a similar energy scale as the softening is found on the hole=doped side, on general grounds one may expect a number of differences in the electron-phonon coupling between p- and n-type doping. Since the purported soft phonon is the oxygen half-breathing mode, one might naively expect a weaker coupling for these modes with electron doping, as Madelung potential considerations(Ohta *et al.*, 1991; Torrance and Metzger, 1989) indicate that doped electrons will preferentially sit on the Cu site, whereas doped holes have primarily oxygen character. The biggest changes in the phonon density of states probed by Kang *et al.* (2002) happen at similar doping levels in $La_{2-x}Sr_xCuO_4$ and $Nd_{2-x}Ce_xCuO_4$ ($x \approx 0.04$), however the doping levels are at very different relative positions in the phase diagram, with $x = 0.04$ being still well into the antiferromagnetic and more insulating phase for the electron-doped compound. As such modifications in the phonon spectrum may be associated generally with screening changes (and hence electron-phonon coupling) with the onset of metallicity, this demonstrates the possibility that the changes in the NCCO phonon spectrum, although superficially similar in the electron and hole-doped materials, may have some differences.

Irrespective of these expectations and differences, a number of similar signatures of phonon anomalies have been found in the electron-doped compounds. As mentioned above, although initial measurements of the electron-phonon coupling in the ARPES spectra seemed to give little sign of the 'kink' in the angle-resolved photoemission spectra (Armitage *et al.*, 2003), which has been taken to be indicative of strong electron-phonon coupling on the hole-doped side of the phase diagram, more recent measurements show evidence for such a kink (Liu *et al.*, 2008; Park *et al.*, 2008; Schmitt *et al.*, 2008). This work gives some evidence that electron-phonon interaction may not be so different on the two sides of the phase diagram.

A number of features in the optical conductivity also have been assigned to polaron-like absorptions and Fano antiresonance features (Calvani *et al.*, 1996; Lupi *et al.*, 1998, 1999). For instance, pseudogap features and renormalizations in the infrared response have been interpreted (Cappelluti *et al.*, 2009) in terms of lattice polaron formation within the Holstein$-t-J$ model in the context of DMFT. Cappelluti *et al.* (2009) point that the moderately large electron-phonon coupling of $\lambda \approx 0.7$ they extract is still not large enough to induce lattice polaron effects in the absence of exchange coupling. This means that if lattice polaronic features exist in these compounds, they can be found only in the presence of (short-range) AF correlations. The disappearance of pseudogap features near the termination of the AF phase is then consistent with this interpretation.

d'Astuto *et al.* (2002) measured NCCO's phonon dispersions *via* inelastic x-ray scattering and assigned the softening in a similar 55 - 75 meV energy range to the same oxygen half-breathing mode in which softening is found in the p-type materials. They claimed that the general softening of the phonon dispersion appears in a roughly similar way at a similar energy scale as in the $p-$types compounds, and that differences in the precise shape of the anomaly in the phonon dispersion are due to an anti-crossing behavior of the bond-stretching modes with the lower energy O(2) mode in the [100] direction. Braden *et al.* (2005) later confirmed that with higher accuracy neutron scattering measurements (which present similar oxygen and heavy-ion dynamic structure factors) that all cuprates including NCCO are found to have roughly similar phonon anomalies along the [100] direction, showing a drop of ≈ 3 THz (12.4 meV) as shown in Fig. 51. The differences between compounds are larger along the [110] direction (Fig. 51), but still small overall. This indicates that all these systems (as well as many other perovskites (Fig. 51) have aspects of their electron-phonon coupling that have roughly similar character.

We should point out that very recent even higher resolution scattering experiments have shown that there are some specific phonon features in p-type compounds that are likely related to charge ordering instabilities (i.e. stripes) (d'Astuto *et al.*, 2008; Reznik *et al.*, 2006). These studies show that in the phonon dispersions one of the two normally degenerate components follows the smoother cosine-like dispersion while the other presents a much sharper dip, which has been interpreted as a Kohn-like anomaly at the stripe ordering wavevector. Considering that there is little evidence for stripes in the electron-doped compounds, it would be very interesting to do such similar high resolution measurements on $n-$type materials.
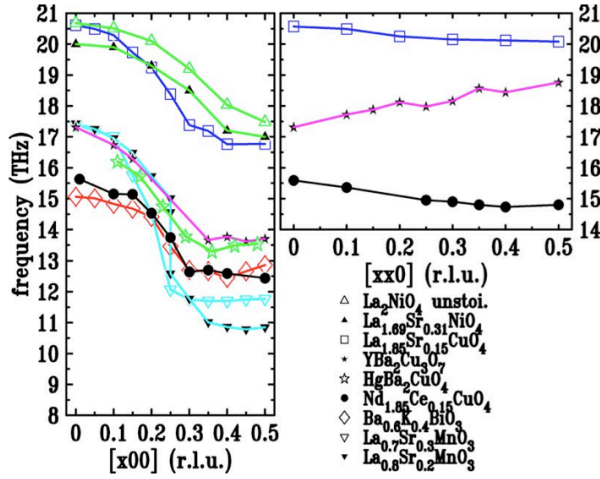
FIG. 51 (Color) Comparison of the phonon anomaly in the bond-stretching branches observed *via* neutron scattering in a number of metallic oxide perovskites. (left) [100] direction. (right) [110] direction. From Braden *et al.* (2005).

E. Inhomogeneous charge distributions

Doping a Mott insulator does not automatically result in a spatially homogenous state (Emery and Kivelson, 1993; Lee and Kivelson, 2003). The magnetic energy loss that comes from breaking magnetic bonds by doping charge can be minimized by forming segregated charge rich regions. This tendency towards phase separation can lead to scenarios in which charges phase separate into various structures including charge puddles, stripes (Carlson *et al.*, 2003; Emery and Kivelson, 1993; Kivelson *et al.*, 2003; Machida, 1989; Mook *et al.*, 1998, 2002; Tranquada *et al.*, 1995; Zaanen and Gunnarsson, 1989), or checkerboard patterns (Hanaguri *et al.*, 2004; Seo *et al.*, 2007). There is extensive evidence for such correlations in the hole-doped cuprates (Kivelson *et al.*, 2003).

The situation is much less clear in the n-type compounds. As some of the strongest evidence for 'stripe' correlations in the hole-doped materials has come from the preponderance of incommensurate spin and charge correlations, the commensurate magnetic response has been taken as evidence for a lack of such forms of phase separation in these materials. However, Yamada *et al.* (2003) has pointed out that the commensurate short range spin correlations detected by neutron scattering in the SC phase of the n-type cuprates can reflect an inhomogeneous distribution of doped electrons in the form of droplets/bubbles in the CuO_2 planes. The commensurate magnetic signatures may also arise from 'in-phase' stripe domains as contrasted to the 'antiphase' domains of stripes in the p-type compounds (Sun *et al.*, 2004). This issue of stripe-like structures in the n-type materials has been investigated theoretically and numerically (See Aichhorn and Arrigoni (2005); Kusko *et al.* (2002);

Sadori and Grilli (2000) for instance.). There is some evidence that numerical models which give stripes on the hole-doped side, give a homogeneous state on the electron-doped side (Aichhorn *et al.*, 2006). One can then consider the possibility of phase separation and inhomogeneity an open issue.

There has been a number of studies that have argued for an inhomogeneous state in the electron-doped curpates. Sun *et al.* (2004) found in $Pr_{1.3-x}La_{0.7}Ce_xCuO_4$ the same unusual transport features that have been argued to be evidence for stripe formation in LSCO (Ando *et al.*, 2001). They measured the *ab*-plane and c-axis thermal conductivity and found an anomalous damping of the c-axis phonons, which has been associated with scattering off of lattice distortions induced by stripes which are relatively well ordered in the plane, but disordered along the c axis. In the AF state the *ab*-plane resistivity is consistent with "high mobility" metallic transport, consistent with motion along "rivers of charge." They interpret these peculiar transport features as evidence for stripe formation in the underdoped n-type cuprates. In $Pr_{1.85}Ce_{0.15}CuO_4$ Zamborszky *et al.* (2004) found signatures in the NMR spin-echo decay rate ($1/T_2$) for static inhomogeneous electronic structure. Similarly, Bakharev *et al.* (2004) found *via* Cu NMR evidence for an inhomogeneous "blob-phase" (bubble) in reoxygenated superconducting $Nd_{1.85}Sr_{0.15}CuO_4$. Moreover, Granath (2004) has shown that some unusual aspects of the doping evolution of the FS found by ARPES (Armitage *et al.*, 2002) could be explained by an inhomogeneous in-phase stripes or 'bubble' phases. 'Bubble' phases, where the doped charge is confined to small zero-dimensional droplets instead of the one-dimensional stripes, arise naturally instead of stripes in $t - J$ type models with long-range Coulomb repulsion in the limit of $t << J$, because of the lower magnetic energy (Granath, 2004). They may be favored in the electron-doped materials, which have more robust antiferromagnetism than the hole-doped materials. From their neutron scattering Dai *et al.* (2005) argue that $x = 0.12$ PLCCO is electronically phase separated and has a superconducting state, which coexists with both a 3D AF state and a 2D commensurate magnetic order that is consistent with in-phase stripes. Onose *et al.* (1999) found infrared and Raman Cu-O phonon modes that grew in intensity with decreasing temperature in unreduced crystals. This was interpreted as being due to a charge ordering instability promoted by a small amount of apical oxygen.

In contrast to these measurements, Williams *et al.* (2005) found no sign of the Cu NMR "wipe out" effect in x=0.15 PCCO which has been interpreted to be consistent with spatial inhomogeneity in $La_{2-x}Sr_xCuO_4$ (Singer *et al.*, 1999). Similarly, in the first spatially resolved STM measurements Niestemski *et al.* (2007) showed that $T_c = 12K$ PLCCO had a relatively narrow gap distribution of 6.5 - 7.0 meV (Fig. 27), with no signs of the gross inhomogeneity of some p-type compounds (Howald *et al.*, 2001; Lang *et al.*, 2002). In

neutron scattering Motoyama *et al.* (2006) found that the field induced response at low temperature is momentum resolution limited, which implies that the dynamic magnetic correlations are long-range (¿200 Å) with correlation lengths that span vortex-core and SC regions. This provides further evidence that NCCO forms a uniform state. Circumstantial evidence for a homogeneous doped state also comes from other neutron measurements, where it has been found that the spin pseudogap closes with increasing temperature and field, in contrast to the hole-doped material where it is better described as "filling in" (Motoyama *et al.*, 2007; Yamada *et al.*, 2003). This 'filling-in' behavior has been associated with phase separation and so its absence argues against such phenomena in the *n*-type cuprates.

Finally there is the very interesting result of Harima *et al.* (2001) (Fig. 52) who demonstrated that the chemical potential shifts very differently with hole and electron doping, which argues against phase separation in the *n*-type compounds. Harima *et al.* (2001) compared the chemical potential shifts in NCCO and LSCO *via* measurements of core-level photoemission spectra. Although the relative shift between LCO and NCO was uncertain in such measurements due to different crystal structures, they found that the chemical potential monotonously increases with electron doping, in contrast to the case of hole doping, where the shift is suppressed in the underdoped region (Fig. 52 (top)). The differences were ascribed to a tendency towards phase separation and mid-gap states in LSCO as compared to NCCO in this doping region (Fig. 52 (middle)). We should note however that this suppression of the chemical potential shift in the hole-doped compounds does not seem to be universal as Bi2212 shows a much smaller suppression (Harima *et al.*, 2003) and Na doped CCOC (Yagi *et al.*, 2006) apparently none at all. Interestingly however, they found that the previously discussed electron-hole asymmetry of the NCCO/LSCO phase diagram with respect to the extent of antiferromagnetism and superconductivity is actually symmetric if plotted in terms of chemical potential (Fig. 52 (bottom)). This is a fascinating result that deserves further investigation.

F. Nature of normal state near optimal doping

A central subject of debate in the field of cuprate superconductivity is the nature of the 'normal' state. Is the metal above T_c well described by Fermi liquid theory or are interactions such as to drive the system into a non-Fermi liquid state of some variety? One of the problems with the resolution of this question experimentally is the "unfortunate" intervention of superconductivity at relatively high temperatures and energy scales. The matter of whether a material is or is not a Fermi liquid can only be resolved definitively at low energy scales as the criteria to have well-defined quasiparticles will always break down at sufficiently high temperatures or en-
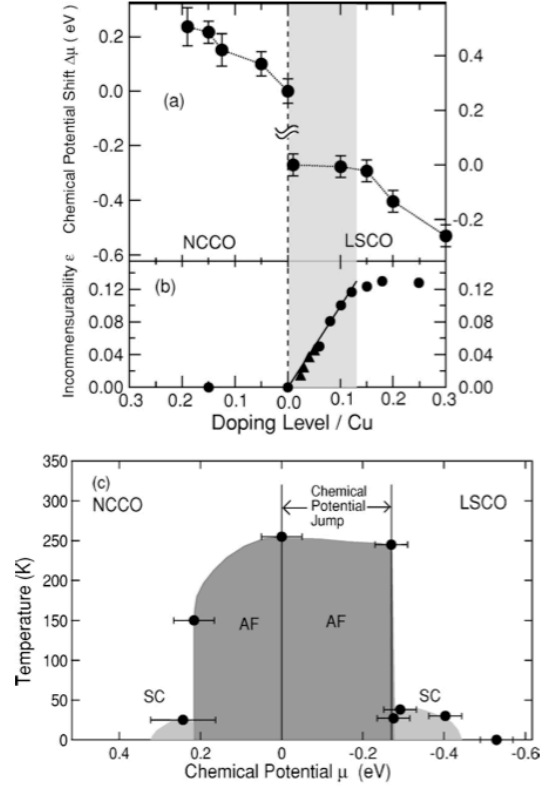

FIG. 52 (top) Chemical potential shift μ in NCCO and LSCO. (middle) Incommensurability measured by inelastic neutron scattering experiments as given in Refs. (Yamada *et al.*, 1998) and (Yamada *et al.*, 2003). In the hatched region, the incommensurability varies linearly and $\Delta\mu$ is constant as functions of doping level. (bottom) μ-T phase diagram of NCCO and LSCO. Note that there is an uncertainty in the absolute value of the chemical potential jump between NCO and LCO. From Harima *et al.* (2001).

ergies. The advantage of trying to answer these question for the electron-doped cuprates as opposed to the *p*-type materials is that superconductivity can be suppressed by modest magnetic fields (≈ 10 T) allowing access to the low temperature behavior of the normal state.

This issue has been discussed frequently in the context of the electron-doped cuprates due to the approximately quadratic dependence of the resistivity above T_c (Fournier *et al.*, 1998a; Hidaka and Suzuki, 1989; Tsuei *et al.*, 1989). For further discussion see Sec. III.A.1. The conventional wisdom is that this is evidence of a "more Fermi liquid-like" normal state (T^2 being the nominal functional form for electron-electron scattering in a conventional metal at low temperature). It is not. While it is certainly true that the quadratic temperature dependence is very different than the remarkable linear dependence found in the hole-doped materials (Gurvitch and Fiory, 1987), it is not likely evidence for a Fermi liquid state. The temperature range over which T^2 is found (from T_c to room temperature) is much larger than that
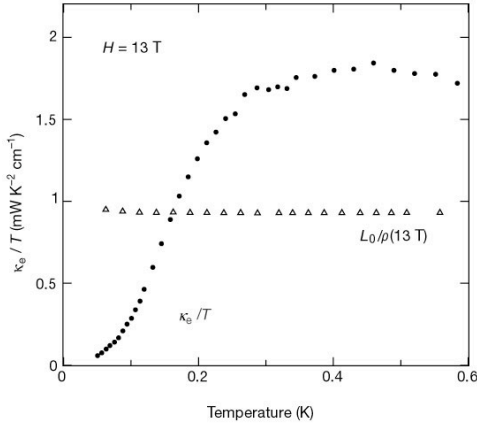
FIG. 53 A comparison of charge conductivity $\sigma(T) = 1/\rho(T)$, plotted as $L_0/\rho(T)$ (triangles) (i.e. given by the Wiedemann-Franz expectation), and electronic contribution to the heat conductivity κ_e, plotted as κ_e/T (circles), as a function of temperature in the normal state at H = 13 T. A clear violation of the Wiedemann-Franz law is found (Hill *et al.*, 2001). The downturn below 300 mK is an artifact of thermal decoupling of the electronic and phononic degrees of freedom (Smith *et al.*, 2005), but an approximately factor of two discrepancy remains in the magnitude of the thermal conductivity and the value inferred from the charge conductivity at low temperature.

ever expected for purely electron-electron scattering to manifest. Within conventional transport theory, one will almost invariably have a phonon contribution that in certain limits will give a linear dependence to the resistivity and destroy the T^2 form except at the lowest temperatures. Moreover, realistic treatments for electron-electron scattering give functional forms for various temperature ranges that depend on such factors as the Fermi surface geometry (Hodges *et al.*, 1971) and it is seldom that a pure T^2 functional form is observed even in conventional metals. Whatever is causing the T^2 functional form almost certainly cannot be electron-electron scattering of a conventional variety and is therefore not evidence of a Fermi liquid ground state. In a similar fashion the quadratic frequency dependence of the effective scattering rate that is found by Wang *et al.* (2006a) up to the high frequency scale of 6000 cm^{-1} (0.74eV) in overdoped NCCO is also unlikely to be evidence for a Fermi-liquid.

Recently however this issue of the Fermi liquid nature of the electron-doped cuprates has been put on more rigorous ground with sensitive measurements of the thermal conductivity of x=0.15 PCCO. Taking advantage of the low critical magnetic fields of these compounds, Hill *et al.* (2001) measured the thermal and electric conductivity of the normal state and discovered a clear violation of the "Wiedemann-Franz law" (Fig. 53). The Wiedemann-Franz law is one of the defining experimental signatures of Fermi liquids and states that the ratio $\kappa/\sigma T$ where κ is the thermal conductivity and σ is the electri-

cal conductivity should be universally close to Sommerfeld's value for the Lorenz ratio $L_0 = \pi^2/3(k_B/e)^2 = 2.45 \times 10^{-8} W\Omega K^{-2}$. This relation reflects the fact that at low temperature the particles that carry charge are the same as those that carry heat. No known metal has been found to be in violation of it[26]. Hill *et al.* (2001) demonstrated that there was no correspondence between thermal and electrical conductivities in PCCO at low temperature. For much of the temperature range, the heat conductivity was found to be greater than expected. Because the Wiedemann-Franz law is a natural property of Fermi liquids, this violation had consequences for understanding the ground state and elementary excitations of these materials. It implies that charge and heat are not carried by the same electronic excitations. A similar violation of the WF law has now been reported in underdoped $Bi_{2+x}Sr_{2-x}CuO_{6-\delta}$ (Proust *et al.*, 2005). On the other hand, agreement with the WF law is found in some overdoped cuprates (Nakamae *et al.*, 2003; Proust *et al.*, 2002). In counter to these measurements Jin *et al.* (2003) have pointed out that rare earth ordering and crystal field levels can affect heat as well as electrical transport. They found large changes in the non-electronic portion of the thermal conductivity of NCO in a magnetic field, which may be responsible for the larger than expected heat current.

In NMR Zheng *et al.* (2003) have measured a similar ratio that should also show universal behavior in a Fermi liquid. They demonstrated that when the superconducting state was suppressed by magnetic field in x=0.11 PLCCO the spin relaxation rate obeyed the Fermi-liquid Korringa law $1/T_1 \propto T$ down to the lowest measured temperature (0.2K). With the measured value for the Knight shift K_s, it was found that the even stronger condition $T_1 T K_s^2 = $ constant was obeyed below 55K albeit with a small $T_1 T K_s^2$ value of 7.5×10^{-8} sec K, which is 50 times less than the non-interacting value. This points to the significance of strong correlations, but gives indication that the ground state revealed by application of a strong magnetic field is actually a Fermi liquid.

Clearly, this is a subject that deserves much more indepth investigation. It would be worthwhile to search for both Wiedemann-Franz and Korringa law violations over the larger phase diagram of electron-doped cuprates to see for what doping ranges - if any - violations exist.

G. Spin-density wave description of the normal state

As originally noticed by Armitage *et al.* (2001a), electron-doped samples near optimal doping present a FS, that while very close to that predicted by band structure calculations, have near-E_F ARPES spectral weight

---

[26] Subsequent to the measurements described herein, violations of the Wiedemann-Franz law has been found near heavy-electron quantum critical points (Tanatar *et al.*, 2007).

that is strongly suppressed (pseudogapped) at the momentum space positions where the underlying Fermi surface (FS) contour crosses the AF Brillouin zone boundary. This suggests the existence of a (π,π) scattering channel and a strong importance of this wavevector.

As discussed by Armitage (2001); Armitage *et al.* (2001a), one possible way to view the results - at least qualitatively - for samples near optimal doping is as a manifestation of a $\sqrt{2} \times \sqrt{2}$ band reconstruction from a static (or slowly fluctuating) spin density wave (SDW) or similar order with characteristic wavevector (π,π). This distortion or symmetry reduction is such that if the order is long-range and static the BZ decreases in volume by $1/2$ and rotates by $45°$. The AFBZ boundary becomes the new BZ boundary and gaps form at the BZ edge in the usual way. Although an SDW is the natural choice based on the close proximity of the antiferromagnetic phase, the data are consistent with any ordering of characteristic wave vector (π,π) such as DDW (Chakravarty *et al.*, 2001).

The $\sqrt{2} \times \sqrt{2}$ reconstructed band structure can be obtained *via* simple degenerate perturbation theory Armitage (2001); Matsui *et al.* (2005b); Park *et al.* (2007). This treatment gives

$$E_k = E_0 + 4t'(\cos k_x \cos k_y) + 2t''(\cos 2k_x + \cos 2k_y)$$
$$\pm \sqrt{4t^2(\cos k_x + \cos k_y)^2 + |V_{\pi\pi}|^2} \; (2)$$

where $V_{\pi\pi}$ is the strength of the effective (π,π) scattering, and t, t' and t'' are nearest, next-nearest, and next-next-nearest hopping amplitudes. The even and odd solutions correspond to new band sheets that appear due to the additional Bragg scattering potential. With realistic hopping parameters for the cuprates (as discussed in Sec. II.B) a small hole pocket centered around $(\pi/2,\pi/2)$ and a small electron pocket around $(\pi,0)$ appears at optimal doping as shown in Fig. 54b. All measured n-type cuprates near optimal doping show a FS phenomenology roughly consistent with this band structure (Armitage, 2001; Armitage *et al.*, 2001b; Matsui *et al.*, 2007; Zimmers *et al.*, 2005)[27]. The $2V_{\pi,\pi}$ splitting between the two band sheets in Fig 54b can be measured directly in a measurement of the ARPES spectral function along the AFBZ boundary as shown for SCCO in Fig. 54a. Note that within this picture one expects differences with the p-type compounds as due to their smaller Luttinger volume the underlying 'bare' FS comes closer to the $(\pi,0)$ position.

This derivation is for a potential with long-range order, which according the Motoyama *et al.* (2007) does not exist above $x \approx 0.134$. Due to the ambiguity associated with the exact position of the phase boundary, possibly
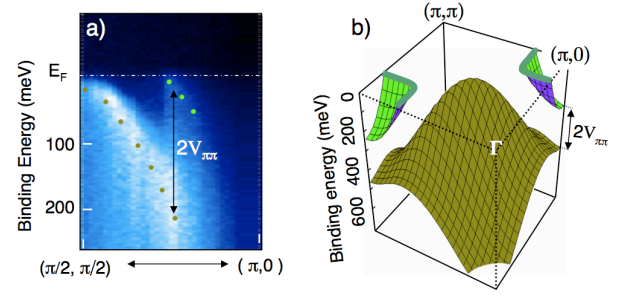
---

[27] Small differences between material classes do exist (Fig. 31). See the discussion in Sec. III.C.

FIG. 54 (a) Measured ARPES spectral function along the AFBZ as given by the arrow in (b). The SDW gap $2V_{\pi,\pi}$ is readily visible in the raw spectra. (b) Schematic of the band structure from a $\sqrt{2} \times \sqrt{2}$ reconstruction. Adapted from Park *et al.* (2007).

more relevant to the typical experimental case may be a situation where true long range order of the $\sqrt{2} \times \sqrt{2}$ phase does not exist, but where the material still has strong (but slow) fluctuations of this order. In this case more complicated treatments are necessary for quantitative treatments. An analysis in the spirit of the above is then much harder, but as long as the fluctuations are slow, then some aspects of the above zone folding picture should remain. For instance depending on their particular time scales, some experiments may be sensitive to the formation of an electron pocket around $(\pi,0)$.
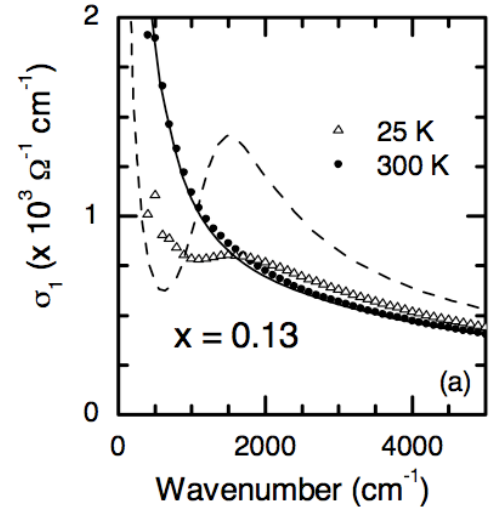
FIG. 55 Calculation of the optical conductivity based on the SDW band structure in Fig. 54. Spectra were calculated for a x=0.13 doping with a value of $2V_{\pi\pi} = 0.25$ eV and a gap opening temperature of 170K. The symbols are the measured optical conductivity for x=0.13 and the lines the spin density wave model calculation. Compare also to the $x = 0.10$ data in Fig. 32. From Zimmers *et al.* (2005).

An interpretation based on such a zone folding scheme enables one to understand - at least qualitatively - issues such as the sign change in the Hall coefficient (Da-

15

gan *et al.*, 2007, 2004; Fournier *et al.*, 1997; Gollnik and Naito, 1998; Wang *et al.*, 1991). It had been a long standing mystery how a simply connected hole-like FS centered around (π,π) (originally thought to be the case from the first ARPES experiments of Anderson *et al.* (1993); King *et al.* (1993)) could give both positive and negative contribution to the Hall coefficient and thermopower. A mean field calculation of the Hall conductance based on the band structure in Eq. 2 shows that the data are qualitatively consistent with the reconstruction of the Fermi surface expected upon density wave ordering (Lin and Millis, 2005), although the calculation has difficulty reproducing the R_H values precisely[28] [29].

Zimmers *et al.* (2005) showed that the notable pseudogaps in the optical conductivity as well as its overall shape can be reasonably modeled by a calculation based on the band structure in Eq. 2 and Fig. 54. As seen in Fig. 55 the overall temperature and frequency dependence matches well to the experimental data seen in the x=0.10 curves in Fig. 32 for instance.

Although it works best for samples near optimal doping, the SDW mean-field picture can also be used to understand the doping dependence of the FS for a limited range near optimal doping. As materials are progressively underdoped and the antiferromagnetic phase is approached, antiferromagnetic correlations become stronger and the "hot spot" regions spread so that the zone-diagonal spectral weight is gapped by the approximate (π,π) nesting of the $(\pi/2,\pi/2)$ section of FS with the $(-\pi/2,-\pi/2)$ section of FS. However a scheme based on nesting obviously breaks down as one approaches the Mott state, where the zone diagonal spectral weight is not only gapped, but also vanishes. Experimentally, the near-E_F spectral weight near $(\pi/2,\pi/2)$ becomes progressively gapped with underdoping and by $x = 0.04$ in NCCO only an electron FS pocket exists around the $(\pi,0)$ point (Fig. 28) (Armitage *et al.*, 2002). On the overdoped side, Matsui *et al.* (2007) have extrapolated that that this hot spot effect would largely disappear in the ARPES spectra by $x = 0.20$ as expected by the virtual disappearance of $V_{\pi,\pi}$ at that doping. That the FS is no longer reconstructed for overdoped samples, was also inferred in the

quantum oscillations experiments of Helm *et al.* (2009).

In an infrared Hall effect study Zimmers *et al.* (2007b) found that at the lowest temperatures their data for $x = 0.12, 0.15, 0.18$ was *qualitatively* consistent with the simple SDW model. However, Jenkins *et al.* (2009a) demonstrated strong *quantitative* discrepancies for underdoped materials of such a model with far infrared Hall measurements when using as input parameters the experimentally measured band structure from ARPES. Additionally, ARPES, IR and IR Hall measurements as high as 300K do not suggest a simple closing of the SDW gap (and hence formation of an unreconstructed Fermi surface around (π, π)) above T_N (Jenkins *et al.*, 2009a; Matsui *et al.*, 2005a; Onose *et al.*, 2004; Wang *et al.*, 2006a; Zimmers *et al.*, 2007b). For instance, there is a strong temperature dependence of the electron contribution to the Hall angle through the whole range up to and even above T_N. Jenkins *et al.* (2009a) ascribed this to the role played by AF fluctuations. It seems clear that experiments like optics, which measure at finite frequency, cannot necessarily distinguish between fluctuations and true long-range order in a model independent way. For instance, despite the success of the extended Drude model in describing σ_{xx} of overdoped $Pr_{2-x}Ce_xCuO_4$, Zimmers *et al.* (2007b) found strong deviations in its description of σ_{xy} in an x=0.18 sample showing that fluctuation effects are playing a role even at this doping. Later work of this group using lower energy far infrared Hall data concludes that these deviations can in general be described by a model that incorporates vertex corrections due to antiferromagnetic fluctuations within the FLEX approximation (Jenkins *et al.*, 2009b; Kontani, 2008). These observations show the obvious limits of a simple mean-field picture to understand all aspects of the data. As discussed elsewhere, the observation of AF-like spectral gap in parts of the phase diagram, which don't exhibit long-range AF might be understandable within models that propose that a PG evinces in the charge spectra when the AF correlation length exceeds the thermal de Broglie wavelength (Kyung *et al.*, 2004).

H. Extent of antiferromagnetism and existence of a quantum critical point

While it has long been known that antiferromagnetism extends to much higher doping level in the *n*-type as compared to the *p*-type compounds, reports differ on what doping level the AF phase actually terminates and whether it coexists or not with superconductivity (Fujita *et al.*, 2003; Kang *et al.*, 2005; Motoyama *et al.*, 2007). There are at least two important questions here: Do the intrinsic regimes of superconductivity and AF coincide? And does the AF regime at higher dopings terminate in a second order transition and a T=0 QCP that manifests itself in the 'scaling forms' of response functions and in physical observables like transport and susceptibility? These are issues of utmost importance with

---

[28] In these calculations long range order has been assumed up to $x = 0.16$. It is difficult to reconcile the reasonable agreement of the data at optimal doping and the mean-field model with the termination of the AF phase at $x \approx 0.134$ as inferred by Motoyama *et al.* (2007). More theoretical work and the explicit calculation of transport coefficients for systems with short range order and AF fluctuations are needed. It is possible however the magnetic field used to suppress superconductivity stabilizes the magnetic state.

[29] More recent calculations by Jenkins *et al.* (2009a) using a band structure that takes into account the very anisotropic Fermi velocities observed experimentally in ARPES results has even worse quantitative agreement with the experimental R_H. However, they claim that one can describe the spectra with the inclusion of vertex corrections within the FLEX approximation (Kontani, 2008).

regards to data interpretation in both $n-$ and p-type compounds. Their resolution impinges on issues of the impact of quantum criticality (Sachdev, 2003), coupling of electrons to antiferromagnetism (Abanov *et al.*, 2001; B. Kyung, 2009; Carbotte *et al.*, 1999; Maier *et al.*, 2008; Schachinger *et al.*, 2003), and $SO(5)$ symmetry (Chen *et al.*, 2004; Zhang, 1997) - yet a complete understanding requires weighing the competing claims of different neutron scattering groups, the information provided by μSR, as well as materials growth and oxygen reduction issues.

It has long been known that samples at superconducting stochiometries show a substantial AF magnetic response, as in for instance the existence of commensurate Bragg peaks (Yamada *et al.*, 1999, 2003). Whether this is because phases truly coexist, or because samples are (chemically or intrinsically) spatially inhomogenous has been unclear[30]. Recently, Motoyama *et al.* (2007) have concluded that they can distinguish these scenarios *via* inelastic scattering by following the spin stiffness ρ_s that sets the instantaneous correlation length. They find it falls to zero at a doping level of $x \approx 0.134$ (Fig. 35a) in NCCO at the onset of superconductivity[31] and hence there is no intrinsic AF/SC coexistence regime. They found that the instantaneous spin-spin correlation length at low temperature remains at some small, but non-neglible value well into the superconducting regime showing the AF correlations are finite but not long range ordered in the superconductor (Fig. 35a). As other inelastic neutron scattering experiments have clearly shown the presence of a superconducting magnetic gap (Yamada *et al.*, 2003), (despite the presence of Bragg peaks in the elastic response) Motoyama *et al.* (2007) concluded that the actual antiferromagnetic phase boundary terminates at $x \approx 0.134$, and that magnetic Bragg peaks observed at higher Ce concentrations originate from rare portions of the sample which were insufficiently oxygen reduced (Fig. 35b)[32]. This group had previously shown that the inner core of large TSFZ annealed crystals have a different oxygen concentration than the outer shell (Mang *et al.*, 2004b). They speculate that the antiferromagnetism of an ideally reduced NCCO sample would terminate in a 1st order transition [possibly rendered 2nd or-

der by quenched randomness (Aizenman and Wehr, 1990; Hui and Berker, 1989; Imry and Wortis, 1979)], which would give no intrinsic QCP.

A similar inference about the termination of AF state near the superconducting phase boundary can be reached from the neutron and μSR PLCCO data of Fujita *et al.* (2003, 2008a). Fujita *et al.* (2008a) found only a narrow coexistence regime near the SC phase boundary ($\Delta x \approx 0.01$ near $x \approx 0.1$) which could also be a consequence of rare slightly less reduced regions. They also find a dramatic decrease in AF signatures near this doping level. However, Li *et al.* (2008a) caution that since both the superconducting coherence length and spin-spin correlation length are both strongly affected by the oxygen annealing process, this issue of the true extent of AF and its coexistence with SC in the n-type cuprates may not be completely solved and there may be some oxygen reduction conditions where superconductivity and antiferromagnetism can genuinely coexist. It is undoubtedly true that the annealing conditions depend on Ce concentration and in this regard it may be challenging to settle the question definitively about whether or not AF and superconductivity intrinsically coexist in any regions of phase space. In support of a scenario of an AF QCP somewhere nearby in PLCCO, Wilson *et al.* (2006b) showed that at higher temperatures and frequencies, the dynamical spin susceptibility $\chi(\omega, T)$ of an $x = 0.12$ sample can be scaled as a function of $\frac{\omega}{T}$ at AF ordering wavevectors. The low energy cut-off of the scaling regime is connected to the onset of AF order, which comes down as the antiferromagnetic phase is suppressed by oxygen reduction.

In seeming contrast to these magnetic measurements that give evidence of no coexistence regime, based on their transport data Dagan *et al.* (2004) claimed that an AF quantum phase transition (QPT) exists at dopings near optimal in PCCO. Their evidence for a quantum critical point (QCP) at $x \approx 0.165$ was: 1) the kink in R_H at 350mK (see Fig 21), 2) the doping dependence of the resistivity's temperature dependent exponent β in the temperature range 0.35 - 20K, 3) the reduced temperature region near x=0.165 over which a T^2 dependence is observed, and 4) the disappearance of the low T resistivity upturn. More recent very high-field (up to 60T) Hall effect and resistivity results support this scenario (Li *et al.*, 2007a).

The 'funnel-like' dependence of the threshold T_0 below which T^2 resistivity is observed shown in Fig 56 (top), is precisely the behavior expected near a quantum phase transition (Dagan *et al.*, 2004). This is particularly striking in the n-type cuprates where the resistivity has a T^2 dependence for all dopings at temperatures above $\approx$30K (or the resistivity minimum). The phase diagram looks qualitatively similar to quantum phase transition diagrams found in the heavy fermions (see for instance Custers *et al.* (2003)). One may also take as evidence the striking linear in T resistivity found from 35mK to 10 K for x=0.17 PCCO (Fournier *et al.*, 1998b) as evi-

---

[30] In this regard see also Sec. IV.E that addresses the question of intrinsic charge inhomogeneity

[31] Note that the definitions for the spin stiffness of Fujita *et al.* (2008a) and Motoyama *et al.* (2007) differ, which may account for their differences of where ρ_s extrapolates to zero. Motoyama *et al.* (2007) derived it from the T dependence of the linewidth of the *instantaneous* spin correlations over a wide range of temperatures, while Fujita *et al.* (2008a) get it from the ω dependence of the peak width at a particular T.

[32] In a related, but ultimately different interpretation, Yamada *et al.* (2003) interpreted their narrow coexistence regime as evidence that the AF/SC phase boundary is first order and therefore these systems should lack a QCP and the associated critical fluctuations
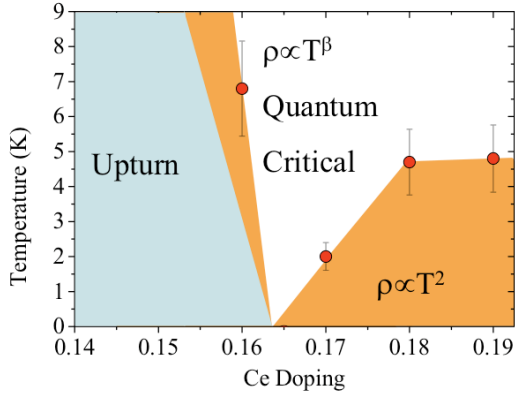
FIG. 56 (top) Schematic illustration of the phase diagram of $Pr_{2-x}Ce_xCuO_4$ from resistivity measurements in magnetic field high enough to suppress superconductivity. Plotted as red dots is T_0, the temperature below which the T^2 behavior is observed (in orange). At dopings lower than that of the nominal QCP the resistivity shows a low temperature upturn (Dagan and Greene, 2004).
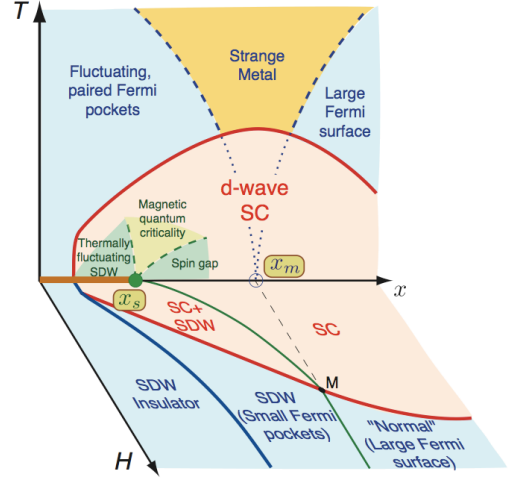

FIG. 57 Proposed phase diagram for field stabilized magnetism for the cuprates. The phase diagram includes a transition from a large FS to a small FS at fields above H_{c2}. The transition happens at a doping x_m which is greater than the doping where the SDW is suppressed at zero field. From (Sachdev et al., 2009).

dence for a QCP near this doping. A recent study of the doping dependence of the low-temperature normal state thermoelectric power has also been interpreted as evidence for a quantum phase transition (QPT) that occurs near x=0.16 doping (Li et al., 2007c). And as discussed elsewhere, a number of other experiments such as optical conductivity (Onose et al., 2004; Zimmers et al., 2005), ARPES (Matsui et al., 2007) and angular magnetoresistance (Yu et al., 2007b) experiments have also suggested that there is a phase transition at a higher doping.

Clearly, the inference of a QCP in PCCO and NCCO at $x \approx 0.165$ dopings is in disagreement with the conclusion of Motoyama et al. (2007) who have found that the AF phase terminates at $x \approx 0.134$, before the occurrence of SC. There are a number of possible different explanations for this.

It may be that the QCP of Dagan et al. (2004) and others is due not to the disappearance of the magnetic phase per se, but instead due to the occurrence of something like a Fermi surface topological transition. For instance, it could be associated with the emergence of the full Fermi surface around the (π, π) position from the pockets around $(\pi, 0)$ in a manner unrelated to the loss of the AF phase. Such behavior, is consistent with the kink-like behavior in the Hall coefficient (Fig 21). It is also consistent with recent magnetic quantum oscillation experiments, which show a drastic change in FS topology between $x = 0.16$ and $x = 0.17$ doping (Helm et al., 2009)[33]. Such a transition could occur just as a result of

the natural evolution of the FS with doping, or it may be that this 2nd transition signifies the termination of an additional order parameter hidden within the superconducting dome(Alff et al., 2003), such as for instance DDW (Chakravarty et al., 2001) or other orbital current states (Varma, 1999). However a transition involving only charge degrees of freedom is superficially at odds with experiments that show a relationship of this transition to magnetism such as the sharp change in angular magnetoresistance at $x \approx 0.165$ (Dagan et al., 2005b; Yu et al., 2007b).

An alternative, but to our minds very natural scenario is that it is the magnetic field used to suppress superconductivity to reveal the low temperature normal state that stabilizes the SDW state. Such a situation is believed to be the case in the hole-doped materials (Demler et al., 2001; Khaykovich et al., 2002; Lake et al., 2001, 2002; Moon and Sachdev, 2009). The situation in the electron-doped materials is inconclusive (see the discussion in Sec. III.F.3), but it has been argued elsewhere that magnetic field enhances the magnetic ordered state in a somewhat similar fashion (Kang et al., 2003b, 2005; Matsuura et al., 2003). Recent calculations by Moon and Sachdev (2009); Sachdev et al. (2009) give a phase diagram (Fig. 57) that is consistent with a zero-field SDW transition at $x \approx 0.134$ and a transition to a large FS at $x \approx 0.165$ at dopings above H_{c2}. Such a scenario naturally explains the doping dependence of quantum oscillation (Helm et al., 2009) and Hall effect measurements

_____

[33] One interesting aspect of these quantum oscillation experiments is the lack of evidence for a small electron pocket on the low doping side, as one would expect that the band structure in Eq. 2 would give both electron and hole contributions. Eun et al.

_____

(2009) has shown that the contribution of the electron pocket is extremely sensitive to disorder.

(Dagan *et al.*, 2004).

However, a scenario of a field induced SDW does not simply explain measurements like ARPES and optics, which have inferred the existence of a QCP by the extrapolated doping level where a magnetic pseudogap closes. However, as mentioned above it is likely that such measurements may be primarily sensitive to the development of short range order or fluctuations. As pointed out by Onose *et al.* (2004); Wang *et al.* (2006a) optical data clearly show the existence of a large pseudogap in underdoped samples at temperatures well above the Néel temperature. (Jenkins *et al.*, 2009b; Zimmers *et al.*, 2007b) showed that gap-like features still appear in infrared Hall angle measurements even above those of the nominal QCP. As this implies that only short-range order is necessary for the existence of relatively well defined magnetic pseudogap in the charge spectra, it calls into question the utility of inferring the critical concentration of a magnetic QCP from such experiments. Theoretically, in Hubbard model calculations Kyung *et al.* (2004) have shown that a pseudogap can develop in the photoemission spectra when the AF correlation length exceeds the thermal de Broglie wavelength (see Sec. IV.I below) i.e. long range order in the ground state is not necessary to develop a PG. However, it seems difficult to imagine however that calculations which only incorporate short range order and fluctuations can reproduce the sharp anomalies in DC transport (Hall effect etc.) found near $x = 0.165$. For this, it seems likely that some sort of long-range order must be involved. These effects are probably due to AF order stabilized by magnetic field as discussed above. More work on this issue is clearly needed; we are not aware of any measurements that show QPT-like anomalies in transport near $x = 0.13$ and so even more detailed studies should be done.

I. Existence of a pseudogap in the electron-doped cuprates?

The pseudogap of the p-type cuprates is one of the most enigmatic aspects of the high-T_c problem. Below a temperature scale T^*, underdoped cuprates are dominated by a suppression in various low-energy excitation spectra (Norman *et al.*, 2005; Randeria, 2007; Timusk and Statt, 1999). It has been a matter of much long standing debate whether this pseudogap is a manifestation of precursor superconductivity at temperatures well above T_c, or rather is indicative of some competing ordered phase.

An answer to the question of whether or not 'The Pseudogap' in the n-type cuprates exists is difficult to address conclusively because of a large ambiguity in its definition in the p-type materials. Moreover, even in the p-type compounds the precise boundary depends on the material system and the experimental probe. Additionally, there has frequently been the distinction made between a 'high-energy' PG, which is associated with physics on the scale of the magnetic exchange J and a 'low-energy' PG, which is of the same order of the superconducting gap. What is clear is that there are undoubtedly a number of competing effects in underdoped cuprates. These have all frequently been confusingly conflated under the rubric of pseudogap phenomena. Here we concentrate on a number of manifestations of the phenomenology which can be directly compared to the p-type side. A number of similarities and differences are found.

At the outset of our discussion, it is interesting to point out that much of the pseudogap phenomena in the electron-doped cuprates seems to be related to antiferromagnetism and this phase's relative robustness in these materials. The issue of whether the PG exists is of course then intimately related to the issues presented above in Secs. IV.H and IV.G on the extent of antiferromagnetism and the SDW description of the normal state.

As mentioned above, both optical conductivity and ARPES of underdoped single crystals ($x = 0$ to 0.125) shows the opening of a high energy gap-like structure at temperatures well above the Néel temperature (Matsui *et al.*, 2005a; Onose *et al.*, 2004). It can be viewed directly in the optical conductivity, which is in contrast to the hole-doped side, where gap-like features do not appear in the ab-plane optical conductivity itself and a 'pseudogap' is only exhibited in the frequency dependent scattering rate (Puchkov *et al.*, 1996). The gap closes gradually with doping and vanishes by superconducting concentrations of approximately $x = 0.15$ (Onose *et al.*, 2004) to $x = 0.17$ (Zimmers *et al.*, 2005). Onose *et al.* (2004) found that both its magnitude (Δ_{PG}) and its onset temperature (T^*) obeys the approximate relation $\Delta_{PG}) = 10k_B T^*$ (Fig. 58). The magnitude of Δ_{PG} is comparable in magnitude to the pseudogap near $(\pi/2, \pi/2)$ in the photoemission spectra reported by (Armitage *et al.*, 2002) (also Fig. 58), which indicates that the pseudogap appearing in the optical spectra is the same as that found in photoemission. Note that this is the same gap-like feature, of which a remarkable number of aspects can be modeled at low T by the SDW band structure as given in Sec. IV.G. Onose *et al.* (2004) identify the pseudogap with the buildup of antiferromagnetic correlations because: (a) In the underdoped region long range AF order develops at a temperature T_N approximately half of T^*. (b) The intrinsic scale of the AF exchange interaction J is on the scale of the pseudogap magnitude (c) The gap anisotropy found in photoemission is consistent with that expected for 2D AF correlations with characteristic wavevector (π, π) as pointed out by Armitage *et al.* (2002).

These PG phenomena may be analogous to the 'high-energy' PG found in the hole-doped cuprates, although there are a number of differences as emphasized by Onose *et al.* (2004). (a) The large pseudogap of the hole-doped system is maximal near $(\pi, 0)$ in contrast with one more centered around $(\pi/2, \pi/2)$ of the n-type cuprate. (b) As mentioned, the pseudogap feature is not discernible in the ab-plane optical conductivity itself in the hole-

doped cuprate, which may be because it is weaker than that in the electron-doped compound. (c) The ground state in the underdoped n-type system, where the pseudogap formation is observed strongest, is antiferromagnetic, while the superconducting phase is present even for underdoped samples in the hole-doped cuprate.
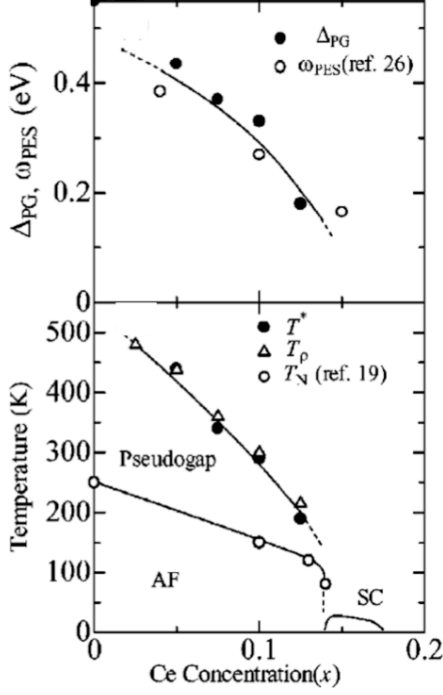

FIG. 58 (top) The x variation of the pseudogap magnitude Δ_{PG} as defined by the higher-lying isosbetic (equal-absorption) point in the temperature-dependent conductivity spectra and the magnitude of the pseudogap (ω_{PES}) in the photoemission spectra (Armitage *et al.*, 2002) (Ref. 26 in the figure). The ω_{PES} is defined as the maximum energy of the quasiparticle peak on the putative large Fermi surface in the ARPES spectra shown in the Figs. 2(c) - (e) of Armitage *et al.* (2002). (bottom) The obtained phase diagram. The onset temperature of pseudogap formation T* and the crossover temperature of out-of-plane resistivity T$_\rho$ (as given by the arrows in Fig. 19 (right) are plotted against x together with the Néel temperature T$_N$ reported previously by Luke *et al.* (1990) (Ref. 19 in the figure).

As pointed out above, it is interesting that for a PG related to AF, it forms at a temperature well above T$_N$. This is presumably related to the fact that the spin correlation length ξ is found to be quite large at temperatures even 100 K above T$_N$, which follows from the quasi-2D nature of the magnetism. In this regard Motoyama *et al.* (2007) found that at the PG temperature T^* (as defined from the optical spectra) the spin correlation length ξ becomes of order the estimated thermal de Broglie wavelegth $\xi_{th} = \hbar v_F / \pi k_B T$. This is a condition for the onset of the PG consistent with a number of theoretical calculations based on $t - t' - t'' - U$ models (Kyung *et al.*, 2004) that emphasize the build-up of AF correlations. In these models, the weaker coupling

regime (smaller U/W) of the electron-doped cuprates allows the identification of the pseudogap with long AF correlation lengths. These theories make quantitative predictions of the momentum dependence of the PG in the ARPES spectra, the pseudogap onset temperature T^*, and the temperature and doping dependence of the AF correlation length that are in accord with experiment. The hole-doped compounds appear to have stronger coupling and similar treatments give a pseudogap that is tied to the stronger local repulsive interaction and has different attributes (Kyung *et al.*, 2004, 2003). Although aspects (such as the PG's momentum space location) are in qualitative agreement with experiment, quantities like the AF correlation length are in strong quantitative disagreement with neutron scattering results.

At lower energy scales, there have been a number of tunneling experiments that have found evidence for a small normal state energy gap (NSG) ($\sim$5 meV) that seems somewhat analogous to the low-energy pseudogap found in the p-type materials. This normal state gap (NSG) is probed in the ab-plane by applying a c-axis magnetic field greater than H_{c2} (Alff *et al.*, 2003; Biswas *et al.*, 2001; Dagan *et al.*, 2005a; Kleefisch *et al.*, 2001). Dagan *et al.* (2005a) find that it is present at all dopings from 0.11 to 0.19 and the temperature at which it disappears correlates with T_c, at least on the overdoped side of the SC dome. However, the NSG survives to very large magnetic fields and this is not obviously explained by the preformed Cooper pair scenario (Biswas *et al.*, 2001; Kleefisch *et al.*, 2001). Recently, Shan *et al.* (2008b) conclude that the NSG and the SC gap are different across the phase diagram, which is consistent with various 'two-gap' scenario in the underdoped p-type cuprates. In PLCCO NMR Zheng *et al.* (2003) found no sign of a *spin* pseudogap opening up at temperatures much larger than T$_c$, which is a hallmark of underdoped p-type cuprates and has been interpreted as singlet formation at high temperatures. Likewise the spin pseudogap observed in neutron scattering appears to close at T$_c$ (Yamada *et al.*, 2003) and not at some higher temperature. This is consistent with a more mean field-like superconducting transition in these compounds, which may be tied to their apparently larger relative superfluid stiffness (4-15 times as compared to hole-doped compounds of similar T$_c$ (Emery and Kivelson, 1995; Shengelaya *et al.*, 2005; Wu *et al.*, 1993)).

In summary, although there are substantial signatures of PG effects in the electron-doped compounds, it is not clear if it is of the same character as in the hole-doped materials. The bulk of PG phenomena in the electron-doped compounds appears to be related to AF correlations. There is, as of yet, no evidence for many of the phenomena associated with pseudogap physics in the p-type materials, such as 'spin pseudogaps' (Alloul *et al.*, 1989; Curro *et al.*, 1997), orbital currents (Fauqué *et al.*, 2006; Li *et al.*, 2008b), stripes (Mook *et al.*, 1998, 2002; Tranquada *et al.*, 1995), or time-reverasal symmetry breaking (Xia *et al.*, 2008). It may be that such phenomena are

obscurred by AF or it may just be that the p- and n-type compounds are just very different when it comes to these effects.

V. CONCLUDING REMARKS

Our understanding of the electron-doped cuprates has advanced tremendously in recent years. Still, some important issues remain unresolved and more research will be needed to gain a full understanding. For instance, the role of oxygen annealing is an important unresolved issue. In the superconducting state, the evidence is now strong that the pairing symmetry in both n- and p-type cuprates is predominately d-wave, although of a non-monotonic form in the n-type. In both n- and p-type cuprates, AFM gives way to SC upon doping and eventually the systems turn to a metallic, non-SC Fermi liquid-like state. For both dopings, the normal state at the SC compositions is anomalous and is not yet well understood, although it is obvious that there is significant and important coupling to antiferromagnetism on at least the electron-doped side. Clearly an understanding of the metallic state on both sides is crucial to an understanding of the mechanism of the high-T_c SC. Similarly, there is convincing evidence for a pseudogap which derives from AFM in the $n-$type compounds. This is in contrast to the pseudogap in the hole-doped compounds, which is as of yet of unknown origin. The issue of whether an additional competing order parameter co-exists with SC and ends at a critical point just before or within the SC dome is still unresolved for both hole and electron doping. Interaction effects play a central role in both classes of cuprates, although they may be weaker on the n-doped side. For instance, numerical cluster calculations have been able to explain the gross features of the n-type phase diagram, pseudogap, and the evolution of the Fermi surface, in a manner not possible on the hole-doped side.

Detailed comparisons between the properties of n- and p-type cuprates will continue to be important areas of future investigation. Such studies should also prove themselves useful for understanding new classes of superconducting materials, such as the recently discovered iron-pnictides, which also show electron- and hole-doped varieties. With regards to the high-T_c problem, our hope is that systematic comparisons between the two sides of the cuprate phase diagram will give unique insight into what aspects of these compounds are universal, what aspects are not universal, and what aspects are crucial for the existence of high temperature superconductivity.

Acknowledgments

References

Abanov, A., A. V. Chubukov, and J. Schmalian, 2001, Phys. Rev. B **63**(18), 180510.

Abrahams, E., and C. M. Varma, 2003, Phys. Rev. B **68**(9), 094502.

Aharony, A., R. J. Birgeneau, A. Coniglio, M. A. Kastner, and H. E. Stanley, 1988, Phys. Rev. Lett. **60**(13), 1330.

Aichhorn, M., and E. Arrigoni, 2005, Europhys. Lett. **72**(1), 117.

Aichhorn, M., E. Arrigoni, M. Potthoff, and W. Hanke, 2006, Phys. Rev. B **74**(23), 235117.

Aizenman, M., and J. Wehr, 1990, Communications in Mathematical Physics **130**(3), 489.

Akimitsu, J., S. Suzuki, M. Watanabe, and H. Sawa, 1988, Jpn. J. Appl. Phys **27**(19), L1859.

Alexander, M., H. Romberg, N. Nücker, P. Adelmann, J. Fink, J. T. Markert, M. B. Maple, S. Uchida, H. Takagi, Y. Tokura, A. C. W. P. James, and D. W. Murphy, 1991, Phys. Rev. B **43**(1), 333.

Alff, L., A. Beck, R. Gross, A. Marx, S. Kleefisch, T. Bauch, H. Sato, M. Naito, and G. Koren, 1998a, Phys. Rev. B **58**(17), 11197.

Alff, L., S. Kleefisch, U. Schoop, M. Zittartz, T. Kemen, T. Bauch, A. Marx, and R. Gross, 1998b, Euro. Phys. J. B - Cond. Matt. Comp. Syst. **5**(3), 423.

Alff, L., Y. Krockenberger, B. Welter, M. Schonecke, R. Gross, D. Manske, and M. Naito, 2003, Nature **422**, 698.

Alff, L., S. Meyer, S. Kleefisch, U. Schoop, A. Marx, H. Sato, M. Naito, and R. Gross, 1999, Phys. Rev. Lett. **83**(13),

2644.

Allen, J. W., C. G. Olson, M. B. Maple, J.-S. Kang, L. Z. Liu, J.-H. Park, R. O. Anderson, W. P. Ellis, J. T. Markert, Y. Dalichaouch, and R. Liu, 1990, Phys. Rev. Lett. **64**(5), 595.

Alloul, H., J. Bobroff, M. Gabay, and P. J. Hirschfeld, 2009, Rev. Mod. Phys. **81**(1), 45.

Alloul, H., T. Ohno, and P. Mendels, 1989, Phys. Rev. Lett. **63**(16), 1700.

Alp, E. E., G. K. Shenoy, D. G. Hinks, D. W. C. II, L. Soderholm, H.-B. Schuttler, J. Guo, D. E. Ellis, P. A. Montano, and M. Ramanathan, 1987, Phys. Rev. B **35**(13), 7199.

Alvarenga, A. D., D. Rao, J. A. Sanjurjo, E. Granado, I. Torriani, C. Rettori, S. Oseroff, J. Sarrao, and Z. Fisk, 1996, Phys. Rev. B **53**(2), 837.

Andersen, O. K., A. I. Liechtenstein, O. Jepsen, and F. Paulsen, 1995, J. Phys. Chem. Sol. **56**(12), 1573.

Anderson, P. W., 1987, Science **235**(4793), 1196.

Anderson, R. O., R. Claessen, J. W. Allen, C. G. Olson, C. Janowitz, L. Z. Liu, J.-H. Park, M. B. Maple, Y. Dalichaouch, M. C. de Andrade, R. F. Jardim, E. A. Early, *et al.*, 1993, Phys. Rev. Lett. **70**(20), 3163.

Ando, Y., A. N. Lavrov, S. Komiya, K. Segawa, and X. F. Sun, 2001, Phys. Rev. Lett. **87**(1), 017001.

Andreone, A., A. Cassinese, A. Di Chiara, R. Vaglio, A. Gupta, and E. Sarnelli, 1994, Phys. Rev. B **49**(9), 6392.

Anlage, S. M., D.-H. Wu, J. Mao, S. N. Mao, X. X. Xi, T. Venkatesan, J. L. Peng, and R. L. Greene, 1994, Phys. Rev. B **50**(1), 523.

Aprili, M., M. Covington, E. Paraoanu, B. Niedermeier, and L. H. Greene, 1998, Phys. Rev. B **57**(14), R8139.

Arai, M., T. Nishijima, Y. Endoh, T. Egami, S. Tajima, K. Tomimoto, Y. Shiohara, M. Takahashi, A. Garrett, and S. M. Bennington, 1999, Phys. Rev. Lett. **83**(3), 608.

Ariando, D. Darminto, H. J. H. Smilde, V. Leca, D. H. A. Blank, H. Rogalla, and H. Hilgenkamp, 2005, Phys. Rev. Lett. **94**(16), 167001.

Arima, T., Y. Tokura, and S. Uchida, 1993, Phys. Rev. B **48**(9), 6597.

Armitage, N. P., 2001, Stanford University Phd. thesis .

Armitage, N. P., 2008, unpublished .

Armitage, N. P., D. H. Lu, D. L. Feng, C. Kim, A. Damascelli, K. M. Shen, F. Ronning, Z.-X. Shen, Y. Onose, Y. Taguchi, and Y. Tokura, 2001a, Phys. Rev. Lett. **86**(6), 1126.

Armitage, N. P., D. H. Lu, C. Kim, A. Damascelli, K. M. Shen, F. Ronning, D. L. Feng, P. Bogdanov, Z.-X. Shen, Y. Onose, Y. Taguchi, Y. Tokura, *et al.*, 2001b, Phys. Rev. Lett. **87**(14), 147003.

Armitage, N. P., D. H. Lu, C. Kim, A. Damascelli, K. M. Shen, F. Ronning, D. L. Feng, P. Bogdanov, X. J. Zhou, W. L. Yang, Z. Hussain, P. K. Mang, *et al.*, 2003, Phys. Rev. B **68**(6), 064517.

Armitage, N. P., F. Ronning, D. H. Lu, C. Kim, A. Damascelli, K. M. Shen, D. L. Feng, H. Eisaki, Z.-X. Shen, P. K. Mang, N. Kaneko, M. Greven, *et al.*, 2002, Phys. Rev. Lett. **88**(25), 257001.

Asayama, K., Y. Kitaoka, G. qing Zheng, and K. Ishida, 1996, Progress in Nuclear Magnetic Resonance Spectroscopy **28**(3-4), 221 .

B. Kyung, A.-M. T., D. Sénéchal, 2009, arXiv:0812.1228 .

Bacci, S. B., E. R. Gagliano, R. M. Martin, and J. F. Annett, 1991, Phys. Rev. B **44**(14), 7504.

Bakharev, O. N., I. M. Abu-Shiekah, H. B. Brom, A. A. Nugroho, I. P. McCulloch, and J. Zaanen, 2004, Phys. Rev.

Lett. **93**(3), 037002.

Balci, H., and R. L. Greene, 2004, Phys. Rev. Lett. **93**(6), 067001.

Balci, H., C. P. Hill, M. M. Qazilbash, and R. L. Greene, 2003, Phys. Rev. B **68**(5), 054520.

Balci, H., V. N. Smolyaninova, P. Fournier, A. Biswas, and R. L. Greene, 2002, Phys. Rev. B **66**, 174510.

Basov, D. N., and T. Timusk, 2005, Rev. Mod. Phys. **77**(2), 721.

Beck, R., Y. Dagan, A. Milner, A. Gerber, and G. Deutscher, 2004, Phys. Rev. B **69**(14), 144506.

Bednorz, J., and K. A. Müller, 1986, Z. Phys. B **64**, 189.

Beesabathina, D. P., L. Salamanca-Riba, S. N. Mao, X. X. Xi, and T. Venkatesan, 1993, Appl. Phys. Lett. **62**(23), 3022.

Billinge, S. J. L., and T. Egami, 1993, Phys. Rev. B **47**(21), 14386.

Biswas, A., P. Fournier, M. M. Qazilbash, V. N. Smolyaninova, H. Balci, and R. L. Greene, 2002, Phys. Rev. Lett. **88**(20), 207004.

Biswas, A., P. Fournier, V. N. Smolyaninova, R. C. Budhani, J. S. Higgins, and R. L. Greene, 2001, Phys. Rev. B **64**, 104519.

Blonder, G. E., M. Tinkham, and T. M. Klapwijk, 1982, Phys. Rev. B **25**(7), 4515.

Blumberg, G., P. Abbamonte, M. V. Klein, W. C. Lee, D. M. Ginsberg, L. L. Miller, and A. Zibold, 1996, Phys. Rev. B **53**(18), R11930.

Blumberg, G., M. Kang, and M. V. Klein, 1997, Phys. Rev. Lett. **78**(12), 2461.

Blumberg, G., A. Koitzsch, A. Gozar, B. S. Dennis, C. A. Kendziora, P. Fournier, and R. L. Greene, 2002, Phys. Rev. Lett. **88**, 107002.

Blumberg, G., A. Koitzsch, A. Gozar, B. S. Dennis, C. A. Kendziora, P. Fournier, and R. L. Greene, 2003, Phys. Rev. Lett. **90**(14), 149702.

Boebinger, G. S., Y. Ando, A. Passner, T. Kimura, M. Okuya, J. Shimoyama, K. Kishio, K. Tamasaku, N. Ichikawa, and S. Uchida, 1996, Phys. Rev. Lett. **77**(27), 5417.

Bogdanov, P. V., A. Lanzara, S. A. Kellar, X. J. Zhou, E. D. Lu, W. J. Zheng, G. Gu, J.-I. Shimoyama, K. Kishio, H. Ikeda, R. Yoshizaki, Z. Hussain, *et al.*, 2000, Phys. Rev. Lett. **85**(12), 2581.

Bonn, D., and W. Hardy, 1996, in *Physical Properties of High Temperature Superconductors V*, edited by D. Ginsberg (World Scientific, Singapore), p. 7.

Borsa, F., P. Carreta, J. H. Cho, F. C. Chou, Q. Hu, D. C. Johnston, A. Lascialfari, D. R. Torgeson, R. J. Gooding, N. M. Salem, and K. J. E. Vos, 1995, Phys. Rev. B **52**(10), 7334.

Bourges, P., 1999, in *The gap Symmetry and Fluctuations in High Temperature Superconductors: Proceedings of NATO ASI summer school held September 1-13, 1997 in Carg'ese, France*, edited by D. P. J. Bok, G. Deutscher and S. Wolf (Plenum Press, 1998), pp. 349–371.

Bourges, P., L. Boudarene, D. Petitgrand, and P. Galez, 1992, Physica B **180**, 447.

Bourges, P., H. Casalta, A. S. Ivanov, and D. Petitgrand, 1997, Phys. Rev. Lett. **79**(24), 4906.

Braden, M., W. Paulius, A. Cousson, P. Vigoureux, G. Heger, A. Goukassov, P. Bourges, and D. Petitgrand, 1994, Europhys. Lett. **25**, 625 .

Braden, M., L. Pintschovius, T. Uefuji, and K. Yamada, 2005, Phys. Rev. B **72**(18), 184517.

Brinkmann, M., T. Rex, H. Bach, and K. Westerholt, 1996a,

J. Crystal Growth **163**(4), 369 .

Brinkmann, M., T. Rex, M. Stief, H. Bach, and K. Westerholt, 1996b, Physica C **269**(1-2), 76.

Budhani, R. C., M. C. Sullivan, C. J. Lobb, and R. L. Greene, 2002, Phys. Rev. B **65**(10), 100517.

Bulut, N., and D. J. Scalapino, 1996, Phys. Rev. B **53**(9), 5149.

Calvani, P., M. Capizzi, S. Lupi, P. Maselli, A. Paolone, and P. Roy, 1996, Phys. Rev. B **53**(5), 2756.

Campuzano, J. C., M. R. Norman, and M. Randeria, 2004, in *Physics of Conventional and Unconventional Superconductors*, edited by K. H. Bennemann and J. B. Ketterson (Springer-Verlag, Berlin), volume II, pp. 167–273.

Cappelluti, E., S. Ciuchi, and S. Fratini, 2009, Phys. Rev. B **79**(1), 012502.

Carbotte, J., D. N. Basov, and E. Schachinger, 1999, Nature **401**, 354.

Carlson, E. W., V. J. Emery, S. A. Kivelson, and D. Orgad, 2003, The Physics of Conventional and Unconventional Superconductors, edited by K. H. Bennemann, and J. B. Ketterson .

Cassanho, A., D. R. Gabbe, and H. P. Jenssen, 1989, J. Crystal Growth **96**(4), 999.

Chakravarty, S., R. B. Laughlin, D. K. Morr, and C. Nayak, 2001, Phys. Rev. B **63**(9), 094503.

Chakravarty, S., A. Sudbo, P. W. Anderson, and S. Strong, 1993, Science **261**, 337.

Chattopadhyay, T., J. W. Lynn, N. Rosov, T. E. Grigereit, S. N. Barilo, and D. I. Zhigunov, 1994, Phys. Rev. B **49**(14), 9944.

Chen, C.-T., P. Seneor, N.-C. Yeh, R. P. Vasquez, L. D. Bell, C. U. Jung, J. Y. Kim, M.-S. Park, H.-J. Kim, and S.-I. Lee, 2002, Phys. Rev. Lett. **88**(22), 227002.

Chen, H.-D., O. Vafek, A. Yazdani, and S.-C. Zhang, 2004, Phys. Rev. Lett. **93**(18), 187002.

Chen, X. H., C. H. Wang, G. Y. Wang, X. G. Luo, J. L. Luo, G. T. Liu, and N. L. Wang, 2005, Phys. Rev. B **72**(6), 064517.

Cherny, A. S., E. N. Khats'ko, G. Chouteau, J. M. Louis, A. A. Stepanov, P. Wyder, S. N. Barilo, and D. I. Zhigunov, 1992, Phys. Rev. B **45**(21), 12600.

Chesca, B., K. Ehrhardt, M. Mossle, R. Straub, D. Koelle, R. Kleiner, and A. Tsukada, 2003, Phys. Rev. Lett. **90**(5), 057004.

Chesca, B., M. Seifried, T. Dahm, N. Schopohl, D. Koelle, R. Kleiner, and A. Tsukada, 2005, Phys. Rev. B **71**(10), 104504.

Chiao, M., R. W. Hill, C. Lupien, B. Popić, R. Gagnon, and L. Taillefer, 1999, Phys. Rev. Lett. **82**(14), 2943.

Chiao, M., R. W. Hill, C. Lupien, L. Taillefer, P. Lambert, R. Gagnon, and P. Fournier, 2000, Phys. Rev. B **62**(5), 3554.

Cho, B. K., J. H. Kim, Y. J. Kim, B.-h. O, J. S. Kim, and G. R. Stewart, 2001, Phys. Rev. B **63**(21), 214504.

Chou, F. C., F. Borsa, J. H. Cho, D. C. Johnston, A. Lascialfari, D. R. Torgeson, and J. Ziolo, 1993, Phys. Rev. Lett. **71**(14), 2323.

Claesson, T., M. Mnsson, C. Dallera, F. Venturini, C. D. Nadai, N. B. Brookes, and O. Tjernberg, 2004, Phys. Rev. Lett. **93**(13), 136402.

Coldea, R., S. M. Hayden, G. Aeppli, T. G. Perring, C. D. Frost, T. E. Mason, S.-W. Cheong, and Z. Fisk, 2001, Phys. Rev. Lett. **86**(23), 5377.

Coleman, P., 2007, in *Handbook of Magnetism and Advanced Magnetic Materials*, edited by H. Kronmuller and S. Parkin (J. Wiley and Sons), volume 1, pp. 95–148.

Cooper, J. R., 1996, Phys. Rev. B **54**(6), R3753.

Côté, G., M. Poirier, and P. Fournier, 2008, J. of Appl. Phys. **104**(12), 123914.

Covington, M., M. Aprili, E. Paraoanu, L. H. Greene, F. Xu, J. Zhu, and C. A. Mirkin, 1997, Phys. Rev. Lett. **79**(2), 277.

Covington, M., R. Scheuerer, K. Bloom, and L. H. Greene, 1996, Appl. Phys. Lett. **68**(12), 1717.

Cox, D. E., A. I. Goldman, M. A. Subramanian, J. Gopalakrishnan, and A. W. Sleight, 1989, Phys. Rev. B **40**(10), 6998.

Cummins, T. R., and R. G. Egdell, 1993, Phys. Rev. B **48**(9), 6556.

Curro, N. J., T. Imai, C. P. Slichter, and B. Dabrowski, 1997, Phys. Rev. B **56**(2), 877.

Custers, J., P. Gegenwart, H. Wilhelm, K. Neumaier, Y. Tokiwa, O. Trovarelli, C. Geibel, F. Steglich, C. Pépin, and P. Coleman, 2003, Nature **424**, 524.

Cyr-Choiniere, O., R. Daou, F. Laliberte, D. LeBoeuf, N. Doiron-Leyraud, J. Chang, J.-Q. Yan, J.-G. Cheng, J.-S. Zhou, J. B. Goodenough, S. Pyon, T. Takayama, *et al.*, 2009, Nature **458**(7239), 743.

Dagan, Y., M. C. Barr, W. M. Fisher, R. Beck, T. Dhakal, A. Biswas, and R. L. Greene, 2005a, Phys. Rev. Lett. **94**(5), 057005.

Dagan, Y., R. Beck, and R. L. Greene, 2007, Phys. Rev. Lett. **99**(14), 147004.

Dagan, Y., and R. L. Greene, 2004, unpublished .

Dagan, Y., and R. L. Greene, 2007, Phys. Rev. B **76**(2), 024506.

Dagan, Y., M. M. Qazilbash, and R. L. Greene, 2005b, Phys. Rev. Lett. **94**(18), 187003.

Dagan, Y., M. M. Qazilbash, C. P. Hill, V. N. Kulkarni, and R. L. Greene, 2004, Phys. Rev. Lett. **92**(16), 167001.

Dai, P., H. J. Kang, H. A. Mook, M. Matsuura, J. W. Lynn, Y. Kurita, S. Komiya, and Y. Ando, 2005, Phys. Rev. B **71**(10), 100502.

Dalichaouch, Y., M. de Andrade, and M. Maple, 1993, Physica C **218**(1-2), 309 .

Damascelli, A., Z. Hussain, and Z.-X. Shen, 2003, Rev. Mod. Phys. **75**(2), 473.

Das, T., R. S. Markiewicz, and A. Bansil, 2007, Phys. Rev. Lett. **98**(19), 197004.

d'Astuto, M., G. Dhalenne, J. Graf, M. Hoesch, P. Giura, M. Krisch, P. Berthet, A. Lanzara, and A. Shukla, 2008, Phys. Rev. B **78**(14), 140511.

d'Astuto, M., P. K. Mang, P. Giura, A. Shukla, P. Ghigna, A. Mirone, M. Braden, M. Greven, M. Krisch, and F. Sette, 2002, Phys. Rev. Lett. **88**(16), 167002.

Demler, E., S. Sachdev, and Y. Zhang, 2001, Phys. Rev. Lett. **87**(6), 067202.

Deutscher, G., 1999, Nature **397**, 410.

Deutscher, G., 2005, Rev. Mod. Phys. **77**(1), 109.

Devereaux, T. P., D. Einzel, B. Stadlober, R. Hackl, D. H. Leach, and J. J. Neumeier, 1994, Phys. Rev. Lett. **72**(3), 396.

Devereaux, T. P., and R. Hackl, 2007, Rev. Mod. Phys. **79**(1), 175.

Dierker, S. B., M. V. Klein, G. W. Webb, and Z. Fisk, 1983, Phys. Rev. Lett. **50**(11), 853.

Ding, H., M. R. Norman, J. C. Campuzano, M. Randeria, A. F. Bellman, T. Yokoya, T. Takahashi, T. Mochiku, and

K. Kadowaki, 1996, Phys. Rev. B **54**(14), R9678.

Doiron-Leyraud, N., C. Proust, D. LeBoeuf, J. Levallois, J.-B. Bonnemaison, R. Liang, D. Bonn, W. Hardy, and L. Taillefer, 2007, Nature **447**, 565.

Durst, A. C., and P. A. Lee, 2000, Phys. Rev. B **62**(2), 1270.

Emery, V. J., and S. A. Kivelson, 1992, J. Phys. Chem. Sol. **53**(12), 1499.

Emery, V. J., and S. A. Kivelson, 1993, Physica C **209**, 597.

Emery, V. J., and S. A. Kivelson, 1995, Nature **374**, 434.

Emery, V. J., and G. Reiter, 1988, Phys. Rev. B **38**(16), 11938.

Endoh, Y., M. Matsuda, K. Yamada, K. Kakurai, Y. Hidaka, G. Shirane, and R. J. Birgeneau, 1989, Phys. Rev. B **40**(10), 7023.

Eskes, H., G. Sawatzky, and L. Feiner, 1989, Physica C **160**, 424.

Eun, J., X. Jia, and S. Chakravarty, 2009, arXiv:0912.0728v2 .

Fauqué, B., Y. Sidis, V. Hinkov, S. Pailhès, C. T. Lin, X. Chaud, and P. Bourges, 2006, Phys. Rev. Lett. **96**(19), 197001.

Fischer, O., M. Kugler, I. Maggio-Aprile, C. Berthod, and C. Renner, 2007, Rev. Mod. Phys. **79**(1), 353.

Fisher, D. S., G. Kotliar, and G. Moeller, 1995, Phys. Rev. B **52**(24), 17112.

Fogelström, M., D. Rainer, and J. A. Sauls, 1997, Phys. Rev. Lett. **79**(2), 281.

Fontcuberta, J. T., and L. Fabrega, 1996, in *Studies of High Temperature Superconductors*, edited by A. V. Narlikar (Nova Science Publishers, Commack, NY), volume 16, p. 185.

Fournier, P., M.-E. Gosselin, S. Savard, J. Renaud, I. Hetel, P. Richard, and G. Riou, 2004, Phys. Rev. B **69**, 220501.

Fournier, P., and R. L. Greene, 2003, Phys. Rev. B **68**, 094507.

Fournier, P., J. Higgins, H. Balci, E. Maiser, C. J. Lobb, and R. L. Greene, 2000, Phys. Rev. B **62**, 11 993.

Fournier, P., X. Jiang, W. Jiang, S. N. Mao, T. Venkatesan, C. J. Lobb, and R. L. Greene, 1997, Phys. Rev. B **56**, 14149.

Fournier, P., E. Maiser, and R. L. Greene, 1998a, in *The Gap Symmetry and Fluctuations in High-T_c Superconductors*, edited by J. Bok, G. Deutscher, D. Pavuna, and S. Wolf (NATO ASI Series B), volume 371, p. 145.

Fournier, P., P. Mohanty, E. Maiser, S. Darzens, T. Venkatesan, C. J. Lobb, G. Czjzek, R. A. Webb, and R. L. Greene, 1998b, Phys. Rev. Lett. **81**, 4720.

Fujimori, A., Y. Tokura, H. Eisaki, H. Takagi, S. Uchida, and E. Takayama-Muromachi, 1990, Phys. Rev. B **42**(1), 325.

Fujita, M., T. Kubo, S. Kuroshima, T. Uefuji, K. Kawashima, K. Yamada, I. Watanabe, and K. Nagamine, 2003, Phys. Rev. B **67**(1), 014514.

Fujita, M., M. Matsuda, B. Fak, C. D. Frost, and K. Yamada, 2006, J. Phys. Soc. Jap. **75**, 093704.

Fujita, M., M. Matsuda, S. Katano, and K. Yamada, 2004, Phys. Rev. Lett. **93**(14), 147003.

Fujita, M., M. Matsuda, S.-H. Lee, M. Nakagawa, and K. Yamada, 2008a, Phys. Rev. Lett. **101**(10), 107003.

Fujita, M., M. Nakagawa, C. D. Frost, and K. Yamada, 2008b, Journal of Physics: Conference Series **108**, 012006 (4pp).

Fukuda, M., M. K. Zalalutdinov, V. Kovacik, T. Minoguchi, T. Obata, M. Kubota, and E. B. Sonin, 2005, Phys. Rev. B **71**(21), 212502.

Gamayunov, K., I. Tanaka, and H. Kojima, 1994, Physica C **228**(1-2), 58.

Gantmakher, V. F., S. N. Ermolov, G. E. Tsydynzhapov, A. A. Zhukov, and T. I. Baturina, 2003, JETP Lett. **77**(8), 424.

Gasumyants, V., V. Kaidanov, and E. Vladimirskaya, 1995, Physica C: Superconductivity and its applications **248**(3-4), 255.

Gauthier, J., S. Gagné, J. Renaud, M.-E. Gosselin, P. Fournier, and P. Richard, 2007, Phys. Rev. B **75**(2), 024424.

Ghamaty, S., B. Lee, J. Markert, E. Early, T. Bjrnholm, C. Seaman, and M. Maple, 1989, Physica C **160**(2), 217 .

Gilardi, R., A. Hiess, N. Momono, M. Oda, M. Ido, and J. Mesot, 2004, Europhys. Lett. **66**(6), 840.

Goldman, A. M., and N. Markovic, 1998, Physics Today **51**(11), 39.

Gollnik, F., and M. Naito, 1998, Phys. Rev. B **58**(17), 11734.

Gooding, R. J., K. J. E. Vos, and P. W. Leung, 1994, Phys. Rev. B **50**(17), 12866.

Graf, J., G.-H. Gweon, K. McElroy, S. Y. Zhou, C. Jozwiak, E. Rotenberg, A. Bill, T. Sasagawa, H. Eisaki, S. Uchida, H. Takagi, D.-H. Lee, *et al.*, 2007, Phys. Rev. Lett. **98**(6), 067004.

Granath, M., 2004, Phys. Rev. B **69**(21), 214433.

Gupta, A., G. Koren, C. C. Tsuei, A. Segmüller, and T. R. McGuire, 1989, Appl. Phys. Lett. **55**(17), 1795.

Gurvitch, M., and A. T. Fiory, 1987, Phys. Rev. Lett. **59**(12), 1337.

Hackl, A., and S. Sachdev, 2009, Physical Review B (Condensed Matter and Materials Physics) **79**(23), 235124 (pages 9).

Hagen, S. J., J. L. Peng, Z. Y. Li, and R. L. Greene, 1991, Phys. Rev. B **43**(16), 13606.

Hanaguri, T., C. Lupien, Y. Kohsaka, D. H. Lee, M. Azuma, M. Takano, H. Takagi, and J. C. Davis, 2004, Nature **430**, 1001.

Hardy, W. N., D. A. Bonn, D. C. Morgan, R. Liang, and K. Zhang, 1993, Phys. Rev. Lett. **70**(25), 3999.

Harima, N., A. Fujimori, T. Sugaya, and I. Terasaki, 2003, Phys. Rev. B **67**(17), 172501.

Harima, N., J. Matsuno, A. Fujimori, Y. Onose, Y. Taguchi, and Y. Tokura, 2001, Phys. Rev. B **64**(22), 220507.

van Harlingen, D. J., 1995, Rev. Mod. Phys. **67**(2), 515.

Harshman, D. R., G. Aeppli, G. P. Espinosa, A. S. Cooper, J. P. Remeika, E. J. Ansaldo, T. M. Riseman, D. L. Williams, D. R. Noakes, B. Ellman, and T. F. Rosenbaum, 1988, Phys. Rev. B **38**(1), 852.

Helm, T., M. V. Kartsovnik, M. Bartkowiak, N. Bittner, M. Lambacher, A. Erb, J. Wosnitza, and R. Gross, 2009, Phys. Rev. Lett. **103**(15), 157002.

Heyen, E. T., R. Liu, M. Cardona, S. Piol, R. J. Melville, D. M. Paul, E. Morán, and M. A. Alario-Franco, 1991, Phys. Rev. B **43**(4), 2857.

Hidaka, Y., and M. Suzuki, 1989, Nature **338**, 635 .

Higgins, J. S., Y. Dagan, M. C. Barr, B. D. Weaver, and R. L. Greene, 2006, Phys. Rev. B **73**(10), 104510.

Hilgenkamp, H., and J. Mannhart, 2002, Rev. Mod. Phys. **74**(2), 485.

Hill, R. W., C. Proust, L. Taillefer, P. Fournier, and R. L. Greene, 2001, Nature **414**, 711.

Hirsch, J., and F. Marsiglio, 1989, Physica C **162-164**, 591.

Hirsch, J. E., 1995, Physica C **243**, 319.

Hirschfeld, P. J., and N. Goldenfeld, 1993, Phys. Rev. B

48(6), 4219.

Hlubina, R., and T. M. Rice, 1995, Phys. Rev. B **51**(14), 9253.

Hodges, C., H. Smith, and J. W. Wilkins, 1971, Phys. Rev. B **4**(2), 302.

Homes, C. C., B. P. Clayman, J. L. Peng, and R. L. Greene, 1997, Phys. Rev. B **56**(9), 5525.

Homes, C. C., R. P. S. M. Lobo, P. Fournier, A. Zimmers, and R. L. Greene, 2006, Phys. Rev. B **74**(21), 214515.

Howald, C., P. Fournier, and A. Kapitulnik, 2001, Phys. Rev. B **64**(10), 100504.

Hozoi, L., M. S. Laad, and P. Fulde, 2008, Phys. Rev. B **78**(16), 165107.

Hu, C.-R., 1994, Phys. Rev. Lett. **72**(10), 1526.

Hui, K., and A. N. Berker, 1989, Phys. Rev. Lett. **62**(21), 2507.

Hundley, M. F., J. D. Thompson, S.-W. Cheong, Z. Fisk, and B. Oseroff, 1989, Physica C **158**, 102.

Hybertsen, M. S., E. B. Stechel, M. Schluter, and D. R. Jennison, 1990, Phys. Rev. B **41**(16), 11068.

Ignatov, A. Y., A. A. Ivanov, A. P. Menushenkov, S. Iacobucci, and P. Lagarde, 1998, Phys. Rev. B **57**(14), 8671.

Ikeda, M., M. Takizawa, T. Yoshida, A. Fujimori, K. Segawa, and Y. Ando, 2009a, unpublished **arXiv:1001.0102v1**.

Ikeda, M., T. Yoshida, A. Fujimori, M. Kubota, K. Ono, H. Das, T. Saha-Dasgupta, K. Unozawa, Y. Kaga, T. Sasagawa, and H. Takagi, 2009b, Phys. Rev. B **80**(1), 014510.

Ikeda, M., T. Yoshida, A. Fujimori, M. Kubota, K. Ono, K. Unozawa, T. Sasagawa, and H. Takagi, 2007, J. Supercond. Nov. Mag. **20**, 563.

Ikeda, N., Z. Hiroi, M. Azuma, M. Takano, Y. Bando, and Y. Takeda, 1993, Physica C **210**(3-4), 367 .

Imai, T., C. P. Slichter, J. L. Cobb, and J. T. Markert, 1995, J. Phys. Chem. Solids **56**, 1921.

Imry, Y., and M. Wortis, 1979, Phys. Rev. B **19**(7), 3580.

Ino, A., C. Kim, M. Nakamura, T. Yoshida, T. Mizokawa, Z.-X. Shen, A. Fujimori, T. Kakeshita, H. Eisaki, and S. Uchida, 2000, Phys. Rev. B **62**(6), 4137.

Ishii, H., T. Koshizawa, H. Kataura, T. Hanyu, H. Takai, K. Mizoguchi, K. Kume, I. Shiozaki, and S. Yamaguchi, 1989, Jpn. J. Appl. Phys **28**, L1952.

Ismer, J.-P., I. Eremin, E. Rossi, and D. K. Morr, 2007, Phys. Rev. Lett. **99**(4), 047005.

James, A. C. W. P., S. M. Zahurak, and D. W. Murphy, 1989, Nature **338**, 240.

Jandl, S., P. Dufour, T. Strach, T. Ruf, M. Cardona, V. Nekvasil, C. Chen, B. M. Wanklyn, and S. Piñol, 1996, Phys. Rev. B **53**(13), 8632.

Jandl, S., M. Iliev, C. Thomsen, T. Ruf, M. Cardona, B. M. Wanklyn, and C. Chen, 1993, Solid State Comm. **87**(7), 609.

Jandl, S., P. Richard, V. Nekvasil, D. I. Zhigunov, S. N. Barilo, and S. V. Shiryaev, 1999, Physica C **314**, 189.

Jenkins, G. S., D. C. Schmadel, P. L. Bach, R. L. Greene, X. Béchamp-Laganière, G. Roberge, P. Fournier, and H. D. Drew, 2009a, Phys. Rev. B **79**(22), 224525.

Jenkins, G. S., D. C. Schmadel, P. L. Bach, R. L. Greene, X. B.-L. G. Roberge, P. Fournier, H. Kontani, and H. D. Drew, 2009b, arXiv:0901.1701v1 .

Jiang, W., S. N. Mao, X. X. Xi, X. Jiang, J. L. Peng, T. Venkatesan, C. J. Lobb, and R. L. Greene, 1994, Phys. Rev. Lett. **73**(9), 1291.

Jin, K., X. H. Zhang, P. Bach, and R. L. Greene, 2009, Phys. Rev. B **80**(1), 012501.

Jin, R., Y. Onose, Y. Tokura, D. Mandrus, P. Dai, and B. C. Sales, 2003, Phys. Rev. Lett. **91**(14), 146601.

Jorgensen, J. D., P. G. Radaelli, D. G. Hinks, J. L. Wagner, S. Kikkawa, G. Er, and F. Kanamaru, 1993, Phys. Rev. B **47**(21), 14654.

Joynt, R., and L. Taillefer, 2002, Rev. Mod. Phys. **74**(1), 235.

Jung, C. U., J. Y. Kim, M.-S. Park, M.-S. Kim, H.-J. Kim, S. Y. Lee, and S.-I. Lee, 2002, Phys. Rev. B **65**(17), 172501.

Kadono, R., W. Higemoto, A. Koda, M. I. Larkin, G. M. Luke, A. T. Savici, Y. J. Uemura, K. M. Kojima, T. Okamoto, T. Kakeshita, S. Uchida, T. Ito, *et al.*, 2004a, Phys. Rev. B **69**(10), 104523.

Kadono, R., K. Ohishi, A. Koda, , W. Higemoto, K. M. Kojima, S. ichi Kuroshima, M. Fujita, and K. Yamada, 2004b, J. Phys. Soc. Japan **73**(11), 2944.

Kadono, R., K. Ohishi, A. Koda, S. R. Saha, W. Higemoto, M. Fujita, and K. Yamada, 2005, J. Phys. Soc. Japan **74**(10), 2806.

Kakuyanagi, K., K.-i. Kumagai, and Y. Matsuda, 2002, Phys. Rev. B **65**(6), 060503.

Kancharla, S. S., B. Kyung, D. Senechal, M. Civelli, M. Capone, G. Kotliar, and A.-M. S. Tremblay, 2008, Phys. Rev. B **77**(18), 184516.

Kaneko, N., Y. Hidaka, S. Hosoya, K. Yamada, Y. Endoh, S. Takekawa, and K. Kitamura, 1999, J. Crystal Growth **197**(4), 818 .

Kang, H. J., P. Dai, B. J. Campbell, P. J. Chupas, S. Rosenkranz, P. L. Lee, Q. Huang, S. Li, S. Komiya, and Y. Ando, 2007, Nat Mater **6**(3), 224.

Kang, H. J., P. Dai, J. W. Lynn, M. Matsuura, J. R. Thompson, S.-C. Zhang, D. N. Argyriou, Y. Onose, and Y. Tokura, 2003a, Nature **423**(6939), 522.

Kang, H. J., P. Dai, J. W. Lynn, M. Matsuura, J. R. Thompson, S.-C. Zhang, D. N. Argyriouk, Y. Onose, and Y. Tokura, 2003b, Nature **429**, 140.

Kang, H. J., P. Dai, D. Mandrus, R. Jin, H. A. Mook, D. T. Adroja, S. M. Bennington, S.-H. Lee, and J. W. Lynn, 2002, Phys. Rev. B **66**(6), 064506.

Kang, H. J., P. Dai, H. A. Mook, D. N. Argyriou, V. Sikolenko, J. W. Lynn, Y. Kurita, S. Komiya, and Y. Ando, 2005, Phys. Rev. B **71**(21), 214512.

ichi Karimoto, S., and M. Naito, 2004, Appl. Phys. Lett. **84**(12), 2136.

Kashiwaya, S., T. Ito, K. Oka, S. Ueno, H. Takashima, M. Koyanagi, Y. Tanaka, and K. Kajimura, 1998, Phys. Rev. B **57**(14), 8680.

Kashiwaya, S., Y. Tanaka, M. Koyanagi, H. Takashima, and K. Kajimura, 1995, Phys. Rev. B **51**(2), 1350.

Kastner, M. A., R. J. Birgeneau, G. Shirane, and Y. Endoh, 1998, Rev. Mod. Phys. **70**(3), 897.

Katano, S., M. Sato, K. Yamada, T. Suzuki, and T. Fukase, 2000, Phys. Rev. B **62**(22), R14677.

Kawakami, T., T. Shibauchi, Y. Terao, and M. Suzuki, 2006, Phys. Rev. B **74**(14), 144520.

Kawakami, T., T. Shibauchi, Y. Terao, M. Suzuki, and L. Krusin-Elbaum, 2005, Phys. Rev. Lett. **95**(1), 017001.

Keimer, B., A. Aharony, A. Auerbach, R. J. Birgeneau, A. Cassanho, Y. Endoh, R. W. Erwin, M. A. Kastner, and G. Shirane, 1992, Phys. Rev. B **45**(13), 7430.

Kendziora, C., B. Nachumi, P. Fournier, Z. Y. Li, R. L. Greene, and D. G. Hinks, 2001, Physica C **364-365**, 541.

Khasanov, R., A. Shengelaya, A. Maisuradze, D. D. Castro, I. M. Savić, S. Weyeneth, M. S. Park, D. J. Jang, S.-I. Lee, and H. Keller, 2008, Phys. Rev. B **77**(18), 184512.

Khaykovich, B., Y. S. Lee, R. W. Erwin, S.-H. Lee, S. Wakimoto, K. J. Thomas, M. A. Kastner, and R. J. Birgeneau, 2002, Phys. Rev. B **66**(1), 014528.

Khurana, A., 1989, Physics Today **42**, 17.

Kikkawa, G., F. Kanamaru, Y. Miyamoto, S. Tanaka, M. Sera, M. Sato, Z. Hiroi, M. Takano, and Y. Bando, 1992, Physica C **196**(3-4), 271 .

Kim, J. S., and D. R. Gaskell, 1993, Physica C **209**(4), 381.

Kim, M.-S., T. R. Lemberger, C. U. Jung, J.-H. Choi, J. Y. Kim, H.-J. Kim, and S.-I. Lee, 2002, Phys. Rev. B **66**(21), 214509.

Kim, M.-S., J. A. Skinta, T. R. Lemberger, A. Tsukada, and M. Naito, 2003, Phys. Rev. Lett. **91**(8), 087001.

King, D. M., Z.-X. Shen, D. S. Dessau, B. O. Wells, W. E. Spicer, A. J. Arko, D. S. Marshall, J. DiCarlo, A. G. Loeser, C. H. Park, E. R. Ratner, J. L. Peng, *et al.*, 1993, Phys. Rev. Lett. **70**(20), 3159.

Kirtley, J. R., C. C. Tsuei, M. Rupp, J. Z. Sun, L. S. Yu-Jahnes, A. Gupta, M. B. Ketchen, K. A. Moler, and M. Bhushan, 1996, Phys. Rev. Lett. **76**(8), 1336.

Kivelson, S. A., I. P. Bindloss, E. Fradkin, V. Oganesyan, J. M. Tranquada, A. Kapitulnik, and C. Howald, 2003, Rev. Mod. Phys. **75**(4), 1201.

Klamut, P., A. Sikora, Z. Bukowski, B. Dabrowski, and J. Klamut, 1997, Physica C **282-287**, 541.

Kleefisch, S., B. Welter, A. Marx, L. Alff, R. Gross, and M. Naito, 2001, Phys. Rev. B **63**(10), 100507.

Koike, Y., A. Kakimoto, M. Mochida, H. Sato, T. Noji, M. Kato, and Y. Saito, 1992, Jpn. J. Appl. Phys **31**, 2721.

Koitzsch, A., G. Blumberg, A. Gozar, B. Dennis, P. Fournier, and R. Greene, 2003, Phys. Rev. B **67**, 184522.

Kokales, J. D., P. Fournier, L. V. Mercaldo, V. V. Talanov, R. L. Greene, and S. M. Anlage, 2000, Phys. Rev. Lett. **85**, 3696.

Kontani, H., 2008, Rep. Prog. Phys. **71**, 026501.

Kordyuk, A. A., S. V. Borisenko, M. S. Golden, S. Legner, K. A. Nenkov, M. Knupfer, J. Fink, H. Berger, L. Forró, and R. Follath, 2002, Phys. Rev. B **66**(1), 014502.

Kramers, H., 1930, Proc. Amsterdam Acad. **33**, 959.

Krockenberger, Y., J. Kurian, A. Winkler, A. Tsukada, M. Naito, and L. Alff, 2008, Phys. Rev. B **77**(6), 060505.

Krüger, F., S. D. Wilson, L. Shan, S. Li, Y. Huang, H.-H. Wen, S.-C. Zhang, P. Dai, and J. Zaanen, 2007, Phys. Rev. B **76**(9), 094506.

Kuiper, P., G. Kruizinga, J. Ghijsen, M. Grioni, P. J. W. Weijs, F. M. F. de Groot, G. A. Sawatzky, H. Verweij, L. F. Feiner, and H. Petersen, 1988, Phys. Rev. B **38**(10), 6483.

Kurahashi, K., H. Matsushita, M. Fujita, and K. Yamada, 2002, J. Phys. Soc. Japan **71**(3), 910.

Kuroshima, S., M. Fujita, T. Uefuji, M. Matsuda, and K. Yamada, 2003, Physica C **392–396**, 216.

Kusko, C., R. S. Markiewicz, M. Lindroos, and A. Bansil, 2002, Phys. Rev. B **66**(14), 140513.

Kwei, G. H., S.-W. Cheong, Z. Fisk, F. H. Garzon, J. A. Goldstone, and J. D. Thompson, 1989, Phys. Rev. B **40**(13), 9370.

Kyung, B., V. Hankevych, A.-M. Dare, and A.-M. S. Tremblay, 2004, Phys. Rev. Lett. **93**(14), 147004.

Kyung, B., J.-S. Landry, and A.-M. S. Tremblay, 2003, Phys. Rev. B **68**(17), 174502.

Lake, B., G. Aeppli, K. N. Clausen, D. F. McMorrow, K. Lefmann, N. E. Hussey, N. Mangkorntong, M. Nohara, H. Takagi, T. E. Mason, and A. Schroeder, 2001, Science **291**(5509), 1759 .

Lake, B., H. M. Rønnow, N. B. Christensen, G. Aeppli, K. Lefmann, D. F. McMorrow, P. Vorderwisch, P. Smeibidl, N. Mangkorntong, T. Sasagawa, M. Nohara, H. Takagi, *et al.*, 2002, Nature **415**, 299.

Lanfredi, A., S. Sergeenkov, and F. Araujo-Moreira, 2006, Physica C **450**(1-2), 40.

Lang, K., V. Madhavan, J. Hoffman, E. Hudson, H. Eisaki, S. Uchida, and J. Davis, 2002, Nature **415**, 412.

Lanzara, A., P. V. Bogdanov, S. A. K. X. J. Zhou and, D. L. Feng, E. D. Lu, T. Yoshida, H. Eisaki, A. Fujimori, K. Kishio, J.-I. Shimoyama, T. Noda, S. Uchida, *et al.*, 2001, Nature **412**, 510.

Lavrov, A. N., H. J. Kang, Y. Kurita, T. Suzuki, S. Komiya, J. W. Lynn, S.-H. Lee, P. Dai, and Y. Ando, 2004, Phys. Rev. Lett. **92**(22), 227003.

LeBoeuf, D., N. Doiron-Leyraud, J. Levallois, R. Daou, J.-B. Bonnemaison, N. Hussey, L. B. andB.J. Ramshaw, R. Liang, D. Bonn, W. Hardy, C. Proust, and L. Taillefer, 2007, Nature **450**, 533.

Leca, V., D. H. A. Blank, G. Rijnders, S. Bals, and G. van Tendeloo, 2006, Appl. Phys. Lett. **89**(9), 092504.

Lee, D.-H., and S. A. Kivelson, 2003, Phys. Rev. B **67**(2), 024506.

Lee, J., K. Fujita, K. McElroy, J. A. Slezak, M. Wang, Y. Aiura, H. Bando, M. Ishikado, T. Masui, J. X. Zhu, A. V. Balatsky, H. Eisaki, *et al.*, 2006a, Nature **442**(7102), 546.

Lee, P. A., N. Nagaosa, and X.-G. Wen, 2006b, Rev. Mod. Phys. **78**(1), 17.

Lefebvre, S., P. Wzietek, S. Brown, C. Bourbonnais, D. Jérome, C. Mézière, M. Fourmigué, and P. Batail, 2000, Phys. Rev. Lett. **85**(25), 5420.

Li, J.-X., J. Zhang, and J. Luo, 2003, Phys. Rev. B **68**(22), 224503.

Li, P., F. F. Balakirev, and R. L. Greene, 2007a, Phys. Rev. Lett. **99**(4), 047003.

Li, P., F. F. Balakirev, and R. L. Greene, 2007b, Phys. Rev. B **75**(17), 172508.

Li, P., K. Behnia, and R. L. Greene, 2007c, Phys. Rev. B **75**(2), 020506.

Li, P., and R. L. Greene, 2007, Phys. Rev. B **76**(17), 174512.

Li, S., S. Chi, J. Zhao, H.-H. Wen, M. B. Stone, J. W. Lynn, and P. Dai, 2008a, Phys. Rev. B **78**(1), 014520.

Li, S., S. D. Wilson, D. Mandrus, B. Zhao, Y. Onose, Y. Tokura, and P. Dai, 2005a, Phys. Rev. B **71**(5), 054505.

Li, S. Y., L. Taillefer, C. H. Wang, and X. H. Chen, 2005b, Phys. Rev. Lett. **95**(15), 156603.

Li, Y., V. Balédent, N. Barisic, Y. Cho, B. Fauqué, Y. Sidis, G. Yu, X. Zhao, P. Bourges, and M. Greven, 2008b, Nature **455**, 372.

Li, Z., V. Jovanovic, H. Raffy, and S. Megtert, 2009, Physica C **469**(2-3), 73 .

Liang, G., Y. Guo, D. Badresingh, W. Xu, Y. Tang, M. Croft, J. Chen, A. Sahiner, B.-h. O, and J. T. Markert, 1995, Phys. Rev. B **51**(2), 1258.

Lin, J., and A. J. Millis, 2005, Phys. Rev. B **72**(21), 214506.

Liu, C. S., and W. C. Wu, 2007, Phys. Rev. B **76**(22), 220504.

Liu, H., G. Liu, W. Zhang, L. Zhao, J. Meng, X. D. Xiaowen Jia, W. Lu, G. Wang, Y. Zhou, Y. Zhu, X. Wang, T. Wu, *et al.*, 2008, arXiv:0808.0802v1 .

Liu, R., J. Chen, P. Nachimuthu, R. Gundakaram, C. Jung, J. Kim, and S. Lee, 2001, Solid State Comm. **118**, 367.

Liu, Z. Y., H. H. Wen, L. Shan, H. P. Yang, X. F. Lu, H. Gao,

M.-S. Park, C. U. Jung, and S.-I. Lee, 2005, Europhys. Lett. **69**(2), 263.

Lofwander, T., V. S. Shumeiko, and G. Wendin, 2001, Supercond. Sci. Technol. **14**(5), R53.

Luke, G. M., L. P. Le, B. J. Sternlieb, Y. J. Uemura, J. H. Brewer, R. Kadono, R. F. Kiefl, S. R. Kreitzman, T. M. Riseman, C. E. Stronach, M. R. Davis, S. Uchida, *et al.*, 1990, Phys. Rev. B **42**(13), 7981.

Luo, H. G., and T. Xiang, 2005, Phys. Rev. Lett. **94**(2), 027001.

Lupi, S., M. Capizzi, P. Calvani, B. Ruzicka, P. Maselli, P. Dore, and A. Paolone, 1998, Phys. Rev. B **57**(2), 1248.

Lupi, S., P. Maselli, M. Capizzi, P. Calvani, P. Giura, and P. Roy, 1999, Phys. Rev. Lett. **83**(23), 4852.

Luttinger, J. M., 1960, Phys. Rev. **119**(4), 1153.

Lynn, J., and S. Skanthakumar, 2001, in *Handbook on the Physics and Chemistry of Rare Earths*, edited by L. E. K.A. Gschneidner, Jr. and M. Maple (Elsevier Science B.V), volume 31, p. 313.

Lynn, J. W., I. W. Sumarlin, S. Skanthakumar, W.-H. Li, R. N. Shelton, J. L. Peng, Z. Fisk, and S.-W. Cheong, 1990, Phys. Rev. B **41**(4), 2569.

Lyons, K. B., P. A. Fleury, J. P. Remeika, A. S. Cooper, and T. J. Negran, 1988, Phys. Rev. B **37**(4), 2353.

Ma, Z., R. C. Taber, L. W. Lombardo, A. Kapitulnik, M. R. Beasley, P. Merchant, C. B. Eom, S. Y. Hou, and J. M. Phillips, 1993, Phys. Rev. Lett. **71**(5), 781.

Machida, K., 1989, Physica C **158**(1-2), 192.

Macridin, A., M. Jarrell, T. Maier, P. R. C. Kent, and E. D'Azevedo, 2006, Phys. Rev. Lett. **97**(3), 036401.

Maier, T. A., D. Poilblanc, and D. J. Scalapino, 2008, Phys. Rev. Lett. **100**(23), 237001.

Maiser, E., P. Fournier, J.-L. Peng, F. M. Araujo-Moreira, T. Venkatesan, R. Greene, and G. Czjzek, 1998, Physica C **297**, 15.

Maljuk, A. N., G. A. Emel'chenko, and A. V. Kosenko, 1996, Journal of Alloys and Compounds **234**(1), 52.

Maljuk, A. N., A. A. Jokhov, I. G. Naumenko, I. K. Bdikin, S. A. Zver'kov, and G. A. Emel'chenko, 2000, Physica C **329**(1), 51.

Mang, P. K., S. Larochelle, A. Mehta, O. P. Vajk, A. S. Erickson, L. Lu, W. J. L. Buyers, A. F. Marshall, K. Prokes, and M. Greven, 2004a, Phys. Rev. B **70**(9), 094507.

Mang, P. K., S. Larochelle, and M.Greven, 2003, Nature **429**, 139.

Mang, P. K., O. P. Vajk, A. Arvanitaki, J. W. Lynn, and M. Greven, 2004b, Phys. Rev. Lett. **93**(2), 027002.

Manske, D., I. Eremin, and K. H. Bennemann, 2001a, Phys. Rev. B **63**(5), 054517.

Manske, D., I. Eremin, and K. H. Bennemann, 2001b, Europhys. Lett. **53**(3), 371.

Mao, S. N., X. X. Xi, S. Bhattacharya, Q. Li, T. Venkatesan, J. L. Peng, R. L. Greene, J. Mao, D. H. Wu, and S. M. Anlage, 1992, Appl. Phys. Lett. **61**(19), 2356.

Mao, S. N., X. X. Xi, Q. Li, T. Venkatesan, D. P. Beesabathina, L. Salamanca-Riba, and X. D. Wu, 1994, J. of Appl. Phys. **75**(4), 2119.

Maple, M. B., 1990, Mater. Res. Bull. **15**, 60.

Marcenat, C., R. Calemczuk, A. F. Khoder, E. Bonjour, C. Marin, and J. Y. Henry, 1993, Physica C **216**(3-4), 443.

Marcenat, C., J. Y. Henry, and R. Calemczuk, 1994, Physica C **235-240**(Part 3), 1747.

Marin, C., J. Y. Henry, and J. X. Boucherle, 1993, Solid State Comm. **86**(7), 425.

Markert, J. T., J. Beille, J. J. Neumeier, E. A. Early, C. L. Seaman, T. Moran, and M. B. Maple, 1990, Phys. Rev. Lett. **64**(1), 80.

Marshall, D. S., D. S. Dessau, A. G. Loeser, C.-H. Park, A. Y. Matsuura, J. N. Eckstein, I. Bozovic, P. Fournier, A. Kapitulnik, W. E. Spicer, and Z.-X. Shen, 1996, Phys. Rev. Lett. **76**(25), 4841.

Massidda, S., N. Hamada, J. Yu, and A. J. Freeman, 1989, Physica C **157**, 571.

Matsuda, M., Y. Endoh, and Y. Hidaka, 1991, Physica C **179**(4-6), 347.

Matsuda, M., Y. Endoh, K. Yamada, H. Kojima, I. Tanaka, R. J. Birgeneau, M. A. Kastner, and G. Shirane, 1992, Phys. Rev. B **45**(21), 12548.

Matsuda, M., M. Fujita, K. Yamada, R. J. Birgeneau, Y. Endoh, and G. Shirane, 2002, Phys. Rev. B **65**(13), 134515.

Matsuda, M., K. Yamada, K. Kakurai, H. Kadowaki, T. R. Thurston, Y. Endoh, Y. Hidaka, R. J. Birgeneau, M. A. Kastner, P. M. Gehring, A. H. Moudden, and G. Shirane, 1990, Phys. Rev. B **42**(16), 10098.

Matsui, H., T. Takahashi, T. Sato, K. Terashima, H. Ding, T. Uefuji, and K. Yamada, 2007, Phys. Rev. B **75**(22), 224514.

Matsui, H., K. Terashima, T. Sato, T. Takahashi, M. Fujita, and K. Yamada, 2005a, Phys. Rev. Lett. **95**(1), 017003.

Matsui, H., K. Terashima, T. Sato, T. Takahashi, S.-C. Wang, H.-B. Yang, H. Ding, T. Uefuji, and K. Yamada, 2005b, Phys. Rev. Lett. **94**(4), 047005.

Matsumoto, O., A. Utsuki, A. Tsukada, H. Yamamoto, T. Manabe, and M. Naito, 2009, Phys. Rev. B **79**(10), 100508.

Matsuura, M., P. Dai, H. J. Kang, J. W. Lynn, D. N. Argyriou, K. Prokes, Y. Onose, and Y. Tokura, 2003, Phys. Rev. B **68**(14), 144503.

Matsuyama, H., T. Takahashi, H. Katayama-Yoshida, T. Kashiwakura, Y. Okabe, S. Sato, N. Kosugi, A. Yagishita, K. Tanaka, H. Fujimoto, and H. Inokuchi, 1989, Physica C **160**(5-6), 567 .

McKenzie, R. H., 1997, Science **278**(5339), 820.

McQueeney, R. J., Y. Petrov, T. Egami, M. Yethiraj, G. Shirane, and Y. Endoh, 1999, Phys. Rev. Lett. **82**(3), 628.

McQueeney, R. J., J. L. Sarrao, P. G. Pagliuso, P. W. Stephens, and R. Osborn, 2001, Phys. Rev. Lett. **87**(7), 077001.

Meevasana, W., X. J. Zhou, S. Sahrakorpi, W. S. Lee, W. L. Yang, K. Tanaka, N. Mannella, T. Yoshida, D. H. Lu, Y. L. Chen, R. H. He, H. Lin, *et al.*, 2007, Phys. Rev. B **75**(17), 174506.

Meinders, M. B. J., H. Eskes, and G. A. Sawatzky, 1993, Phys. Rev. B **48**(6), 3916.

Miller, R. I., R. F. Kiefl, J. H. Brewer, J. E. Sonier, J. Chakhalian, S. Dunsiger, G. D. Morris, A. N. Price, D. A. Bonn, W. H. Hardy, and R. Liang, 2002, Phys. Rev. Lett. **88**(13), 137002.

Mira, J., J. Rivas, D. Fiorani, R. Caciuffo, D. Rinaldi, C. Vázquez-Vázquez, J. Mahía, M. A. López-Quintela, and S. B. Oseroff, 1995, Phys. Rev. B **52**(22), 16020.

Mitrovic, V. F., E. E. Sigmund, M. Eschrig, H. N. Bachman, W. P. Halperin, A. P. Reyes, P. Kuhns, and W. G. Moulton, 2001, Nature **413**, 501.

Moler, K. A., D. J. Baar, J. S. Urbach, R. Liang, W. N. Hardy, and A. Kapitulnik, 1994, Phys. Rev. Lett. **73**(20), 2744.

Moler, K. A., D. L. Sisson, J. S. Urbach, M. R. Beasley, A. Kapitulnik, D. J. Baar, R. Liang, and W. N. Hardy, 1997,

Phys. Rev. B **55**(6), 3954.

Mook, H. A., P. Dai, S. M. Hayden, G. Aeppli, T. G. Perring, and F. Dogan, 1998, Nature **395**, 580.

Mook, H. A., P. Dai, and F. Doğan, 2002, Phys. Rev. Lett. **88**(9), 097004.

Moon, E. G., and S. Sachdev, 2009, arXiv:0905.2608 .

Moran, E., A. I. Nazzal, T. C. Huang, and J. B. Torrance, 1989, Physica C **160**, 30.

Moritz, B., F. Schmitt, W. Meevasana, S. Johnston, E. M. Motoyama, M. Greven, D. H. Lu, C. Kim, R. T. Scalettar, Z.-X. Shen, and T. P. Devereaux, 2009, New Journal of Physics **11**(9), 093020.

Motoyama, E. M., P. K. Mang, D. Petitgrand, G. Yu, O. P. Vajk, I. M. Vishik, and M. Greven, 2006, Phys. Rev. Lett. **96**(13), 137002.

Motoyama, E. M., G. Yu, I. M. Vishik, O. P. Vajk, P. K. Mang, and M. Greven, 2007, Nature **445**(7124), 186.

Muller-Buschbaum, X., and X. Wollschlager, 1975, Z. Anorg. Allg. Chem. **414**, 76.

Naito, M., and M. Hepp, 2000, Jap. J. Appl. Phys. **39**(Part 2, No. 6A), L485.

Naito, M., S. Karimoto, and A. Tsukada2, 2002, Supercond. Sci. Technol. **15**, 1663.

Naito, M., H. Sato, and H. Yamamoto, 1997, Physica C **293**(1-4), 36 , intrinsic Josephson Effects and THz Plasma Oscillations in High-Tc Superconductors.

Nakamae, S., K. Behnia, N. Mangkorntong, M. Nohara, H. Takagi, S. J. C. Yates, and N. E. Hussey, 2003, Phys. Rev. B **68**(10), 100502.

Namatame, H., A. Fujimori, Y. Tokura, M. Nakamura, K. Yamaguchi, A. Misu, H. Matsubara, S. Suga, H. Eisaki, T. Ito, H. Takagi, and S. Uchida, 1990, Phys. Rev. B **41**(10), 7205.

Navarro, E., D. Jaque, J. Villegas, J. Martyn, A. Serquis, F. Prado, A. Caneiro, , and J. Vicent, 2001, J. of Alloys and Compounds **323-324**, 580.

Nedil'ko, A., 1982, Russian J. Inorg. Chem. **27**, 634.

Nekvasil, V., and M. Divis, 2001, in *Encyclopedia of Materials: Science and Technology*, edited by K. H. J. Buschow, R. W. Cahn, M. C. Flemings, B. I. (print), E. J. Kramer, S. Mahajan, , and P. V. (updates) (Elsevier, Oxford), pp. 4613 – 4627.

Nie, J. C., P. Badica, M. Hirai, A. Sundaresan, A. Crisan, H. Kito, N. Terada, Y. Kodama, A. Iyo, Y. Tanaka, and H. Ihara, 2003, Supercond. Sci. Technol. **16**(1), L1.

Niestemski, F. C., S. Kunwar, S. Zhou, S. Li, H. Ding, Z. Wang, P. Dai, and V. Madhavan, 2007, Nature **450**(7172), 1058.

Norman, M. R., D. Pines, and C. Kallin, 2005, Advances In Physics **54**(8), 715, ISSN 0001-8732.

Nücker, N., P. Adelmann, M. Alexander, H. Romberg, S. Nakai, J. Fink, H. Rietschel, G. Roth, H. Schmidt, and H. Spille, 1989, Z. Phys. B **75**, 421.

Ohta, Y., T. Tohyama, and S. Maekawa, 1991, Phys. Rev. B **43**(4), 2968.

Oka, K., H. Shibata, S. Kashiwaya, and H. Eisaki, 2003, Physica C **388**, 389.

Oka, K., and H. Unoki, 1990, Jap. J. Appl. Phys. **29**, L909.

Okada, K., Y. Seino, and A. Kotani, 1990, J. Phys. Soc. Japan **59**(8), 2639.

Onose, Y., Y. Taguchi, T. Ishikawa, S. Shinomori, K. Ishizaka, and Y. Tokura, 1999, Phys. Rev. Lett. **82**(25), 5120.

Onose, Y., Y. Taguchi, K. Ishizaka, and Y. Tokura, 2001, Phys. Rev. Lett. **87**(21), 217001.

Onose, Y., Y. Taguchi, K. Ishizaka, and Y. Tokura, 2004,

Phys. Rev. B **69**(2), 024504.

Orenstein, J., and A. J. Millis, 2000, Science **288**(5465), 468.

Oseroff, S. B., D. Rao, F. Wright, D. C. Vier, S. Schultz, J. D. Thompson, Z. Fisk, S.-W. Cheong, M. F. Hundley, and M. Tovar, 1990, Phys. Rev. B **41**(4), 1934.

Pan, Z.-H., P. Richard, A. V. Fedrov, T. Kondo, T. Takeuchi, S. L. Li, P. Dai, G. Gu, W. Ku, Z. Wang, and H. Ding, 2006, arXiv:cond-mat/0610442 .

Park, S. R., Y. S. Roh, Y. K. Yoon, C. S. Leem, J. H. Kim, B. J. Kim, H. Koh, H. Eisaki, N. P. Armitage, and C. Kim, 2007, Phys. Rev. B **75**(6), 060501.

Park, S. R., D. J. Song, C. S. Leem, C. Kim, C. Kim, B. J. Kim, and H. Eisaki, 2008, Phys. Rev. Lett. **101**(11), 117006.

Pathak, S., V. B. Shenoy, M. Randeria, and N. Trivedi, 2009, Phys. Rev. Lett. **102**(2), 027002.

Pellegrin, E., N. Nücker, J. Fink, S. L. Molodtsov, A. Gutiérrez, E. Navas, O. Strebel, Z. Hu, M. Domke, G. Kaindl, S. Uchida, Y. Nakamura, *et al.*, 1993, Phys. Rev. B **47**(6), 3354.

Peng, J. L., Z. Y. Li, and R. L. Greene, 1991, Physica C **177**(1-3), 79.

Peters, C. J., R. J. Birgeneau, M. A. Kastner, H. Yoshizawa, Y. Endoh, J. Tranquada, G. Shirane, Y. Hidaka, M. Oda, M. Suzuki, and T. Murakami, 1988, Phys. Rev. B **37**(16), 9761.

Petitgrand, D., S. V. Maleyev, P. Bourges, and A. S. Ivanov, 1999, Phys. Rev. B **59**(2), 1079.

Pfleiderer, C., 2009, Rev. Mod. Phys. .

Pimenov, A., A. V. Pronin, A. Loidl, U. Michelucci, A. P. Kampf, S. I. Krasnosvobodtsev, V. S. Nozdrin, and D. Rainer, 2000, Phys. Rev. B **62**(14), 9822.

Pinol, S., J. Fontcuberta, C. Miravitlles, and D. M. Paul, 1990, Physica C **165**(3-4), 265.

Pintschovius, L., and M. Braden, 1999, Phys. Rev. B **60**(22), R15039.

Pintschovius, L., D. Reznik, and K. Yamada, 2006, Phys. Rev. B **74**(17), 174514.

Plakhty, V. P., S. V. Maleyev, S. V. Gavrilov, E. Bourdarot, S. Pouget, and S. N. Barilo, 2003, Europhys. Lett. **61**, 534.

Podolsky, D., S. Raghu, and A. Vishwanath, 2007, Phys. Rev. Lett. **99**(11), 117004.

Ponomarev, A. I., T. B. Charikova, A. N. Ignatenkov, A. O. Tashlykov, and A. A. Ivanov, 2004, Low Temp. Phys. **30**(11), 885.

Prijamboedi, B., and S. Kashiwaya, 2006, Journal of Materials Science: Materials in Electronics **17**(7), 483.

Pronin, A. V., A. Pimenov, A. Loidl, A. Tsukada, and M. Naito, 2003, Phys. Rev. B **68**(5), 054511.

Proust, C., K. Behnia, R. Bel, D. Maude, and S. I. Vedeneev, 2005, Phys. Rev. B **72**(21), 214511.

Proust, C., E. Boaknin, R. W. Hill, L. Taillefer, and A. P. Mackenzie, 2002, Phys. Rev. Lett. **89**(14), 147003.

Prozorov, R., R. Giannetta, P. Fournier, and R. L. Greene, 2000, Phys. Rev. Lett. **85**, 3700.

Puchkov, A., D. B. DN, and T. Timusk, 1996, J. Phys. Condens. Matter **8**(10), 10049.

Qazilbash, M. M., A. Biswas, Y. Dagan, R. A. Ott, and R. L. Greene, 2003, Phys. Rev. B **68**(2), 024502.

Qazilbash, M. M., A. Koitzsch, B. S. Dennis, A. Gozar, H. Balci, C. A. Kendziora, R. L. Greene, and G. Blumberg, 2005, Phys. Rev. B **72**(21), 214510.

Radaelli, P. G., J. D. Jorgensen, A. J. Schultz, J. L. Peng, and R. L. Greene, 1994, Phys. Rev. B **49**(21), 15322.

Randeria, M., 2007, in *Models and Phenomenology for Conventional and High-temperature Superconductivity*, edited by G. Iadonisi, J. R. Schrieffer, and M. Chiofalo (Ios Pr Inc), pp. 53–75.

Reznik, D., L. Pintschovius, M. Ito, S. Iikubo, M. Sato, H. Goka, M. Fujita, K. Yamada, G. Gu, and J. Tranquada, 2006, Nature **440**(1170), 1170.

Richard, P., S. Jandl, M. Poirier, P. Fournier, V. Nekvasil, and M. L. Sadowski, 2005a, Phys. Rev. B **72**(1), 014506.

Richard, P., M. Neupane, Y.-M. Xu, P. Fournier, S. Li, P. Dai, Z. Wang, and H. Ding, 2007, Phys. Rev. Lett. **99**(15), 157002.

Richard, P., M. Poirier, and S. Jandl, 2005b, Phys. Rev. B **71**(14), 144425.

Richard, P., G. Riou, I. Hetel, S. Jandl, M. Poirier, and P. Fournier, 2004, Phys. Rev. B **70**(6), 064513.

Riou, G., S. Jandl, M. Poirier, V. Nekvasil, M. Divis, P. Fournier, R. Greene, D. Zhigunov, and S. Barilo, 2001, Eur. Phys. J. B **23**, 179.

Riou, G., P. Richard, S. Jandl, M. Poirier, P. Fournier, V. Nekvasil, S. N. Barilo, and L. A. Kurnevich, 2004, Phys. Rev. B **69**(2), 024511.

Roberge, G., S. Charpentier, S. Godin-Proulx, P. Rauwel, K. Truong, and P. Fournier, 2009, J. Crystal Growth **311**(5), 1340 .

Ronning, F., C. Kim, D. L. Feng, D. S. Marshall, A. G. Loeser, L. L. Miller, J. N. Eckstein, I. Bozovic, and Z.-X. Shen, 1998, Science **282**(5396), 2067.

Ronning, F., T. Sasagawa, Y. Kohsaka, K. M. Shen, A. Damascelli, C. Kim, T. Yoshida, N. P. Armitage, D. H. Lu, D. L. Feng, L. L. Miller, H. Takagi, *et al.*, 2003, Phys. Rev. B **67**(16), 165101.

Ronning, F., K. M. Shen, N. P. Armitage, A. Damascelli, D. H. Lu, Z.-X. Shen, L. L. Miller, and C. Kim, 2005, Phys. Rev. B **71**(9), 094518.

Rossat-Mignod, J. M., L. P. Regnault, C. Vettier, P. Bourges, P. Burlet, J. Bossy, J. Y. Henry, and G. Lapertot, 1991, Physica C **185**, 86.

Rullier-Albenque, F., H. Alloul, F. Balakirev, and C. Proust, 2008, Europhys. Lett. **81**(3), 37008.

Rullier-Albenque, F., H. Alloul, and R. Tourbot, 2003, Phys. Rev. Lett. **91**(4), 047001.

Sachdev, S., 2003, Rev. Mod. Phys. **75**(3), 913.

Sachdev, S., M. A. Metlitski, Y. Qi, and C. Xu, 2009, Phys. Rev. B **80**(15), 155129.

Sachidanandam, R., T. Yildirim, A. B. Harris, A. Aharony, and O. Entin-Wohlman, 1997, Phys. Rev. B **56**(1), 260.

Sadori, A., and M. Grilli, 2000, Phys. Rev. Lett. **84**(23), 5375.

Sadowski, W., H. Hagemann, M. Franois, H. Bill, M. Peter, E. Walker, and K. Yvon, 1990, Physica C **170**(1-2), 103 .

Sakisaka, Y., T. Maruyama, Y. Morikawa, H. Kato, K. Edamoto, M. Okusawa, Y. Aiura, H. Yanashima, T. Terashima, Y. Bando, K. Iijima, K. Yamamoto, *et al.*, 1990, Phys. Rev. B **42**(7), 4189.

Santander-Syro, A. F., T. Kondo, J. Chang, A. Kaminski, S. Pailhes, M. Shi, L. Patthey, A. Zimmers, B. Liang, P. Li, and R. L. Greene, 2009, arXiv:0903.3413v1 .

Sato, T., T. Kamiyama, T. Takahashi, K. Kurahashi, and K. Yamada, 2001, Science **291**(5508), 1517.

Savici, A. T., A. Fukaya, I. M. Gat-Malureanu, T. Ito, P. L. Russo, Y. J. Uemura, C. R. Wiebe, P. P. Kyriakou, G. J. MacDougall, M. T. Rovers, G. M. Luke, K. M. Kojima, *et al.*, 2005, Phys. Rev. Lett. **95**(15), 157001.

Sawa, A., M. Kawasaki, H. Takagi, and Y. Tokura, 2002,

Phys. Rev. B **66**(1), 014531.

Scalapino, D. J., 1995, Physics Reports **250**, 329.

Schachinger, E., C. C. Homes, R. P. S. M. Lobo, and J. P. Carbotte, 2008, Phys. Rev. B **78**(13), 134522.

Schachinger, E., J. J. Tu, and J. P. Carbotte, 2003, Phys. Rev. B **67**(21), 214508.

Schmitt, F., W. S. Lee, D.-H. Lu, W. Meevasana, E. Motoyama, M. Greven, and Z.-X. Shen, 2008, Phys. Rev. B **78**(10), 100505.

Schneider, C. W., Z. H. Barber, J. E. Evetts, S. N. Mao, X. X. Xi, and T. Venkatesan, 1994, Physica C **233**, 77.

Schultz, A. J., J. D. Jorgensen, J. L. Peng, and R. L. Greene, 1996, Phys. Rev. B **53**(9), 5157.

Segawa, K., and Y. Ando, 2006, Phys. Rev. B **74**(10), 100508.

Sekitani, T., M. Naito, and N. Miura, 2003, Phys. Rev. B **67**(17), 174503.

Senechal, D., and A.-M. S. Tremblay, 2004, Phys. Rev. Lett. **92**(12), 126401.

Seo, K., H.-D. Chen, and J. Hu, 2007, Phys. Rev. B **76**(2), 020511.

Shan, L., Y. Huang, H. Gao, Y. Wang, S. L. Li, P. C. Dai, F. Zhou, J. W. Xiong, W. X. Ti, and H. H. Wen, 2005, Phys. Rev. B **72**(14), 144506.

Shan, L., Y. Huang, Y. L. Wang, S. Li, J. Zhao, P. Dai, Y. Zhang, C. Ren, and H. H. Wen, 2008a, http://arxiv.org/abs/cond-mat/0703256 .

Shan, L., Y. L. Wang, Y. Huang, S. L. Li, J. Zhao, P. Dai, and H. H. Wen, 2008b, Phys. Rev. B **78**(1), 014505.

Shannon, R. D., 1976, Acta Crystallographica Section A **32**, 751.

Shen, K. M., F. Ronning, D. H. Lu, W. S. Lee, N. J. C. Ingle, W. Meevasana, F. Baumberger, A. Damascelli, N. P. Armitage, L. L. Miller, Y. Kohsaka, M. Azuma, *et al.*, 2004, Phys. Rev. Lett. **93**(26), 267002.

Shen, Z.-X., D. S. Dessau, B. O. Wells, D. M. King, W. E. Spicer, A. J. Arko, D. Marshall, L. W. Lombardo, A. Kapitulnik, P. Dickinson, S. Doniach, J. DiCarlo, *et al.*, 1993, Phys. Rev. Lett. **70**(10), 1553.

Shengelaya, A., R. Khasanov, D. G. Eshchenko, D. D. Castro, I. M. Savic, M. S. Park, K. H. Kim, S.-I. Lee, K. A. Muller, and H. Keller, 2005, Phys. Rev. Lett. **94**(12), 127001.

Shibauchi, T., L. Krusin-Elbaum, M. Li, M. P. Maley, and P. H. Kes, 2001, Phys. Rev. Lett. **86**(25), 5763.

Siegrist, T., S. M. Zahurak, D. Murphy, , and R. S. Roth, 1988, Nature **334**, 231.

Singer, P. M., A. W. Hunt, A. F. Cederström, and T. Imai, 1999, Phys. Rev. B **60**(22), 15345.

Singh, A., and H. Ghosh, 2002, Phys. Rev. B **65**(13), 134414.

Singh, R. R. P., P. A. Fleury, K. B. Lyons, and P. E. Sulewski, 1989, Phys. Rev. Lett. **62**(23), 2736.

Singley, E. J., D. N. Basov, K. Kurahashi, T. Uefuji, and K. Yamada, 2001, Phys. Rev. B **64**(22), 224503.

Skanthakumar, S., J. W. Lynn, J. L. Peng, and Z. Y. Li, 1991, J. Appl. Phys. **69**(8), 4866.

Skanthakumar, S., J. W. Lynn, J. L. Peng, and Z. Y. Li, 1993, Phys. Rev. B **47**(10), 6173.

Skanthakumar, S., J. W. Lynn, and I. W. Sumarlin, 1995, Phys. Rev. Lett. **74**(14), 2842.

Skelton, E. F., A. R. Drews, M. S. Osofsky, S. B. Qadi, J. Z. Hu, T. A. Vanderah, J. L. Peng, and R. L. Greene, 1994, Science **263**, 1416.

Skinta, J. A., M.-S. Kim, T. R. Lemberger, T. Greibe, and M. Naito, 2002, Phys. Rev. Lett. **88**(20), 207005.

Smith, M. F., J. Paglione, M. B. Walker, and L. Taillefer,

2005, Phys. Rev. B **71**(1), 014506.

Smith, M. G., A. Manthiram, J. Zhou, J. B. Goodenough, and J. T. Markert, 1991, Nature **351**(6327), 549.

Snezhko, A., R. Prozorov, D. D. Lawrie, R. Giannetta, J. Gauthier, J. Renaud, and P. Fournier, 2004, Phys. Rev. Lett. **92**, 157005.

Sondheimer, E. H., 1948, Royal Society of London Proceedings Series A **193**, 484.

Sonier, J. E., J. H. Brewer, and R. F. Kiefl, 2000, Rev. Mod. Phys. **72**(3), 769.

Sonier, J. E., K. F. Poon, G. M. Luke, P. Kyriakou, R. I. Miller, R. Liang, C. R. Wiebe, P. Fournier, and R. L. Greene, 2003, Phys. Rev. Lett. **91**(14), 147002.

Sooryakumar, R., and M. V. Klein, 1980, Phys. Rev. Lett. **45**(8), 660.

Sooryakumar, R., and M. V. Klein, 1981, Phys. Rev. B **23**(7), 3213.

Stadlober, B., G. Krug, R. Nemetschek, R. Hackl, J. L. Cobb, and J. T. Markert, 1995, Phys. Rev. Lett. **74**(24), 4911.

Steeneken, P. G., L. H. Tjeng, G. A. Sawatzky, A. Tanaka, O. Tjernberg, G. Ghiringhelli, N. B. Brookes, A. A. Nugroho, and A. A. Menovsky, 2003, Phys. Rev. Lett. **90**(24), 247005.

Stepanov, A. A., P. Wyder, T. Chattopadhyay, P. J. Brown, G. Fillion, I. M. Vitebsky, A. Deville, B. Gaillard, S. N. Barilo, and D. I. Zhigunov, 1993, Phys. Rev. B **48**(17), 12979.

Sugai, S., T. Kobayashi, and J. Akimitsu, 1989, Phys. Rev. B **40**(4), 2686.

Sulewski, P. E., P. A. Fleury, K. B. Lyons, S.-W. Cheong, and Z. Fisk, 1990, Phys. Rev. B **41**(1), 225.

Sumarlin, I. W., J. W. Lynn, T. Chattopadhyay, S. N. Barilo, D. I. Zhigunov, and J. L. Peng, 1995, Phys. Rev. B **51**(9), 5824.

Sumarlin, I. W., S. Skanthakumar, J. W. Lynn, J. L. Peng, Z. Y. Li, W. Jiang, and R. L. Greene, 1992, Phys. Rev. Lett. **68**(14), 2228.

Sun, C., H. Yang, L. Cheng, J. Wang, X. Xu, S. Ke, and L. Cao, 2008, Phys. Rev. B **78**(10), 104518.

Sun, X. F., Y. Kurita, T. Suzuki, S. Komiya, and Y. Ando, 2004, Phys. Rev. Lett. **92**(4), 047001.

Suzuki, K., K. Kishio, T. Hasegawa, and K. Kitazawa, 1990, Physica C **166**, 357.

Taguchi, M., A. Chainani, K. Horiba, Y. Takata, M. Yabashi, K. Tamasaku, Y. Nishino, D. Miwa, T. Ishikawa, T. Takeuchi, K. Yamamoto, M. Matsunami, *et al.*, 2005, Phys. Rev. Lett. **95**(17), 177002.

Taillefer, L., B. Lussier, R. Gagnon, K. Behnia, and H. Aubin, 1997, Phys. Rev. Lett. **79**(3), 483.

Takagi, H., S. Uchida, and Y. Tokura, 1989, Phys. Rev. Lett. **62**, 1197.

Takayama-Muromachi, E., F. Izumi, Y. Uchida, K. Kato, and H. Asano, 1989, Physica C **159**, 634.

Tan, Z., J. I. Budnick, C. E. Bouldin, J. C. Woicik, S.-W. Cheong, A. S. Cooper, G. P. Espinosa, and Z. Fisk, 1990, Phys. Rev. B **42**(1), 1037.

Tanaka, I., T. Watanabe, N. Komai, and H. Kojima, 1991, Physica C **185-189**(Part 1), 437.

Tanaka, Y., and S. Kashiwaya, 1995, Phys. Rev. Lett. **74**(17), 3451.

Tanatar, M. A., J. Paglione, C. Petrovic, and L. Taillefer, 2007, Science **316**(5829), 1320.

Tanda, S., S. Ohzeki, and T. Nakayama, 1992, Phys. Rev. Lett. **69**(3), 530.

Tarascon, J.-M., E. Wang, L. H. Greene, B. G. Bagley, G. W. Hull, S. M. D'Egidio, P. F. Miceli, Z. Z. Wang, T. W. Jing, J. Clayhold, D. Brawner, and N. P. Ong, 1989, Phys. Rev. B **40**(7), 4494.

Thompson, J. D., S.-W. Cheong, S. E. Brown, Z. Fisk, S. B. Oseroff, M. Tovar, D. C. Vier, and S. Schultz, 1989, Phys. Rev. B **39**(10), 6660.

Thurston, T. R., M. Matsuda, K. Kakurai, K. Yamada, Y. Endoh, R. J. Birgeneau, P. M. Gehring, Y. Hidaka, M. A. Kastner, T. Murakami, and G. Shirane, 1990, Phys. Rev. Lett. **65**(2), 263.

Timusk, T., and B. Statt, 1999, Rep. Prog. Phys. **62**(1), 61.

Tinkham, M., 1996, *Introduction to superconductivity* (McGraw-Hill), second edition edition.

Tohyama, T., 2004, Phys. Rev. B **70**(17), 174517.

Tohyama, T., and S. Maekawa, 1990, J. Phys. Soc. Jap. **59**, 1760.

Tohyama, T., and S. Maekawa, 1994, Phys. Rev. B **49**(5), 3596.

Tohyama, T., and S. Maekawa, 2001, Phys. Rev. B **64**(21), 212505.

Tokura, Y., A. Fujimori, H. Matsubara, H. Watabe, H. Takagi, S. Uchida, M. Sakai, H. Ikeda, S. Okuda, and S. Tanaka, 1989a, Phys. Rev. B **39**(13), 9704.

Tokura, Y., S. Koshihara, T. Arima, H. Takagi, S. Ishibashi, T. Ido, and S. Uchida, 1990, Phys. Rev. B **41**(16), 11657.

Tokura, Y., H. Takagi, and S. Uchida, 1989b, Nature **337**, 345.

Torrance, J. B., and R. M. Metzger, 1989, Phys. Rev. Lett. **63**(14), 1515.

Tranquada, J., Y. N. B.J. Sternlieb J.D. Axe, and S. Uchida, 1995, Nature **375**, 561.

Tranquada, J., S. Heald, A. Moodenbaugh, G. Liang, and M. Croft, 1989, Nature **337**, 720.

Tranquada, J. M., C. H. Lee, K. Yamada, Y. S. Lee, L. P. Regnault, and H. M. Ronnow, 2004a, Phys. Rev. B **69**(17), 174507.

Tranquada, J. M., H. Woo, T. G. Perring, H. Goka, G. D. Gu, G. Xu, M. Fujita, and K. Yamada, 2004b, Nature **429**(6991), 534.

Tremblay, A. M. S., B. Kyung, and D. Senechal, 2006, Low Temp. Phys. **32**(4-5), 424.

Tsuei, C. C., A. Gupta, and G. Koren, 1989, Physica C **161**, 415.

Tsuei, C. C., and J. R. Kirtley, 2000a, Rev. Mod. Phys. **72**(4), 969.

Tsuei, C. C., and J. R. Kirtley, 2000b, Phys. Rev. Lett. **85**(1), 182.

Tsukada, A., Y. Krockenberger, M. Noda, H. Yamamoto, D. Manske, L. Alff, and M. Naito, 2005, Solid State Comm. **133**, 427.

Tsukada, A., M. Naito, and H. Yamamoto, 2007, Physica C **463-465**, 64 , proceedings of the 19th International Symposium on Superconductivity (ISS 2006).

Tsunekawa, M., A. Sekiyama, S. Kasai, S. Imada, H. Fujiwara, T. Muro, Y. Onose, Y. Tokura, , and S. Suga, 2008, New Journal of Physics **10**, 073005.

Uchiyama, H., A. Q. R. Baron, S. Tsutsui, Y. Tanaka, W.-Z. Hu, A. Yamamoto, S. Tajima, and Y. Endoh, 2004, Phys. Rev. Lett. **92**(19), 197005.

Uefuji, T., T. Kubo, K. Yamada, M. Fujita, K. Kurahashi, I. Watanabe, and K. Nagamine, 2001, Physica C **357-360**(Part 1), 208.

Uemura, Y. J., L. P. Le, G. M. Luke, B. J. Sternlieb, W. D.

Wu, J. H. Brewer, T. M. Riseman, C. L. Seaman, M. B. Maple, M. Ishikawa, D. G. Hinks, J. D. Jorgensen, *et al.*, 1991, Phys. Rev. Lett. **66**(20), 2665.

Uemura, Y. J., G. M. Luke, B. J. Sternlieb, J. H. Brewer, J. F. Carolan, W. N. Hardy, R. Kadono, J. R. Kempton, R. F. Kiefl, S. R. Kreitzman, P. Mulhern, T. M. Riseman, *et al.*, 1989, Phys. Rev. Lett. **62**(19), 2317.

Uzumaki, X., X. Kamehura, and X. Niwa, 1991, Jap. J. Appl. Phys. **30**, 981.

Varma, C. M., 1997, Phys. Rev. B **55**(21), 14554.

Varma, C. M., 1999, Phys. Rev. Lett. **83**(17), 3538.

Varma, C. M., S. Schmitt-Rink, and E. Abrahams, 1987, Solid State Comm. **62**, 681.

Venturini, F., R. Hackl, and U. Michelucci, 2003, Phys. Rev. Lett. **90**(14), 149701.

Vigoureux, P., 1995, *Études structurales des composés supra-conducteurs de type n : $R_{2-x}Ce_xCuO_{4d}$ (R = Gd, Eu, Sm, Nd, Pr); influences des traitements chimiques sur les pro-priétés physiques*, Ph.D. thesis, Université Paris XI, Orsay, France.

Vigoureux, P., M. Braden, A. Gukasov, W. Paulus, P. Bourges, A. Cousson, D. Petitgrand, J.-P. Lauriat, M. Meven, S. N. Barilo, D. Zhigunov, P. Adelmann, *et al.*, 1997, Physica C **273**, 239 .

Volovik, G. E., 1993, JETP Lett. **58**, 469.

Wagenknecht, M., D. Koelle, R. Kleiner, S. Graser, N. Schopohl, B. Chesca, A. Tsukada, S. T. B. Goennenwein, and R. Gross, 2008, Phys. Rev. Lett. **100**(22), 227001.

Wang, C. H., G. Y. Wang, T. Wu, Z. Feng, X. G. Luo, and X. H. Chen, 2005, Phys. Rev. B **72**(13), 132506.

Wang, N. L., G. Li, D. Wu, X. H. Chen, C. H. Wang, and H. Ding, 2006a, Phys. Rev. B **73**(18), 184502.

Wang, Y., L. Li, and N. P. Ong, 2006b, Phys. Rev. B **73**(2), 024510.

Wang, Y., B. Revaz, A. Erb, and A. Junod, 2001, Phys. Rev. B **63**(9), 094508.

Wang, Z. Z., T. R. Chien, N. P. Ong, J. M. Tarascon, and E. Wang, 1991, Phys. Rev. B **43**(4), 3020.

Weber, C., K. Haule, and G. Kotliar, 2009, preprint .

Wells, B. O., Z.-X. Shen, A. Matsuura, D. M. King, M. A. Kastner, M. Greven, and R. J. Birgeneau, 1995, Phys. Rev. Lett. **74**(6), 964.

Williams, G. V. M., J. Haase, M.-S. Park, K. H. Kim, and S.-I. Lee, 2005, Phys. Rev. B **72**(21), 212511.

Wilson, S. D., P. Dai, S. Li, S. Chi, H. J. Kang, and J. W. Lynn, 2006a, Nature **442**, 59 .

Wilson, S. D., S. Li, P. Dai, W. Bao, J.-H. Chung, H. J. Kang, S.-H. Lee, S. Komiya, Y. Ando, and Q. Si, 2006b, Phys. Rev. B **74**(14), 144514.

Wilson, S. D., S. Li, H. Woo, P. Dai, H. A. Mook, C. D. Frost, S. Komiya, and Y. Ando, 2006c, Phys. Rev. Lett. **96**(15), 157001.

Wilson, S. D., S. Li, J. Zhao, G. Mu, H.-H. Wen, J. W. Lynn, P. G. Freeman, L.-P. Regnault, K. Habicht, and P. Dai, 2007, Proceedings of the National Academy of Sciences **104**(39), 15259.

Woods, S. I., A. S. Katz, M. C. de Andrade, J. Herrmann, M. B. Maple, and R. C. Dynes, 1998, Phys. Rev. B **58**(13), 8800.

Woods, S. I., A. S. Katz, S. I. Applebaum, M. C. de Andrade, M. B. Maple, and R. C. Dynes, 2002, Phys. Rev. B **66**(1), 014538.

Woynarovich, F., 1982, J. Phys. C: Solid State Physics **15**(1), 97.

Wu, B., K. Jin, J. Yuan, H. Wang, T. Hatano, B. Zhao, and B. Zhu, 2009, Physica C **469**, 1945.

Wu, D. H., J. Mao, S. N. Mao, J. L. Peng, X. X. Xi, T. Venkatesan, R. L. Greene, and S. M. Anlage, 1993, Phys. Rev. Lett. **70**(1), 85.

Wu, H., L. Zhao, J. Yuan, L. X. Cao, J. P. Zhong, L. J. Gao, B. Xu, P. C. Dai, B. Y. Zhu, X. G. Qiu, and B. R. Zhao, 2006, Phys. Rev. B **73**(10), 104512.

Wu, T., C. H. Wang, G. Wu, D. F. Fang, J. L. Luo, G. T. Liu, and X. H. Chen, 2008, J. Phys. Condens. Matter **20**(27), 275226.

Xia, J., E. Schemm, G. Deutscher, S. A. Kivelson, D. A. Bonn, W. N. Hardy, R. Liang, W. Siemons, G. Koster, M. M. Fejer, and A. Kapitulnik, 2008, Phys. Rev. Lett. **100**(12), 127002.

Xiang, T., H. G. Luo, D. H. Lu, K. M. Shen, and Z. X. Shen, 2008, arXiv:0807.2498 .

Xu, X. Q., S. N. Mao, W. Jiang, J. L. Peng, and R. L. Greene, 1996, Phys. Rev. B **53**(2), 871.

Yagi, H., T. Yoshida, A. Fujimori, Y. Kohsaka, M. Misawa, T. Sasagawa, H. Takagi, M. Azuma, and M. Takano, 2006, Phys. Rev. B **73**(17), 172503.

Yamada, K., K. Kurahashi, Y. Endoh, R. J. Birgeneau, and G. Shirane, 1999, J. Phys. Chem. Sol. **8-9**(10), 1025.

Yamada, K., K. Kurahashi, T. Uefuji, M. Fujita, S. Park, S.-H. Lee, and Y. Endoh, 2003, Phys. Rev. Lett. **90**(13), 137004.

Yamada, K., C. H. Lee, K. Kurahashi, J. Wada, S. Wakimoto, S. Ueki, H. Kimura, Y. Endoh, S. Hosoya, G. Shirane, R. J. Birgeneau, M. Greven, *et al.*, 1998, Phys. Rev. B **57**(10), 6165.

Yamada, K., S. Wakimoto, G. Shirane, C. H. Lee, M. A. Kastner, S. Hosoya, M. Greven, Y. Endoh, and R. J. Birgeneau, 1995, Phys. Rev. Lett. **75**(8), 1626.

Yamada, T., K. Kinoshita, and H. Shibata, 1994, Jap. J. Appl. Phys. **33**(Part 2, No. 2A), L168.

Yamamoto, H., M. Naito, and H. Sato, 1997, Phys. Rev. B **56**(5), 2852.

Yildirim, T., A. B. Harris, O. Entin-Wohlman, and A. Aharony, 1994, Phys. Rev. Lett. **72**(23), 3710.

Yildirim, T., A. B. Harris, and E. F. Shender, 1996, Phys. Rev. B **53**(10), 6455.

Yu, G., M. Greven, E. Yamamoto, *et al.*, 2008, arXiv:0803.3250 .

Yu, R. C., M. B. Salamon, J. P. Lu, and W. C. Lee, 1992, Phys. Rev. Lett. **69**(9), 1431.

Yu, W., J. S. Higgins, P. Bach, and R. L. Greene, 2007a, Phys. Rev. B **76**(2), 020503.

Yu, W., J. S. Higgins, P. Bach, and R. L. Greene, 2007b, Phys. Rev. B **76**(2), 020503.

Yu, W., B. Liang, and R. L. Greene, 2005, Phys. Rev. B **72**(21), 212512.

Yu, W., B. Liang, and R. L. Greene, 2006, Phys. Rev. B **74**(21), 212504.

Yuan, Q., X.-Z. Yan, and C. S. Ting, 2006a, Phys. Rev. B **74**(21), 214503.

Yuan, Q., F. Yuan, and C. S. Ting, 2005, Phys. Rev. B **72**(5), 054504.

Yuan, Q., F. Yuan, and C. S. Ting, 2006b, Phys. Rev. B **73**(5), 054501.

Zaanen, J., and O. Gunnarsson, 1989, Phys. Rev. B **40**(10), 7391.

Zaanen, J., G. A. Sawatzky, and J. W. Allen, 1985, Phys. Rev. Lett. **55**(4), 418.

Zamborszky, F., G. Wu, J. Shinagawa, W. Yu, H. Balci, R. L. Greene, W. G. Clark, and S. E. Brown, 2004, Phys. Rev. Lett. **92**(4), 047003.

Zhang, F. C., and T. M. Rice, 1988, Phys. Rev. B **37**(7), 3759.

Zhang, S.-C., 1997, Science **275**(5303), 1089.

Zhao, J., P. Dai, S. Li, P. G. Freeman, Y. Onose, and Y. Tokura, 2007, Phys. Rev. Lett. **99**(1), 017001.

Zhao, L., H. Wu, J. Miao, H. Yang, F. C. Zhang, X. G. Qiu, and B. R. Zhao, 2004, Supercond. Sci. Technol. **17**(11), 1361.

Zheng, G.-q., T. Sato, Y. Kitaoka, M. Fujita, and K. Yamada, 2003, Phys. Rev. Lett. **90**(19), 197005.

Zimmers, A., R. P. S. M. Lobo, N. Bontemps, C. C. Homes, M. C. Barr, Y. Dagan, and R. L. Greene, 2004, Phys. Rev. B **70**(13), 132502.

Zimmers, A., Y. Noat, T. Cren, W. Sacks, D. Roditchev, B. Liang, and R. L. Greene, 2007a, Phys. Rev. B **76**(13), 132505.

Zimmers, A., L. Shi, D. C. Schmadel, W. M. Fisher, R. L. Greene, H. D. Drew, M. Houseknecht, G. Acbas, M.-H. Kim, M.-H. Yang, J. Cerne, J. Lin, *et al.*, 2007b, Phys. Rev. B **76**(6), 064515.

Zimmers, A., J. M. Tomczak, R. P. S. M. Lobo, N. Bontemps, C. P. Hill, M. C. Barr, Y. Dagan, R. L. Greene, A. J. Millis, and C. C. Homes, 2005, Europhys. Lett. **70**(2), 225.